Structure/Function Relationships of [NiFe]- and [FeFe]-Hydrogenases

Juan C. Fontecilla-Camps,* Anne Volbeda, Christine Cavazza, and Yvain Nicolet

Laboratoire de Cristallographie et Cristallogenèse des Proteines, Institut de Biologie Structurale J. P. Ebel, CEA, CNRS, Universitè Joseph Fourier, 41 rue J. Horowitz, 38027 Grenoble Cedex 1, France

Received March 26, 2007

Contents

* Corresponding author (e-mail juan.fontecilla@ibs.fr; telephone 33 4 38785920; fax 33 4 38785122).

1. Introduction

The utilization of hydrogen by micro-organisms as a source of reducing power or of protons as final electron acceptors is mediated by metalloenzymes called hydrogenases. The need for catalytic transition metal centers is explained by the significant increase in the acidity of molecular hydrogen when bound to them.[1] There are three phylogenetically unrelated classes of these enzymes: [NiFe]- and [FeFe]-hydrogenases, in which hydrogen is the only substrate or product, according to $H_2 \leftrightarrow 2H^+ + 2e^-$, and a third class in which hydrogen uptake is coupled to methenyltetrahydromethanopterin reduction.[2] The latter is called FeS cluster-free hydrogenase because, as opposed to the other two enzymes, it lacks FeS cubane centers.[3] Its active site contains a labile light-sensitive cofactor[4] with a mononuclear low-spin iron, most likely Fe(II),[5] that binds two CO ligands.[6,7] The crystal structure of the apoenzyme was published in 2006,[8] and more recently, the three-dimensional structure of the holoenzyme was reported at a Workshop on Biohydrogen, February 21−23, 2007, in Berlin, Germany (S. Shima et al., unpublished work). As we will discuss below, low-spin iron coordinated to CO is also present in [NiFe]- and [FeFe]-hydrogenases, indicating that a $Fe(CO)_x$ unit is central to biological hydrogen catalysis. Here, we will review [NiFe]- and [FeFe]-hydrogenases.

The crystal structures of five periplasmic [NiFe]-hydrogenases from sulfate-reducing bacteria have been reported.[9−13] In addition, the structures of [FeFe]-hydrogenases from the sulfate-reducing bacterium *Desulfovibrio desulfuricans* ATCC 7757 and the carbohydrate-fermenting bacterium *Clostridium pasteurianum* have also been determined.[14,15] The former is a periplasmic uptake enzyme, whereas the latter is cytoplasmic and uses low-potential electrons to reduce protons to hydrogen. Spectroscopic and crystallographic studies have revealed the complex nature of the hydrogenases active sites, which contain biologically unusual ligands. Consequently, a considerable effort is under way to elucidate their synthetic pathways and the catalytic center assembly, and some significant progress has been made in this respect. Because the active sites of [NiFe]- and [FeFe]-hydrogenases are buried within the structures, these enzymes require pathways for transferring electrons and protons between the catalytic center

10.1021/cr050195z CCC: $65.00
Published on Web 09/13/2007

Juan C. Fontecilla-Camps received his undergraduate training at the University of Concepcion, Chile, and his Ph.D. degree in protein crystallography at the University of Alabama in Birmingham under the supervision of Charles E. Bugg in 1980. Subsequently, he moved to Marseilles, France, where he became group leader and then head of a protein crystallography laboratory established by the CNRS and the University of Aix-Marseilles. In 1991, he took a job with the French Commissariat à l'Energie Atomique (CEA) in Grenoble. After having worked on the crystal structure of animal toxins, in 1993 he turned his attention to the structural biology of hydrogenases and other metalloenzymes. He and his group have solved the structures of NiFe and Fe-only hydrogenases, pyruvate-ferredoxin oxidoreductase, and, very recently, carbon monoxide dehydrogenase/acetyl-coenzyme A synthase. In 2000, he was awarded the medal of the European section of the International Society of Biological Inorganic Chemistry for his work on hydrogenases. He is also "Chevalier dans l'Ordre des Palmes Académiques".

Anne Volbeda obtained his Ph.D. degrer in 1988 at the University of Groningen after working with Wim Hol on the crystallographic analysis of spiny lobster hemocyanin, a large hexameric protein that uses binuclear copper centers to transport molecular oxygen. During a postdoctoral fellowship with Dietrich Suck at EMBL Heidelberg, he worked on the crystal structure of P1 nuclease, an enzyme with a trinuclear zinc active site. In 1991 he obtained a permanent position at the laboratory of crystallography and crystallogenesis of proteins (LCCP) led by Juan Fontecilla-Camps in Grenoble. Here he continued doing research on the structure and function of large redox enzymes depending on iron and/or nickel. These include [NiFe]-hydrogenases, pyruvate:ferredoxin oxidoreductase, carbon monoxide dehydrogenase complexed with acetyl coenzyme A synthase, and cytosolic aconitase. His main themes of interest concern the role of cavities inside proteins, transfer pathways for electrons, protons, and gases, and the functioning of metal sites in biochemical energy transformations.

and the molecular surface. By the same token, hydrogen has to reach the active site or escape from it. A major current subject of study concerning hydrogenases is their relative sensibility to molecular oxygen. This is not only of basic scientific interest but also central to the possible use of hydrogenases in bio-fuel cells or the industrial production of "bio-hydrogen". In this chapter we will address the points mentioned above from a structural perspective.

Christine Cavazza received her Ph.D. degree in biochemistry and structural biology in 1996 from the University of Marseilles (France) under the direction of Dr. Mireille Bruschi. She concentrated her research activity on the biochemistry of the *Thiobacillus ferrooxidans* respiratory chain. In 1997 she became a postdoctoral associate with Ivano Bertini at the Uuniversity of Florence (Italy). Subsequently, Christine worked on NiFe hydrogenases during a postdoctoral fellowship with Claude Hatchikian at the University of Marseilles (1999–2000). In 2000, she joined the group of Juan C. Fontecilla-Camps and obtained a permanent position at the Laboratory of Protein Crystallography and Crystallogenesis in 2002, where she continued doing research on the biochemistry and structural biology of NiFe hydrogenases. She also has worked on other metalloenzymes like pyruvate-ferredoxin oxidoreductase. Her main themes of interest focus on the understanding of reaction mechanisms of oxygen-sensitive metalloenzymes.

Yvain Nicolet obtained his Ph.D. degree in 2001 at the University Joseph Fourier in Grenoble, under the supervision of Juan C. Fontecilla-Camps. His thesis research was centered on the crystal structure determination of the FeFe-hydrogenase from *Desulfovibrio desulfuricans*. He stayed an additional year at the University Joseph Fourier as a teaching assistant, where he worked on the crystallographic study of human butyrylcholinesterase. Subsequently, he moved to the Massachusetts Institute of Technology as a postdoctoral fellow in Catherine L. Drennan's laboratory, where he worked on the X-ray structure of biotin synthase and radical SAM enzymes. He then pursued his research as a postdoctoral fellow at the European Synchrotron Radiation Facility in Grenoble working on the general stress response pathway of *Deinococcus radiodurans*. In 2004 he joined the "metalloproteins" group at the Laboratory of Protein Crystallography and Crystallogenesis in Grenoble as a permanent scientist. He is currently involved in the structural study of radical SAM enzymes required for the maturation of metalloprotein active sites.

2. Enzyme Architectures

2.1. [NiFe]-Hydrogenases

Orthorhombic ($P2_12_12_1$) crystals of *Desulfovibrio (D.) vulgaris* Miyazaki [NiFe]-hydrogenase and monoclinic ($C2$) crystals from the *D. gigas* enzyme were reported in 1987.[16,17] The first atomic model, published in 1995, was obtained at

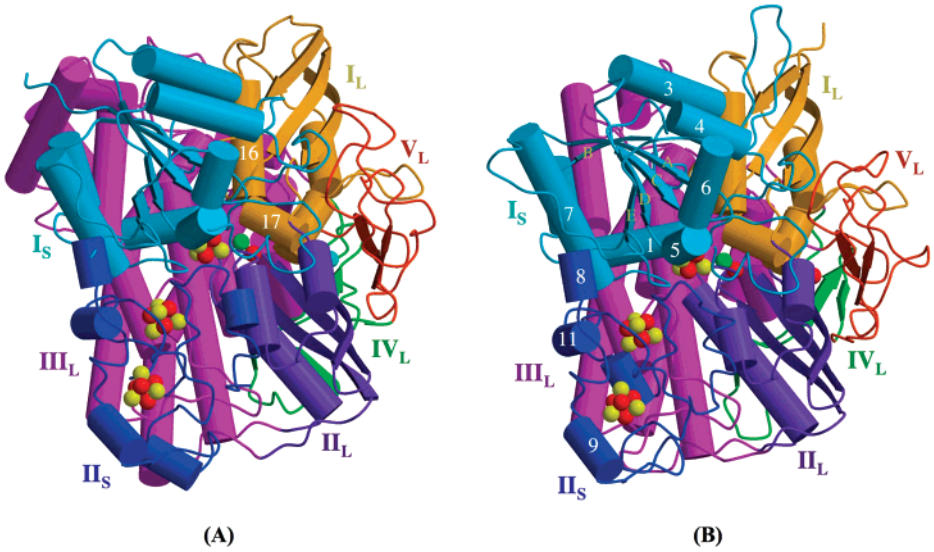

Figure 1. [NiFe]-hydrogenase architectures in **(**A**)** *D. fructosovorans* (PDB code 1YQW), which is very similar to the *D. gigas* enzyme, and **(**B**)** *Dm. baculatum* (PDB code 1CC1), which has a Ni−Fe−Se active site. Atom color codes: green, Ni; red, Fe; light blue, Mg; yellow, S. Structural domains are shown in different colors. Subscripts L and S refer to the large and small subunits, respectively. Selected secondary structure elements are labeled for the large subunit in **(**A**)** and the small subunit in **(**B**)**. This figure and Figures 2−7 and 13 were prepared with the programs MOLSCRIPT[254] and Raster3D.[255]

the Institut de Biologie Structurale in Grenoble from a better quality triclinic (*P*1) crystal form of the *D. gigas* [NiFe]-enzyme.[9] Typically, a freshly aerobically purified enzyme preparation was used,[18] and crystals were grown overnight under air using the vapor diffusion method. X-ray diffraction data were collected the next day with a rotating anode Cu Kα X-ray source at room temperature. It was important to collect X-ray data as soon as possible after crystal growth, because when exposed to air the crystals rapidly became colorless and lost their diffracting power. Six native crystals were used to complete a 2.85 Å resolution X-ray data set, and many additional ones were tested for the binding of heavy atom salts in soaking experiments. The crystal structure was solved by a combination of isomorphous replacement, using three heavy atom derivatives, along with noncrystallographic symmetry density averaging, taking advantage of the presence of two enzyme heterodimers per asymmetric unit.

On the basis of a visual inspection it is possible to define two structural domains in the small subunit, which contains three FeS clusters, and five in the large subunit, which contains the active site (Figure 1A). Alternatively, the large subunit may be described as being composed of four polypeptide layers. The two subunits possess an extensive contact interface of about 3500 Å.[2] The N-terminal domain I_S of the small subunit has a flavodoxin-like fold. It coordinates the [Fe_4S_4] cluster closest to the active site (the proximal cluster) at approximately the location occupied by the phosphate group of FMN in flavodoxin. Structural superposition of this domain to 89 Cα atoms of *Clostridium MP* flavodoxin[19] gave a root-mean-square deviation of 2.7 Å.[9] The superimposed regions represent 65% of flavodoxin and include the central five-stranded parallel β-sheet and five flanking α-helices. The mesial [Fe_3S_4] and distal [Fe_4S_4] clusters are bound to the C-terminal domain II_S that is less rich in secondary structural elements than I_S. One of the ligands of the distal cluster is the Nδ atom of the surface-exposed His185. All of the protein ligands to the 10 other cluster Fe atoms are cysteine thiolates. Domain II_S is absent from some [NiFe]-hydrogenases, such as NAD(P)$^+$-reducing and energy-converting enzymes (see also sections 4 and 7).

A 5 Å resolution anomalous difference map of *D. gigas* hydrogenase displayed four significant peaks disposed in an approximate linear fashion and separated by about 12 Å from center to center.[20] The two strongest peaks were assigned to the two [Fe_4S_4] clusters, the next one to an intermediate [Fe_3S_4] cluster, and the weakest peak to the active site, which at the time was thought to contain only one Ni ion. The same distribution of metal sites was found in a 4 Å resolution analysis of *D. vulgaris* Miyazaki [NiFe]-hydrogenase, performed by Higuchi et al. in Kyoto, Japan.[21] However, in the 2.85 Å resolution analysis of the *D. gigas* enzyme described above, the anomalous dispersion peak at the active site turned out to correspond to a second, different metal ion next to Ni.[9] In retrospect, this made sense because we used Cu Kα X-ray radiation ($\lambda = 1.541$ Å) to collect the diffraction data, which correspond to the low-energy side of the Ni absorption edge (at $\lambda = 1.488$ Å). The Ni site could be assigned in the electron density because it was terminally bound to the thiolate of Cys530. This residue is substituted by selenocysteine in the homologous [NiFeSe]-hydrogenases, and previous EXAFS analyses of these enzymes showed that it was a Ni ligand.[22−24] The second metal ion was tentatively assigned to iron, which has an absorption edge at $\lambda = 1.743$ Å, because of the reported presence of 12 ± 1 iron atoms per hydrogenase heterodimer,[25] a content that was confirmed by an inductively coupled plasma analysis.[9]

Starting in 1996, the use of cryogenic methods and of synchrotron radiation with tunable X-ray wavelengths greatly simplified and improved the crystallographic studies. Crystals were much more stable after storage in liquid nitrogen or when kept at 100 K during data collection. In addition, data collection was much faster with the intense synchrotron X-ray beam, and complete data sets could be measured from single crystals. Direct crystallographic evidence for the presence of iron in the active site was obtained with 3 Å resolution anomalous scattering X-ray data collected for the *D. gigas* enzyme at 1.733 Å and 1.750 Å (high- and low-energy sides of the iron absorption edge, respectively) at the European Synchrotron Radiation Facility (ESRF) in Grenoble, France. Only in the anomalous difference map calculated from data collected at the former wavelength was there a

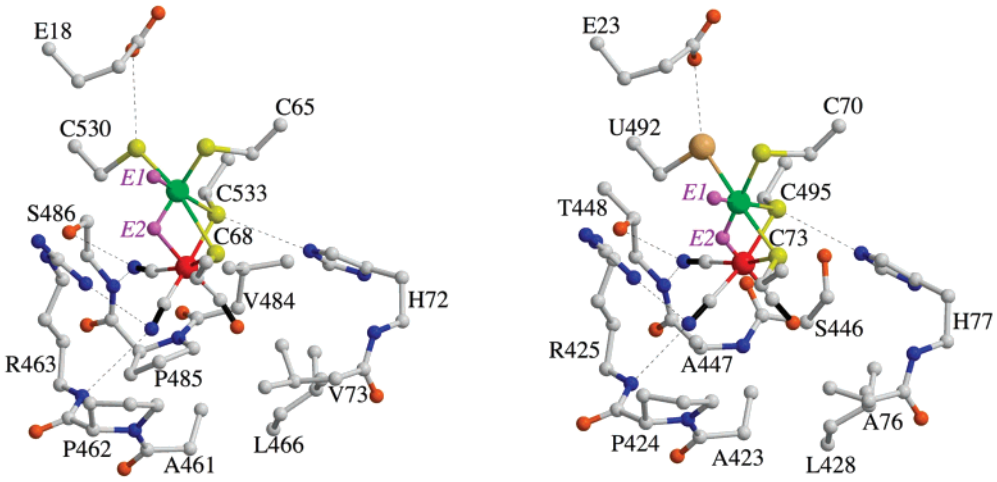

Figure 2. Ni−Fe active site: **(**A**)** *D. gigas* [NiFe]-hydrogenase, oxidized form (see text); **(**B**)** *Dm. baculatum* [NiFeSe]-hydrogenase, reduced form. Atom colors: green, Ni; red, Fe; yellow, S; dark yellow, Se; orange, O; blue, N; white, C. Dashed lines depict putative hydrogen bonds. Two available sites for exogenous ligands are labeled *E1* and *E2*. The occupancy of these sites depends on the functional state of the enzyme (see sections 6 and 8).

significant peak for the second active site metal ion.[26] This result was confirmed by a similar analysis performed by Higuchi et al. at the Photon Factory in Tsukuda, Japan, using *D. vulgaris* Miyazaki [NiFe]-hydrogenase. Its structure was independently solved at 1.8 Å resolution combining multiple isomorphous replacement (MIR) and multiwavelength anomalous dispersion (MAD) methods.[10] In this study crystallographic evidence for the assignment of the nickel ion next to the active site iron was also provided.

The Ni−Fe active site of the *D. gigas* enzyme is located between the two $\alpha\beta$-domains I_L and II_L of the large subunit (Figure 1). A distinctive feature of the extensive helical domain III_L is the presence of a partially bent four-helix bundle that spans most of the large subunit. The less structured domains IV_L and V_L are located on the surface, opposite the interface of the two subunits. Comparison of the amino acid sequences of different hydrogenases indicates that they are the least conserved domains. In the final stages of the large subunit polypeptide chain tracing we were surprised by the absence of electron density beyond His536 because the gene sequence indicated the existence of 15 extra C-terminal residues.[9] This was especially disquieting because His536 is deeply buried in the structure. This apparent problem was solved when we became aware of a paper by Menon et al. reporting the proteolytic cleavage of a 15-residue C-terminal peptide upon maturation of the large subunit of *D. gigas* [NiFe]-hydrogenase.[27] His536 corresponds to the C-terminal residue of a separated 25 residue long third subunit in the homologous cytoplasmic F_{420} nonreducing [NiFeSe]-hydrogenase from *Methanococcus voltae*, which provides two of the four protein ligands to the Ni−Fe site.[28] Interestingly, depending on selenium availability, the third subunit can be synthesized from genes coding for either Cys or SeC at the position corresponding to Cys530 in *D. gigas* hydrogenase. Higher resolution analyses of the *D. vulgaris* Miyazaki[10] and *D. gigas* enzymes (PDB deposition 2FRV) revealed the presence of a Mg ion bound to the C-terminal histidine. Because the C-terminal α-helices 16 and 17 of the large subunit are buried, upon maturation a substantial conformational rearrangement must follow the cleavage of the C-terminal peptide. This will be further discussed in section 3.

Subsequent structures of [NiFe]-hydrogenases from *D. fructosovorans* (by the Grenoble group),[11] *D. desulfuricans* (by Matias et al. in Lisbon, Portugal),[13] and the [NiFeSe]-enzyme from *Desulfomicrobium* (*Dm.*) *baculatum* (again by the Grenoble group)[12] were solved by molecular replacement, using the atomic coordinates of the *D. gigas* enzyme as a search model. All of these structures have essentially the same polypeptide fold and domain structure. Besides the substitution of the terminal *Cys530* Ni ligand (*D. gigas* numbering, given in italics from here on) by a selenocysteine, the [NiFeSe]-enzyme from *Dm. baculatum* shows some additional internal differences,[12] relative to the *Desulfovibrio* [NiFe]-hydrogenases: (1) a third $[Fe_4S_4]$ cluster replaces the mesial $[Fe_3S_4]$ cluster (Figure 1B); (2) the Mg(II) ion bound to the C-terminal histidine of the large subunit in the other enzymes is replaced by a transition metal that, from an inductively coupled plasma analysis, corresponds to a 14th iron ion—it is not known whether this substitution is functionally significant; and (3) there is a H_2S molecule bound inside a cavity near the active site. There are also differences at the enzyme surface. For example, the large subunit stretch between α-helices 4 and 7 is much shorter in the *Dm. baculatum* enzyme and contains only one α-helix, instead of the three observed in the other structures (Figure 1B). A comparison of active site structures is given in Figure 2. A 2.54 Å resolution analysis of *D. gigas* [NiFe]-hydrogenase revealed the presence of three elongated electron density peaks connected to the active site Fe ion.[26] Previous FTIR spectroscopic studies using *Chromatium vinosum* [NiFe]-hydrogenase, now *Allochromatium* (*A.*) *vinosum*, had indicated the presence of three intrinsic high-frequency bands that shifted as a function of changes in the redox state of the enzyme.[29,30] On the basis of isotopic labeling experiments with ^{13}C and ^{15}N, these bands were assigned to two cyanides and one carbon monoxide.[31] As the same FTIR bands were found in the *D. gigas* enzyme we proposed that they corresponded to the three iron diatomic ligands found in our electron density maps and named L1, L2, and L3.[26] L3, sitting in a hydrophobic pocket, was tentatively assigned to CO, whereas L1 and L2, which were hydrogen-bonded to the protein (Figure 2), were modeled as CN^- ligands.[32] The

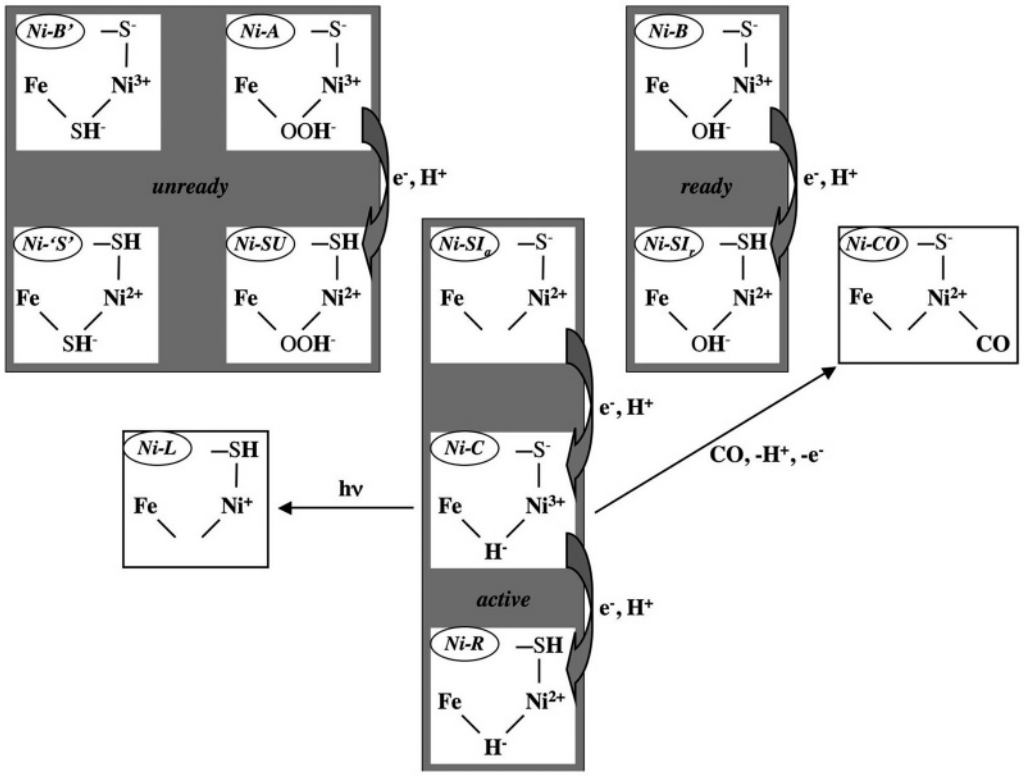

enzyme state	description	alternative name
Ni-A	unready oxidized	Ni_u*
Ni-SU	unready reduced	Ni_u-S
Ni-B	ready oxidized	Ni_r*
Ni-SI$_r$	ready reduced	Ni_r-S
Ni-B'	Na_2S-induced	-
Ni-'S'	idem, diamagnetic	-

enzyme state	description	alternative name
Ni-SI$_a$	active, most oxidized	Ni_a-S
Ni-C	active, paramagnetic	Ni_a-C*
Ni-R	active, most reduced	Ni_a-SR
Ni-L	light-induced,	Ni_a-L*
Ni-CO	CO-induced	Ni_a-SCO

Figure 3. Overview of stable Ni−Fe intermediates with observed and/or suggested hydrogen/inhibitor binding sites and Ni oxidation states. Different nomenclatures are tabulated. For some intermediates, two or more protonation states have been characterized.

two cyanide bands have been found to correspond to vibrationally coupled species.[33]

Initially, there was a controversy concerning the nature of the diatomic iron ligands (Figure 2). In the 1.8 Å resolution structure of the *D. vulgaris* Miyazaki enzyme a strong electron density peak at L1 was assigned to SO, an assumption that was supported by the results of pyrolysis mass spectrometry experiments.[10] The remaining L2 and L3 ligands were assigned to a mixture of CO and CN^-. This model has not been found in any of the other structures,[12,13,26,34] where the electron densities of the three diatomic ligands are very similar. The origin of the strong L1 electron density in the first *D. vulgaris* Miyazaki hydrogenase structure remains unclear as recent high-resolution crystal structures of this enzyme do not show any significant differences between the electron densities of L1, L2, and L3.[35,36] Furthermore, a recent detailed FTIR study has confirmed that this enzyme also contains a $Fe(CN)_2CO$ unit.[37]

The Ni−Fe active site contains two *cis* Ni coordination sites available for substrate binding: a bridging site called E2 and a terminal Ni site called E1 (Figure 2). In this respect, [NiFe]-hydrogenases resemble two other Ni−Fe enzymes that can function in tandem: carbon monoxide dehydrogenase and acetyl-coenzyme A synthase.[38] Air-exposed, oxidized [NiFe]-hydrogenase preparations typically contain two inactive paramagnetic states: one that is called ready because it can be easily activated and another called unready, which can be reductively activated only after an extended period of time (see also Figure 3).[39] The corresponding EPR signals have been called Ni-B and Ni-A. In the initial oxidized [NiFe]-hydrogenase crystal structures E2 seemed to be occupied either by an oxo ligand[26] or by sulfur.[10,13] More recently, we and others have provided crystallographic

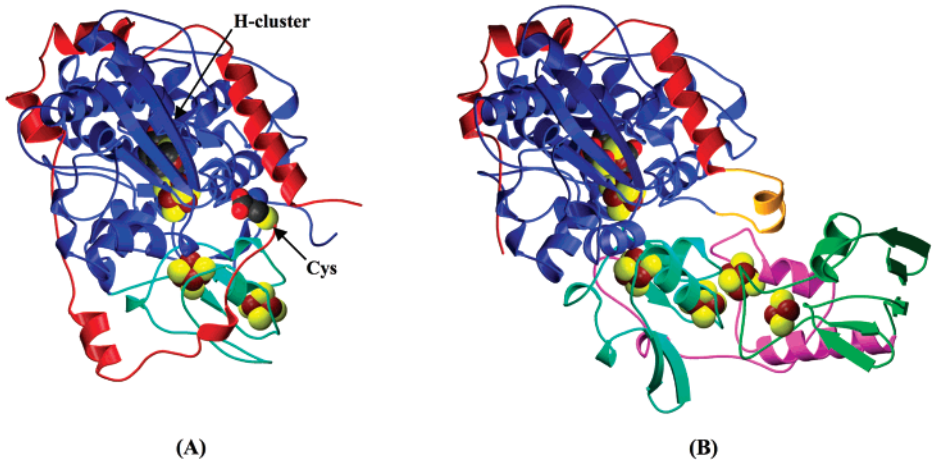

Figure 4. Ribbon depiction of the three-dimensional structures of (A) *D. desulfuricans* (Dd) and (B) *C. pasteurianum* I (CpI) [FeFe]-hydrogenases. FeS clusters are shown as yellow (S) and brown (Fe) spheres; O, N, and C atoms are red, blue, and black spheres, respectively. Other color codes are, for the Dd enzyme, blue, large subunit; red, small subunit; light blue, ferredoxin-like domain. A bound putative cysteine molecule (Cys) is also shown. Topologically equivalent regions of CpI hydrogenase are shown with the same color codes. Additional domains in this enzyme are depicted in purple and green. The loop connecting the two regions equivalent to the Dd hydrogenase small and large subunits is shown in orange.

evidence for peroxide binding to E2 in the unready state.[36,40] The crystal structures of two reductively activated enzymes display no detectable electron density for the Ni E1 or E2 sites.[12,41] This observation does not rule out the possibility of hydride binding to one or both sites in the reduced active center. A hydron species most certainly binds to E1 because the competitive inhibitor CO binds to that site.[35] Possible reactions with molecular oxygen will be discussed in section 6, and the structural properties of the activated enzyme will be developed in section 8.

2.2. [FeFe]-Hydrogenase Structures and Active Sites

[FeFe]-hydrogenases are organized into modular domains (Figure 4), with accessory clusters functioning as inter- and intramolecular electron-transfer centers electronically linked to the catalytic H-cluster that is defined further below.[14,15] The modularity of [FeFe]-hydrogenases was first deduced from the amino acid sequences of *Desulfovibrio* and *Clostridium* enzymes.[42−46] The identical large subunits of the [FeFe]-hydrogenases from *D. desulfuricans* (Dd) and *D. vulgaris* Hildenborough (DvH) consist of a ferredoxin-like domain containing two [Fe_4S_4] clusters and the highly conserved catalytic domain.[14,42] The small subunit of these enzymes cannot be considered as a classical domain because it encircles the large subunit as a belt (Figure 4A) and is structurally equivalent to the C-terminal tail of the single-chain cytoplasmic hydrogenase I from *C. pasteurianum* (CpI; Figure 4B).[10,47] In the Dd hydrogenase the N-terminal stretch of the small subunit lies close the C-terminal end of the large subunit, and both regions are stabilized by a bound cysteine; in the single-chain CpI hydrogenase these two parts are connected and form a loop (Figure 4).

In general, clostridial [FeFe]-hydrogenases are monomeric enzymes containing up to four FeS centers in addition to the catalytic Fe−Fe and proximal clusters (collectively called the H-cluster).[15,43,48−50] There are further examples of multisubunit hydrogenases: the NAD(P)H-dependent [FeFe]-hydrogenases from *Thermotoga maritima* and *Thermoanaerobacter tengcongensis* consist of three and four subunits, respectively.[51,52] The EPR spectra of purified catalytic subunits from these thermophilic organisms indicated the presence of H- and ferredoxin-like clusters. On the other hand, the simplest [FeFe]-hydrogenases are the ones isolated from algae as they contain only the H-cluster and no extra FeS centers.[53−56]

The two initial structural reports (Figure 5A,B) revealed the H-cluster as being composed of (1) a binuclear Fe−Fe cluster with two diatomic ligands bound to each of the metal centers, and three bridging ligands between them consisting of two sulfur atoms and a small molecule and (2) a standard [Fe_4S_4] cluster connected to the Fe−Fe center by the thiolate of a cysteine residue.[14,15] However, both models were not completely right: in CpI hydrogenase, the four terminally bound diatomic molecules were modeled as CO, although FTIR spectroscopy had indicated the presence of two COs and two CN^-s.[57] In addition, a fifth diatomic ligand was modeled as a bridging CO, whereas the bridging sulfur ligands were modeled as labile S^{2-} and a water molecule was placed between them; a second water molecule was modeled as a ligand to the distal Fe (Figure 5B). In the Dd enzyme the small Fe−Fe bridging ligand was modeled as water (Figure 5A). By comparing the two active site structures, a consensus model could be built.[47] In this model each Fe center is ligated by a CO and a CN^-, which were assigned on the basis of their environments: the COs sit in hydrophobic pockets, whereas the CN^-s establish hydrogen bonds with the protein. The small bridging ligand is an additional CO, and the bridging sulfurs belong to a small organic molecule, initially modeled as 1,3-propanedithiolate (Figure 5A). Some of the original differences probably arose from dissimilar redox states in the crystals and oxidative damage. Although the CpI hydrogenase crystals were grown in the presence of dithionite, the initial structure most likely reflects the anaerobically oxidized Hox ($g = 2.10$) enzyme. This is suggested by FTIR spectroscopic results that assigned a bridging CO to that state.[57,58] On the other hand, in the original Dd structure, it is highly likely that the small "monatomic" ligand resulted from a mixture of bridging and terminally bound CO in the crystal. This conclusion is supported by the structure of the reduced Dd enzyme, where the bridging CO ligand becomes terminally bound to the distal Fe, an observation that is consistent with FTIR studies (Figure 5C).[58] Another important result concerning the

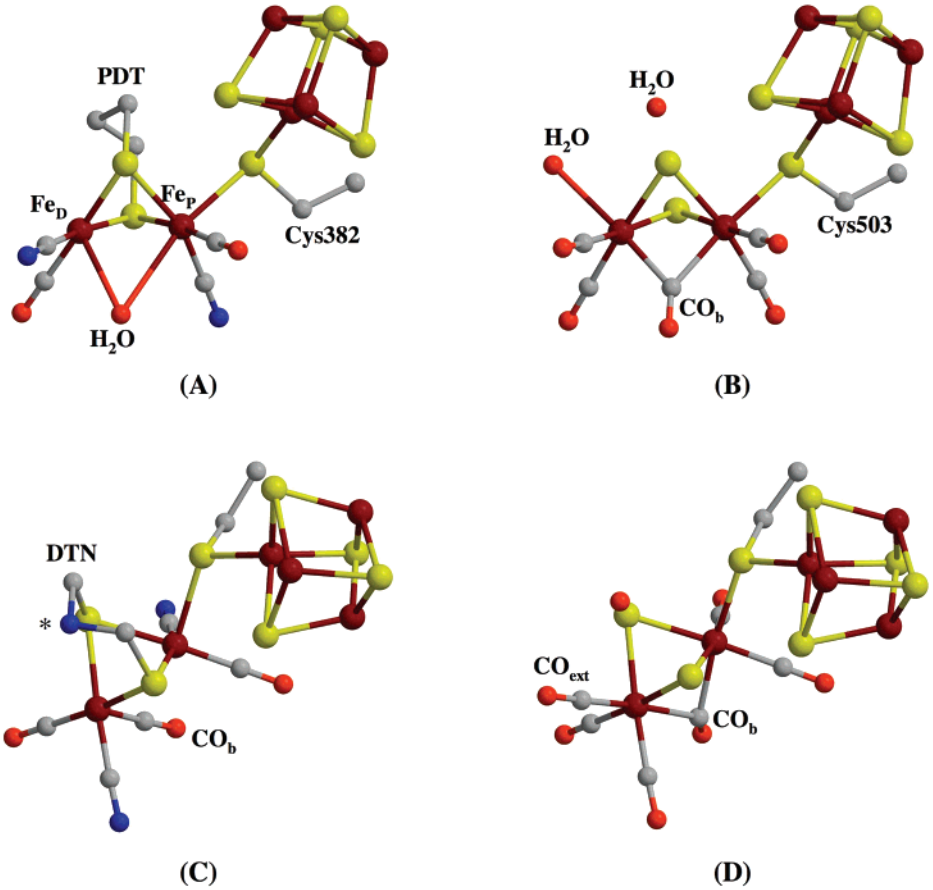

Figure 5. Active site of [FeFe]-hydrogenases: **(**A**)** initial model from *D. desulfuricans* (Dd); **(**B**)** initial model from *C. pasteurianum* hydrogenase I (CpI); **(**C**)** reduced active site in Dd; **(**D**)** CO complex in CpI. Abbreviations: PDT, 1,3-propanedithiolate; DTN, di(thiomethyl)-amine; CO_b, internal bridging CO ligand; CO_{ext}, external CO ligand. See text for further details.

hydrogenase active site is the structural characterization of the complex that it forms with added CO (Figure 5D).[59] As could be expected from the presence of a tunnel connecting the active site to the enzyme surface (section 6.4),[14] extrinsic CO binds to the available coordination site at the distal Fe (Fe_D), which is, most likely, where hydrogen also binds (see below).

Although the small organic molecule was originally modeled as a propanedithiolate, mechanistic considerations suggested that it would make more sense if the bridgehead atom was nitrogen (Figure 5C).[58] A secondary amine would be ideally placed to extract the proton resulting from the heterolytic cleavage of molecular hydrogen. Furthermore, there is a very convincing proton-transfer pathway leading from the small molecule central atom to the hydrogenase surface via a cysteine side chain (section 5.2). Model chemistry supports the N assignment.[60] Evidence for two nitrogen-containing ligands at or near the Fe−Fe cluster has been obtained from ENDOR and ESEEM spectroscopies.[61−63] One signal is reminiscent of a histidine imidazole nitrogen atom. The other has been assigned to a CN^- ligand on the basis of FTIR spectroscopic results indicating the presence of high-frequency bands in DvH hydrogenase.[63,64] The source of the imidizole-like nitrogen remains to be determined as no histidine residue is found near the active site. This N could then correspond to the bridgehead atom in the small molecule (Figure 5C).

3. Hydrogenase Maturation

As stated in the Introduction, the three types of hydrogenases are metalloenzymes, and they represent one of the most intriguing examples of convergent evolution. Although their amino acid sequences are completely unrelated and the metal centers have different architectures and compositions, they share one unique property, namely, CO coordination to an active site low-spin Fe.[5−7] In addition, both the [NiFe]- and [FeFe]-enzymes have CN^- ligands bound to Fe in the active site. The formation of these metal centers and their integration into the apoprotein follow a complex pathway and require the participation of accessory proteins with novel biochemical roles.

Maturation of [FeFe]-hydrogenases appears to require a minimum of three auxiliary proteins, two of which belong to the class of radical *S*-adenosylmethionine (SAM) enzymes[65] and the other, which is also a metalloprotein, to the family of GTPases.[66] They are considered to be sufficient to generate active enzyme when their genes are coexpressed with the structural genes in a heterologous host, otherwise deficient in [FeFe]-hydrogenase expression. On the other hand, maturation of the large subunit of [NiFe]-hydrogenases depends on the activity of at least seven core proteins that catalyze the synthesis of the CN/CO ligands and have a function in the coordination of the active site iron, the insertion of nickel and the proteolytic maturation of the large subunit. In contrast, no information is available yet for the maturation of the [FeS] cluster-free enzyme class.

3.1. Maturation of [NiFe]-Hydrogenases

The maturation process can be divided into several steps: (1) synthesis of the apoenzyme, (2) transport and storage of nickel and iron, (3) ligand synthesis and partial active site assembly, and (4) insertion of nickel, proteolysis of a

C-terminal amino acid stretch, and folding of the nascent C-terminal region into the rest of the large subunit. The FeS clusters are assembled by the general purpose Isc proteins.[67] Step 1 depends on the environment. For instance, under anaerobic conditions, *Escherichia coli* can undergo a major reorganization of its metabolism mediated by the expression of over 300 genes.[68] If hydrogen is present, some microorganisms can sense it due to a cytoplasmic hydrogenase-like regulatory H_2-sensor protein, as reviewed by Vignais and Colbeau.[69] A kinase and a DNA-binding protein complete a signaling pathway that results in the expression of [NiFe]-hydrogenase structural genes.[69] Step 2, iron and nickel transport, is highly regulated in microorganisms because of the toxic effects of these metal ions, for example, through Fenton chemistry (Fe) and glutathione depletion (Ni).[70] In *E. coli*, an ABC transporter coded by the *nik* operon is responsible for nickel transport, a process regulated by another DNA-binding protein of known three-dimensional structure called NikR.[71] Iron transport depends on the synthesis of small molecules called siderophores, and this may also be the case for nickel.[72] In the more complex steps 3 and 4, the active site ligands have to be synthesized and the active site has to be assembled and inserted in the large subunit. This process is under the control of the six genes from the *hyp* operon and a nickel-dependent protease.[73]

3.1.1. CN^- Synthesis

In 1984, Barret and co-workers noticed that inactivation of carbamoylphosphate synthase (PyrA) abolished hydrogenase activity in *Salmonella typhimurium*, although the reason for this was not further investigated.[74] More recently, Paschos et al. have shown that CN^- synthesis in *E. coli* depends on two gene products, HypE and HypF.[75] HypF is an 82 kDa protein that has amino acid sequence homologies to eukaryotic acylphosphatases in its N-terminal region and to *O*-carbamoyltransferases at its C-terminal stretch.[76] The amino acid sequence homology of the N-terminal domain of HypF to acylphosphatases has been more recently extended to its three-dimensional structure.[77] HypF hydrolyzes carbamoyl phosphate (CP) and transfers the carbamoyl group to the C-terminal Cys of HypE. There is experimental evidence that HypF forms a complex with HypE.[78−80]

HypE is a 35 kDa monomeric protein with an amino acid sequence similar to those of aminoimidazole ribonucleotide synthase (PurM) and selenophosphate synthase (SelD).[81] PurM catalyzes the dehydration of aminoimidazole ribonucleotide in an ATP-dependent manner. The ATP-binding motif is conserved in HypE. In addition, HypE has a C-terminal cysteine.[82]

The process of CN^- synthesis can be summarized as follows: HypF transfers carbamoyl to the HypE C-terminal cysteine, where it is dehydrated to form a HypE−SCN complex, which has been identified by mass spectrometry. Subsequently, HypE donates a CN^- to the nascent Fe unit of the hydrogenase active site.

3.1.2. CO Synthesis

It was originally thought that CO was also synthesized from CP.[75] However, this idea has been discarded by recent experiments using $^{13}CO_2$ in which only CN^- was labeled (CO_2 is a CP precursor). Because CO was not labeled, its synthesis must follow a different pathway (Lenz et al.; Forzi et al.; Workshop on Biohydrogen, February 21−23, 2007, Berlin, Germany). Roseboom et al. have suggested that this ligand may be synthesized from acetate or one of its precursors.[83]

3.1.3. HypC and HypD Are Involved in Iron Coordination

HypC interacts very strongly with both the hydrogenase large subunit and with HypD. HypC is a 9.6 kDa protein with a CxxxP motif in its N-terminal region.[84] HypD is a 41.4 kDa protein that has a $[Fe_4S_4]$ cluster.[83,85] The HypCD complex is not detected in the presence of citrulline, a CP source. In the absence of nickel, HypC forms a complex with the hydrogenase large subunit (HycE). It is thought that the HypCD complex gets the CN^- ligands from HypE and then transfers them to the hydrogenase, a notion that is supported by the fact that a HypCDE complex has been characterized.[85] However, the mechanism by which CN^- ligands are transferred to the prospective active site Fe has not been elucidated. Also, it is not clear whether the Fe ion comes from the $[Fe_4S_4]$ cluster in HypD or from some other source. The HypC−preHycE complex is stable under reducing conditions but it dissociates in the presence of alkylating agents. This supports the notion that HypC forms a covalent complex with the hydrogenase large subunit through its C-terminal cysteine.[84] It is thought that iron insertion precedes nickel insertion and that the former binds hydrogenase as a $FeCO(CN)_2$ unit. Nickel is also required for the dissociation of the HypC−preHycE complex.

3.1.4. Ni Insertion: HypA, HypB, and SlyD

The implication of HypB in nickel transport/insertion has been shown in a $HypB^-$ mutant, which lacked hydrogenase activity. However, the enzymatic activity could be restored by adding nickel to the growth medium, suggesting that HypB is not absolutely required for nickel insertion.[86] If zinc is added instead of nickel, the former replaces the latter, but there is no proteolytic maturation because the protease activity is nickel-specific.[87,88] The structure of the protease from *M. jannaschii* has been determined very recently.[89] Similar GTPases are required for nickel insertion in CO dehydrogenase and urease.[90,91] Some HypBs have a histidine-rich stretch at their N terminus, which may serve as a reservoir for nickel ions. If this region is deleted, HypB can bind only one Ni ion per protein molecule.[92] Downstream of the histidine-rich sequence, the N-terminal region of *E. coli* HypB has the CxxCGC motif, which corresponds to a high-affinity Ni-binding site.[93] However, this binding site is not essential for nickel insertion into hydrogenase. On the other hand, mutation of residue C166 or H167 significantly affects nickel insertion.

HypA, which is specific for *E. coli* hydrogenase 3, binds one nickel ion per molecule, and it is known to interact with HypB. Although its role is not clear, it may be the component that ultimately provides nickel to HycE. The GTPase activity of HypB could then induce the conformational change required for nickel insertion by HypA. The isoform of HypA for hydrogenases 1 and 2 is called HybF.[94,95] SlyD is a proline cis/trans isomerase that interacts with HypB.[93] As in the latter, the mutation of this protein reduces hydrogenase activity, but this effect is abolished by added nickel.[96]

3.1.5. Proteolytic Maturation

The last step in the maturation process requires the proteolysis of, if present, a large subunit C-terminal extension.[95] Depending on the hydrogenase, the size of the extension varies from only 5 to as many as 32 amino acid

residues.[97] The enzyme involved in proteolysis is extremely specific, and there are as many isoforms of it as hydrogenases in a given organism. The HybD and HycI endopeptidases have been characterized, and the crystal structure of the former 17.5 kDa protein is available.[98] HybD consists of a twisted five-stranded β-sheet sandwiched between three helices on one side and two on the other. The structure contains an adventitious cadmium ion that is pentacoordinated by the carboxylate oxygens of glutamate (Glu16) and aspartate (Asp62) side chains, the imidazole nitrogen of a histidine (His93), and a water molecule. The as-purified HybD and HycI proteins do not contain metal,[98,99] and in vitro they cleave their substrates only when nickel is added. From this observation and the fact that the enzyme activity is insensitive to standard protease inhibitors,[100,101] it has been concluded that HybD recognizes nickel bound to the large subunit precursor and that in the crystal structure cadmium occupies the physiological nickel-binding site.[101]

Depending on the hydrogenase, the maturation endopeptidase proteolytic site is found between either His or Arg and a nonpolar residue such as Met, Ile, Val, or Ala. Extensive amino acid replacement studies have shown that this relative conservation is not a strict requirement, as most of the exchanges at these sites do not block proteolysis. From this, it is tempting to conclude that it is the nickel ion in the large subunit precursor which determines the properties of the cleavage site in a regiospecific manner.[97,101,102] Almost two-thirds of the C-terminal 25-residue extension of *E. coli* hydrogenase 3 can be removed by site-directed mutagenesis without affecting either cleavage or subunit maturation; however, truncations beyond this critical size strongly reduce precursor stability.[97] It should also be mentioned that some [NiFe]-hydrogenases do not have a C-terminal extension in the large subunit, so they do not require proteolytic processing. Examples are cytoplasmic H_2 sensors and energy-converting hydrogenases.[69]

3.2. Maturation of [FeFe]-Hydrogenases

To date, only three strictly conserved [FeFe]-hydrogenase maturation proteins, HydE, HydF, and HydG, have been identified.[65,103] However, additional proteins, such as TM1420 in *T. maritima*, may also be involved in the maturation of the more complex [FeFe]-hydrogenase from this organism.[104] The HydE and HydG [FeFe]-hydrogenase maturases contain the CxxxCxxC motif that is characteristic of the AdoMet radical protein superfamily. Lysine 2,3-aminomutase (LAM) was the first AdoMet radical enzyme to be reported in seminal experiments carried out by Barker and co-workers in 1970.[105,106] AdoMet radical proteins were recognized as a protein superfamily when advanced sequence profiling methods demonstrated that over 600 proteins involved in diverse cellular processes share significant sequence similarity, including the CxxxCxxC motif.[107] The three cysteines of this motif coordinate a $[Fe_4S_4]$ cluster, and the methionine carboxylate and amine moieties of SAM bind to this cluster at the open iron coordination site in a bidentate fashion.[108−111] The AdoMet radical superfamily may currently be the most intensively studied group of FeS proteins, and several excellent reviews have recently appeared.[111−116]

AdoMet radical enzymes are frequently involved in metabolic pathways, cofactor biosynthesis, production of deoxyribonucleotides, incorporation of sulfur into organic substrates, and the anaerobic synthesis of unique biomolecules.[107,111−116] In addition, there is a precedent for the involvement of a putative AdoMet radical protein in the biosynthesis of metalloenzyme catalytic sites. For instance, the biosynthesis of the iron−molybdenum cofactor (FeMoco) of nitrogenase, another enzyme capable of hydrogen production, requires NifB, also a putative member of the AdoMet radical superfamily.[117] Although its enzymatic activity has not yet been determined,[118] the metabolic product of NifB, the NifB cofactor, incorporates both iron and sulfur into nitrogenase.[117] AdoMet radical proteins also serve as activating enzymes for the generation of protein radicals in anaerobic ribonucleotide reductase, pyruvate formate lyase, and benzylsuccinate synthase.

AdoMet radical enzymes are found in all three kingdoms of life. Radical generation is initiated by the one-electron reduction of AdoMet by the $[Fe_4S_4]$ cluster coordinated to the CxxxCxxC motif. This results in the cleavage of AdoMet, generating the highly reactive 5′-deoxyadenosyl radical and methionine.[119−121] The 5′-deoxyadenosyl radical then abstracts a hydrogen atom from a substrate that is positioned in close proximity to AdoMet and is unique to each subclass of AdoMet radical enzymes. The reductive cleavage of AdoMet in vitro has been observed to proceed in the absence of the appropriate substrate; however, the rate of AdoMet cleavage often increases significantly in its presence. The structures of four AdoMet radical enzymes, biotin synthase (BioB),[122] coproporphyrinogen(III) oxidase (HemN),[123] molybdopterin biosynthetic protein (MoaA),[124] and LAM,[125] have been determined. These structures demonstrate that AdoMet radical proteins share a $(\beta/\alpha)_6$ repeat in their structural core, which is described as an incomplete triosephosphate isomerase (TIM) barrel.[126] In the case of BioB, the protein contains the full $(\beta/\alpha)_8$ TIM-barrel fold. Alignments of the four AdoMet radical structures place the $[Fe_4S_4]$ cluster that coordinates AdoMet in the same location relative to the $(\beta/\alpha)_6$ core within an extended loop.[125] Although the $(\beta/\alpha)_6$ core of the AdoMet radical proteins characterized to date is similar, each protein contains unique N- and/or C-terminal regions that potentially modulate substrate access to the active site. The structural and biophysical characterization of the AdoMet radical superfamily of proteins is providing valuable insights into the properties of these enzymes. This will help elucidate the roles of HydE and HydG in [FeFe]-hydrogenase active site synthesis.

3.2.1. HydE

HydE and BioB, which is involved in S insertion from a FeS cluster during biotin synthesis, have significantly similar amino acid sequences.[127] This similarity has now been extended to their three-dimensional structures (Nicolet et al., unpublished results). An additional CxxxxxxxCxxC motif that is not conserved in all of the HydE gene sequences binds a second FeS cluster.[128] Under reducing conditions, the reconstituted recombinant HydE can cleave AdoMet. This enzyme may be involved in the synthesis of the diatomic ligands CO and CN^-, but this has not been supported by soaking experiments using HydE crystals (unpublished results). At any rate, HydE does not bind glycine, a hypothetical precursor of these ligands[129] (Nicolet et al., unpublished results).

3.2.2. HydF

The deduced amino acid sequence of HydF indicated that it should have GTPase activity at its N-terminal region and that it binds a FeS cluster at its C-terminal stretch.[65,66,103,130]

Table 1. Hydrogenase Redox Partners

EC no.[a]	enzyme type(s)	redox partner	catalyzed reaction
1.12.1.2	[NiFe], [FeFe]	NAD^+	$H_2 + NAD^+ \leftrightarrow H^+ + NADH$
1.12.1.3	[NiFe], [FeFe]	$NADP^+$	$H_2 + NADP^+ \leftrightarrow H^+ + NADPH$
1.12.2.1	[NiFe(Se)], [FeFe]	cytochrome c_3	$2H_2 + cyt\text{-}c_3(ox) \leftrightarrow 4H^+ + cyt\text{-}c_3(red)$
1.12.5.1	[NiFe]	quinone	$H_2 +$ menaquinone $\leftrightarrow$ menaquinol
1.12.7.2	[NiFe], [FeFe]	ferredoxin	$H_2 + Fd(ox) \leftrightarrow 2H^+ + Fd(red)$
1.12.98.1	[NiFe(Se)]	coenzyme F_{420}	$H_2 + F_{420} \leftrightarrow 2H^+ + F_{420}H_2$
1.12.98.2	FeS-free	methenyl-H_4MPT	$H_2 + CH{\equiv}H_4MPT^+ \leftrightarrow H^+ + CH_2{=}H_4MPT$
1.12.98.3	[NiFe]	methanophenazine	$H_2 + Phen \leftrightarrow PhenH_2$
1.12.99.6	[NiFe]	"acceptor"	$H_2 + A \leftrightarrow AH_2$

[a] See ENZYME database: http:///www.expasy.org/enzyme/.

The FeS cluster is required for hydrogenase maturation. By analogy with other systems, HydF could be either a scaffold protein or an insertase or both.

3.2.3. HydG

This protein is similar to ThiH, which is involved in thiamin synthesis.[131] HydG has two FeS clusters that are necessary for activity.[128] It may be involved in the synthesis of the small, dithiolate-containing molecule found at the [FeFe]-hydrogenase active site.

It is difficult to establish whether additional gene products are necessary for [FeFe]-hydrogenase maturation. During heterologous expression, some proteins from the host *E. coli* could also be involved. Other open reading frames are sometimes present in the Hyd operon, such as aspartate ammonia lyase and a gene coding for a small protein of unknown function. The possible role of the former in maturation remains elusive. It is not known whether the proximal [Fe_4S_4] cluster is assembled at the same time as the active site dinuclear iron center. Very recently, McGlynn et al. have reported that when *E. coli* cell extracts lacking [FeFe]-hydrogenase activity are mixed with equivalent extracts containing HydE, HydF, and HydG, the enzyme is activated.[132] The authors suggest that the Hyd proteins act as an assembly complex.

4. Electron Transfer

Hydrogenases may be classified according to their redox partner (Table 1), which can be the same for [NiFe(Se)]- and [FeFe]-enzymes. The identity of the physiological partner depends on the location inside the cell and on the eventual complexation with another protein.[69,133] An example is the diaphorase subunit in the case of cytoplasmic bidirectional hydrogen:$NAD(P)^+$ oxidoreductases found in bacteria and archaea. Soluble periplasmic hydrogenases are hydrogen-oxidizing enzymes. The produced electrons are transferred via *c*-type cytochromes and a membrane-bound complex involving a high molecular weight cytochrome *c* (Hmc) to the cytoplasmic side of the membrane.[134,135] On the other hand, the produced protons remain in the periplasm and contribute to the formation of a transmembrane proton gradient. More common membrane-bound periplasmic hydrogenases are complexed to cytochrome *b*, allowing electron transfer to a quinone. Hydrogen-producing cytoplasmic [FeFe]-hydrogenases and membrane-bound energy-converting [NiFe]-hydrogenases exchange electrons with ferredoxin. In addition, the latter enzymes translocate protons across the cytoplasmic membrane.[136] Electron carriers such as coenzyme F_{420} (a deazaflavin) and methanophenazine are found only in archaea.[137] Unlike other hydrogenases, FeS-free hydrogenases do not catalyze the reduction of artificial dyes, reducing only their specific methanopterin cofactor.[2] A detailed review on hydrogenase diversity is provided elsewhere in this issue.[138] Here we will review only those electron-transfer pathways and complexes for which structural information is available.

4.1. [NiFe(Se)]-Hydrogenases

All of the [NiFe(Se)]-hydrogenase structures solved so far are from periplasmic uptake enzymes found in sulfate-reducing bacteria. In [NiFe]-enzymes from *Desulfovibrio* species, electrons are transferred from the active site to the redox partner via a proximal [Fe_4S_4], a mesial [Fe_3S_4], and a distal [Fe_4S_4] cluster (Figure 1). The center-to-center distance between consecutive redox centers in this pathway is about 12 Å, adequate for electron transfer.[139,140] The mesial location of the [Fe_3S_4] cluster is surprising because it has a redox potential much more positive than that of hydrogen oxidation[141] and, consequently, it is predominantly in its reduced state during enzyme turnover. Direct electron transfer from the proximal to the distal [Fe_4S_4] cluster could be difficult, given the 20 Å long intercluster distance. On the other hand, electron transfer from the active site to the distal cluster needs to be efficient because only the latter is exposed to the molecular surface. Indeed, when the histidine ligand of the distal cluster is replaced by either cysteine or glycine in *D. fructosovorans* [NiFe]-hydrogenase, hydrogen uptake drops by about 2 orders of magnitude.[142] Although uphill electron transfer may be fast enough, reduction of either the proximal or the distal [Fe_4S_4] cluster could cause a transient drop in the redox potential of the [Fe_3S_4] cluster, increasing its electron-transfer efficiency.

It was possible to further investigate the role of the [Fe_3S_4] mesial cluster by converting it to a [Fe_4S_4] center in the *D. fructosovorans* [NiFe]-hydrogenase.[143] Amino acid comparisons with the [NiFeSe]-enzymes, where the mesial center is naturally replaced by a [Fe_4S_4] cluster,[12,144] showed that that could be accomplished by replacing a proline residue facing the empty Fe site of the [Fe_3S_4] cluster by cysteine. Although the mutated and the native enzymes were equally active, the former was also more air-sensitive (section 6). These results indicate that internal electron transfer is not rate limiting. The reaction rate must then depend on either substrate access to the active site (section 6.2), hydrogen heterolytic cleavage (section 8), proton transfer to the solution (section 5), or external electron transfer. In fact, studies using different electron acceptors suggest that their interaction with hydrogenase defines the catalytic rate.[145] A puzzling result was obtained with the conversion in *M. voltae* [NiFeSe]-hydrogenase of its mesial [Fe_4S_4] to a [Fe_3S_4] cluster. The mutation increased the redox potential of the cluster by 400 mV but did not significantly change the enzymatic activity when

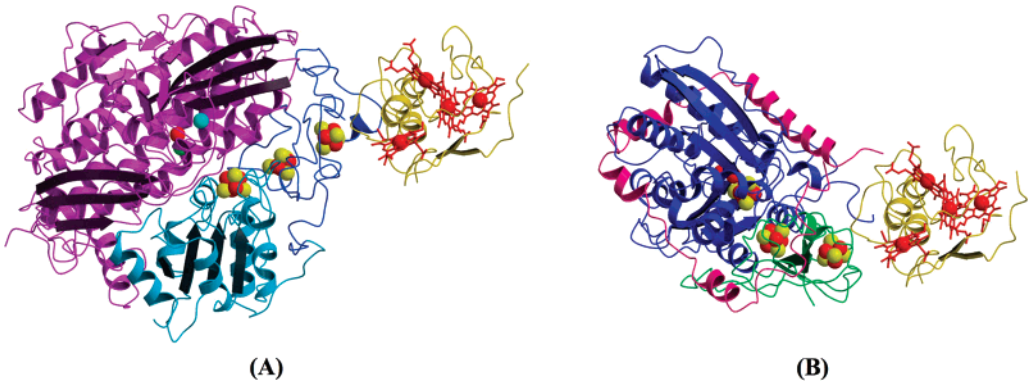

Figure 6. NMR-constrained docking of cytochrome c_3 to hydrogenase structures: **(A)** [NiFe]-hydrogenase (PDB code 1H2A, 1J0O for c_3), after Yahata et al.;[153] **(B)** [FeFe]-hydrogenase (PDB code 1HFE, 2CTH for c_3), after ElAntak et al.[160]

benzylviologen was used as the electron acceptor. However, for unclear reasons, it resulted in a 10-fold drop in activity when the physiological redox partner, F_{420}, was used instead.[144] One possible explanation is that the dye can bypass the mutated cluster and accept electrons directly from either the proximal cluster or the active site, whereas F_{420} cannot. A crystal structure of this archaean hydrogenase is unfortunately lacking.

The presence of specific redox partner recognition sites is illustrated, for example, by the crown of acidic residues surrounding the His ligand of the distal [Fe_4S_4] cluster in *Desulfovibrio* sp. [NiFe]-hydrogenases.[9] This crown most likely interacts with positively charged patches, which surround one of the hemes on soluble *c*-type cytochromes.[146] At any rate, the electron-transfer complex is probably short-lived, considering the relatively high binding K_m values. For example, cytochrome c_3 binding to [NiFe]-hydrogenase in *D. gigas* has a K_m of 7.4 μM.[147] Such type I basic cytochromes subsequently transfer electrons to membrane-bound redox complexes via a type-II (acidic) cytochrome c_3,[148,149] 9-heme,[150,151] and/or 16-heme (Hmc)[134,135] cytochromes. Although all of these proteins share the cytochrome c_3 four-heme structural motif, low amino acid sequence similarities at the molecular surface explain why electron-transfer complexes are species-specific. The electrons are ultimately transferred to sulfate or a variety of different cytoplasmic terminal acceptors in the case of organisms other than sulfate-reducing bacteria.

A first theoretical model of a cytochrome c_3:hydrogenase complex from *D. desulfuricans* ATCC 27774 using the respective crystal structures and a rigid docking protocol was reported by Matias and co-workers.[13,152] The six lowest energy solutions were subjected to a molecular dynamics simulation to optimize side-chain conformations. The best solution, in energy terms, involved the interaction of a patch of six lysines, located around heme IV of the cytochrome, with four acidic residues near the hydrogenase small subunit distal cluster and two aspartates from the large subunit. However, another solution, with the closest distance between heme IV and the distal cluster and probably the fastest electron transfer, had contacts between eight basic residues from the cytochrome and nine acidic residues from the hydrogenase small subunit. This solution used residues described as a carboxylate crown in the original NiFe-hydrogenase X-ray structural publication.[9] Several low-energy complexes are likely to be involved in in vivo electron transfer. In one of the theoretical complexes obtained by Matias et al.[13] the heme II region formed an extensive contact interface with the large subunit, close to the Mg(II) ion. The authors suggested that in this (transient) complex, proton transfer from hydrogenase to c_3 could occur. This is further discussed in section 5.

Automated rigid docking approaches have limited applications because potentially important conformational changes are not explored and possible essential bridging waters and/or ions for the complex may not have been included. Docking experiments can be improved if combined with NMR data. Recently, this approach has been used to investigate the complexation of c_3 of *D. vulgaris* Miyazaki F with the periplasmic [NiFe]-hydrogenase of the same organism,[153] using the available cytochrome NMR structure[154] and the crystal structure of the enzyme.[10] Although, in vivo, different oxidation states should be involved in electron transfer, in vitro only complexes with both redox partners either oxidized or reduced were experimentally accessible. Chemical shift perturbations from the oxidized forms confirmed that the [NiFe]-hydrogenase recognizes the region around heme IV. This result makes sense because, according to electrochemical methods and NMR, this heme has the highest redox potential at pH 7.[155] The docking model with the shortest distance between heme IV and the distal cluster provides a plausible electron-transfer pathway through the conserved *His188* ligand of the cluster (*D. gigas* numbering) and *F197* (sometimes replaced by Y) to heme IV. In this solution, four conserved acidic residues from the enzyme form salt bridges with four lysines from the cytochrome (Figure 6A). A large ionic strength effect on complex formation confirmed a significant contribution of electrostatic contacts. Although the hydrogenase surface structure does not change upon reduction,[41] different chemical shift perturbations were found under oxidizing and reducing conditions. This may be due to the reduction-induced conformational change of cytochrome c_3 detected by NMR.[154] In the reduced complex, some residues between hemes I and III either showed large chemical shift differences or became undetectable. Large shift perturbations were also observed for a cysteine residue that binds heme III and for several residues scattered around heme IV. According to the authors, these results suggest that electron transfer from reduced c_3 to hydrogenase, which in vitro may act as an H_2-evolving enzyme, involves a contact interface close to heme III. As this heme has the lowest redox potential,[155] it makes sense that it should function as the electron donor. Thus, depending on the redox states of hydrogenase and the cytochrome, different hemes could be involved in electron transfer.

4.2. [FeFe]-Hydrogenases

Calculations show that the [FeFe]-hydrogenase from *D. desulfuricans*, as the [NiFe]-hydrogenases, displays a negative electrostatic potential at the region surrounding its distal [Fe_4S_4] cluster.[14] Thus, it is not surprising that type I (basic) cytochrome c_3 is likely to function as a redox partner for both [FeFe]- and [NiFe]-periplasmic hydrogenases.[156] [FeFe]-hydrogenases also contain FeS clusters that provide an electron-transfer pathway between the buried active site and the molecular surface (Figure 4). Their center-to-center intercluster distances are about 11 Å, as in many other redox enzymes. Both the cytoplasmic *C. pasteurianum*[15] and the periplasmic *D. desulfuricans* enzymes[14] have a two-[Fe_4S_4] ferredoxin-like domain not far from the H-cluster. The two clusters in this domain are called mesial (or FS4A) and distal (or FS4B). In addition, the cytoplasmic enzyme has a small domain containing a [Fe_4S_4] cluster (called FS4C) and a plant-like ferredoxin domain with a [Fe_2S_2] cluster (called FS2). FS4C has one histidine ligand that binds Fe through its Nϵ atom, unlike the histidine ligand of the distal cluster of [NiFe]-hydrogenase that uses its Nδ atom instead. Both FS2 and FS4C are located at the surface, close to the distal cluster, but at opposite sides of the enzyme. It is currently not known which of these clusters accepts electrons from ferredoxin, the physiological redox partner.

The first NMR/docking study of a redox complex involving an [FeFe]-hydrogenase was reported by Morelli et al.[157] These authors used the periplasmic enzyme from *D. desulfuricans* ATCC 7757 and cytochrome c_{553} from the same organism, which has many basic residues surrounding its single heme.[158] In their best solution, extensive electrostatic contacts occur between this basic surface and the acidic surface surrounding the distal [Fe_4S_4] cluster of the hydrogenase ferredoxin-like domain.[14] The two redox centers have a center-to-center separation of 12.3 Å, with a putative electron-transfer pathway extending from Cys38, which is a hydrogenase cluster ligand, to Cys10, which is covalently linked to the cytochrome heme. This complex is very similar to the one between cytochrome c_{553} and a two-[Fe_4S_4] ferredoxin that is homologous to the hydrogenase ferredoxin-like domain. In that case, NMR shift information could be used for both redox partners because of their small sizes.[159] In the complex with hydrogenase, the interaction surface is twice as large due to the additional involvement of the small subunit that encircles the ferredoxin domain of the enzyme.

More recently, the NMR/docking approach has been used to study the interaction of DvH [FeFe]-hydrogenase, which is identical to the Dd enzyme (see section 2.2),[46] with c_3.[160] This cytochrome transfers electrons to the membrane-bound Hmc complex.[134] Five residues near heme IV undergo chemical shift variations when the cytochrome forms a complex with either Hmc or hydrogenase. In the best docking solution, the shortest Fe−Fe distance between heme IV and the distal [Fe_4S_4] cluster of the hydrogenase is 8.8 Å (Figure 6B). The interacting surface area is comparable to the one found in the previously discussed cytochrome c_{553}:[FeFe]-hydrogenase complex,[157] but the shorter Fe−Fe distance in the complex with c_3 suggests that, for hydrogenase, c_3 may be a more efficient electron acceptor. A significant role of electrostatic interactions in complex formation is suggested by the presence of eight lysines surrounding heme IV. However, as these lysines interact only loosely with the hydrogenase, the respective oxidation states of the redox partners may be more important for complex formation.[160]

5. Proton Transfer

Protons may move through hydrogen bonds when the donor and acceptor groups have suitable pK_a values. Transfer over longer distances requires rotations and/or translations of a sufficient number of proton-carrying groups, as well as the presence of a driving force. In several enzymes, there is experimental evidence for the existence of tunneling mechanisms responsible for proton transfer,[161] but whether these play any role in hydrogenases has not been determined. At any rate, because of the long distance separating the active sites from the protein surface, efficient proton transfer should be a requirement. Potential proton-transfer pathways have not yet been investigated systematically and, besides the crystal structures, the only available experimental information for such pathways comes from a relatively small number of site-directed mutants.

5.1. [NiFe(Se)]-Hydrogenases

Several proton-transfer pathways have been proposed for [NiFe]-hydrogenases, based on the respective three-dimensional structures. In the 2.8 Å resolution structure of an oxidized form of the *D. gigas* enzyme (PDB entry 1FRV), the side chains of *His72*, *His468*, *His482*, and the C-terminal *His536*, two water molecules, and the carboxylate group of the partially exposed *Glu46* formed a plausible pathway for proton transfer from the Ni−Fe bridging *Cys533* ligand to the protein surface.[9] However, a subsequent study at 2.54 Å resolution showed that the amino acid at position 482 could not be histidine:[26] correction of the sequence showed it to be leucine instead (M. Rousset, personal communication). Moreover, an electron density peak bridging the side chains of *His536* and *Glu46* was wrongly assigned as water and corresponded in fact to the Mg(II) ion discussed above (see PDB entry 2FRV). This was also found to be the case in the 1.8 Å resolution structure of an oxidized form of *D. vulgaris* (Miyazaki) [NiFe]-hydrogenase.[10] The Mg ion could play a role in the large subunit maturation process (section 3). Because *His536*'s main role seems to be the stabilization of the C-terminal region through several bonds, it may not participate in proton transfer. By the same token it may be argued that the bridging *Cys533* may not be an ideal base for proton-transfer either. However, *His536* has been postulated to play a role in this process because it is near the active site,[10] its side chain forming a conserved hydrogen bond with the carbonyl oxygen atom of *Cys533*. A putative proton-transfer pathway to *His536* and the Mg site will be further discussed below.

In *Dm. baculatum* [NiFeSe]-hydrogenase, the SeC that is homologous to *Cys530* in the *D. gigas* enzyme is also a terminal Ni ligand. The 2.1 Å resolution crystal structure of an active, reduced form of this enzyme showed the Se atom to be within hydrogen-bonding distance of the *Glu18* carboxylate, an invariant residue in all [NiFe]-hydrogenases.[12] Both residues, together with the Ni ion, display higher temperature (*B*) factors than atoms in their immediate vicinity. This may be due to a mixture of different protonation states for these species in the crystal. Consequently, *Cys530* and *Glu18* are likely to be part of the proton-transfer pathway. Furthermore, more than one conformation has been found for the *Cys530* thiolate in oxidized forms of *D. desulfuricans* ATCC 27774 and *D. fructosovorans* [NiFe]-hydrogenase,[13,34] and similar high *B* factors for *Glu18* and *Cys530* have been found in other crystal structures. Proton

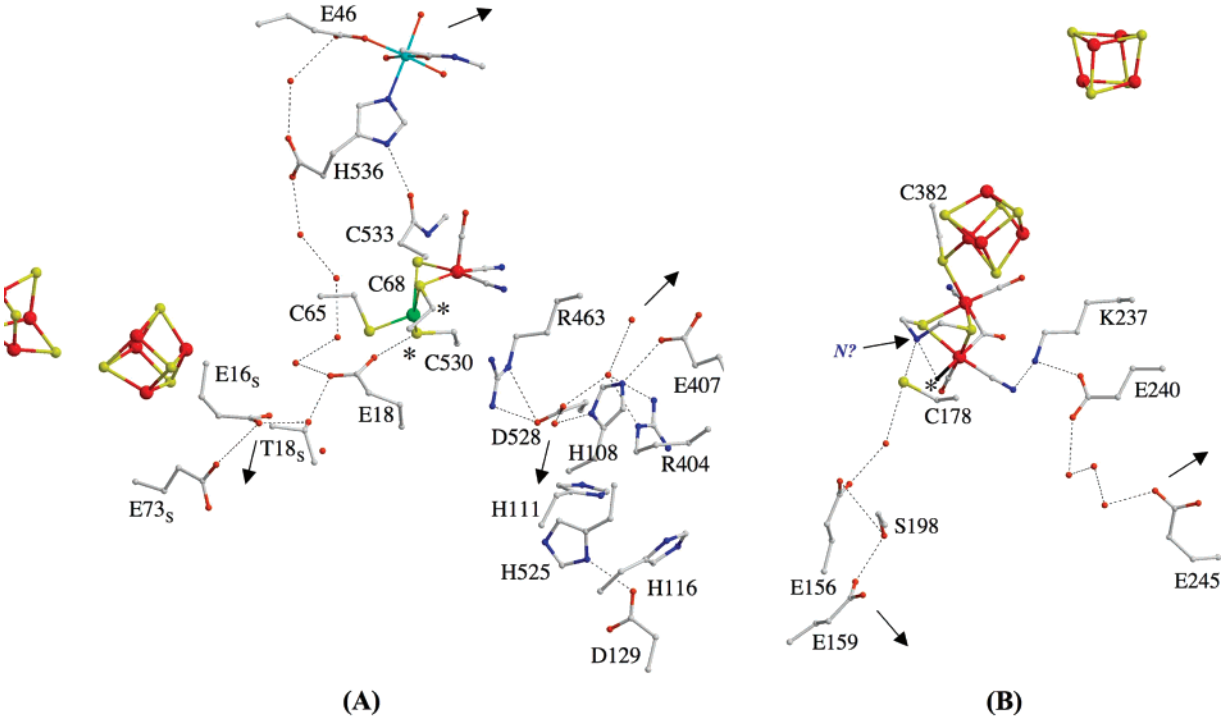

Figure 7. Putative proton-transfer pathways in the two major classes of hydrogenase: **(**A**)** [NiFe]-hydrogenase (residue numbers from the *D. gigas* enzyme); **(B)** [FeFe]-hydrogenase (residue numbers from the *D. desulfuricans* ATCC 7757 enzyme). Asterisks depict possible turnover sites, and arrows indicate proton entrance/exit sites. The "*N*?" indicates nitrogen as a putative bridgehead atom in the dithiolate-containing ligand.

transfer from a Ni site to a thiolate ligand has been documented in a model compound.[162] Mutation of *Glu18* to Gln in the *D. fructosovorans* enzyme did not modify its Ni-based EPR spectroscopic properties but completely abolished catalytic activity and H/D isotope exchange. Only the *para*-H_2/*ortho*-H_2 conversion was still possible.[163] Thus, the mutated enzyme could still perform the heterolytic cleavage of H_2 with *Cys530* acting as a probable base, but proton/deuterion exchange between the active site and solvent was blocked. This confirms the essential role of the invariant *Glu18* in proton transfer, as inferred from the crystallographic results.

The problem in defining proton transfer is that as one moves away from the active site and hence from the *Glu18* carboxylate, a multitude of pathways become plausible (Figure 7A). One of us (A.V.) noted a connection to the proximal [Fe_4S_4] cluster through hydrogen bonds successively involving the side chains of the small subunit *Thr18*, *Glu16*, and *Glu73*, which are conserved in *Desulfovibrio* species.[164] This would imply coupling of electron and proton transfers between the active site and the proximal cluster. In favor of this idea, the potential changes as a function of pH in the $[Fe_4S_4]^{2+}/[Fe_4S_4]^{+}$ and Ni−C/Ni−R redox couples[141] (Figure 3), suggesting that each reduction step is accompanied by protonation. The reduction of the cluster may provide a driving force for proton transfer from the active site. In *Dm. baculatum* [NiFeSe]-hydrogenase *Thr18* and *Glu73* are conserved but *Glu16* is replaced by glycine. However, a water molecule replaces the carboxylate group in the hydrogen-bonding network, so proton transfer should still be possible.

The Mg(II) ion is connected to the large subunit *Glu18* through four linearly disposed water molecules, the C-terminal carboxylate, an additional water molecule, and the already mentioned *Glu46* ligand. These are conserved in all of the crystal structures.[165] The Mg ion has three water ligands. Metal-bound waters may be well suited for proton transfer because they normally have lower pK_a values than bulk water. As mentioned in section 4.1, the putative pathway involving the Mg ion could be instrumental in allowing proton transfer to the redox partner, cytochrome c_3, for which one of the lowest energy docking solutions involves a contact interface close to the Mg site.[13] Electron transfer should take place in a different transient complex having a contact interface close to the distal [4Fe-4S] cluster, either with the same or with another c_3 molecule.[13] The occurrence of both proton and electron transfers would agree with the redox-Bohr effect observed for electron exchange between hydrogenase and cytochrome c_3 in *D. vulgaris* Hildenborough (DvH).[166]

Two processes could be involved in proton transfer between the four water molecules connecting *Glu18* and the C-terminal carboxylate: tunneling[161] and the so-called Grotthuss mechanism (reviewed by Cukierman[167] and by Brezinski and Ädelroth[168]). In the latter, protonation of a water molecule releases a proton at a different site, with subsequent rearrangement. However, in contrast with protons in bulk water, their counterparts in protein water networks do not always get transferred. This is illustrated, for example, by the properties of a water chain in an aquaporin channel.[169] Nearby residues with suitable pK_a values for transient protonation are also required. Whether this condition is satisfied in the proposed pathway for hydrogenase remains to be determined. As indicated above, an Fe(II) ion replaces Mg in the reduced *Dm. baculatum* [NiFeSe]-hydrogenase structure,[12] but the ion coordination sphere remains unchanged. At any rate, the change of metal ion does not seem to affect significantly the proton-transfer capacity of the enzyme. It should be noted that in some hydrogenases the C-terminal histidine is replaced by arginine, the guanidinium

group of which could replace the Mg(II) ion and form a salt bridge with the conserved *Glu46*.

Matias and co-workers have proposed a different pathway based on the crystal structure of oxidized *D. desulfuricans* ATCC 27774 [NiFe]-hydrogenase.[13] This pathway involves a significant movement of the protonated *Glu18* toward a water molecule that is bound to the conserved *Asp528*. Alternatively, the side chain of *Cys530* could rotate and transfer a proton to *Asp528* via *Arg463*. Indeed, in the crystal structures of *D. desulfuricans* ATCC 27774 and *D. fructosovorans* [NiFe]-hydrogenases,[13,34] one of the *Cys530* conformations has its Sγ at hydrogen-bonding distance from the *Arg463* guanidinium group. Beyond *Asp528*, there is a network of buried waters surrounded by several charged residues (Figure 7A). Interestingly, at least four of the concerned residues, namely, *Arg463*, *Asp528*, *His108*, and *Arg404* are not only invariant in [NiFe(Se)]-hydrogenases but are also conserved in the structure of the hydrophilic domain of *T. thermophilus* complex I,[170] the Nqo4 subunit of which is related to the hydrogenase large subunit (in other proposed hydrogenase proton-transfer pathways, only *Glu46* and the C-terminal carboxylate moiety are conserved in subunit Nqo4). Because the Ni−Fe site is replaced by a quinone-binding site in complex I, the structural similarities between the two enzymes cannot be related to catalysis. Instead, they may be due to the conservation of proton-transfer pathways that first evolved in a putative common ancestor (section 7).

5.2. [FeFe]-Hydrogenases

The case of [FeFe]-hydrogenases is simpler than that of the NiFe-enzymes because the former are smaller and, consequently, the distance between the active site and the molecular surface is shorter. Two proton-transfer pathways were initially proposed from the analysis of the crystal structures (Figure 7B). One of these pathways, based on the *D. desulfuricans* structure, starts at the cyanide ligand of Fe_D and subsequently involves two conserved residues, Lys237 and Glu240, the latter being connected through three water molecules to the nonconserved Glu245 at the protein surface.[14] In this proposition, the proton resulting from the heterolytic cleavage of H_2 would transiently bind the distal Fe_D cyanide ligand. This may not be feasible. In the alternative hypothesis, postulated on the basis of the *C. pasterianum* structure, the proton resulting from heterolytic cleavage at Fe_D would bind to a neighboring water molecule, then to *Cys178* (Dd hydrogenase numbering, *in italics*),[15] an additional water molecule, *Glu156*, *Ser198*, and *Glu159*. This proton-transfer pathway has been made more plausible due to a proposition by some of us:[58] In the first structural report of Dd hydrogenase the small organic molecule bridging Fe_P and Fe_D was modeled as a propane dithiolate.[14] However, it would make more sense if the bridgehead atom of this ligand were nitrogen because, as a secondary amine, it could be involved in the heterolytic cleavage of molecular hydrogen, be protonated on the distal Fe_D side, and then transfer the proton to *Cys178* via the well-known Walden inversion (section 8). Residues and water molecules involved in this putative pathway are conserved in the two enzymes with known crystal structures.

As a concluding remark concerning proton transfer we note that it heavily depends on the characteristics of the protein environment. The proton, being a charged species, will require stabilization through the presence of nearby residues with suitable pK_a values all along the transfer pathway. It is known that the pK_a of a residue is not constant but changes with the oxidation state of the metal centers and of the protonation state of the other residues in the structure.[171,172] Significant pK_a changes, caused even by distant variations of charges elsewhere in the structure, can inactivate a proton pathway, as exemplified by mutagenesis studies of proton pumping by *R. sphaeroides* cytochrome *c* oxidase.[168,173] These observations illustrate the difficulty in predicting proton-transfer pathways and in determining how they are regulated. There is certainly a need for additional studies on this crucial aspect of hydrogenase function. FTIR difference spectroscopy may turn out to be a powerful technique for such studies.[174]

6. Oxygen Sensitivity

Depending on their environment, microorganisms can have hydrogenases with different levels of resistance to oxygen-induced inactivation, as defined by the (ir)reversibility of inactivation by O_2 and the maximum concentration of this gas that is compatible with enzymatic activity. Understanding the structural basis of this phenomenon is a major goal in current technologically oriented hydrogenase research (see F. Armstrong's paper).[175] As discussed below, one important parameter in oxygen resistance is the narrowness of the hydrophobic tunnels connecting the active site to the molecular surface. All of the available [NiFe]-hydrogenase structures come from anaerobic bacteria and, consequently, are quite oxygen-sensitive. An exception is the [NiFeSe]-hydrogenase from *Dm. baculatum*,[12] which is not significantly inactivated by dioxygen and does not display the EPR signals that are typical of oxidized, inactive unready (Ni-A) and ready (Ni-B) states (Figure 3).[176−178] In this section we will discuss how dioxygen reacts with hydrogenases, which pathways it uses to reach the active sites, and which factors could be involved in the oxygen tolerance of both the [NiFeSe]-enzymes and the extensively studied and remarkable enzymes from *Ralstonia* Knallgas bacteria.

6.1. Oxidized Inactive States of the Ni–Fe Site and Radiation Effects

Several years ago, an orthorhombic hydrogenase crystal was used to determine the 1.8 Å resolution structure of the as-prepared *D. fructosovorans* enzyme.[179] This structure showed clear signs of radiation damage, such as reduction of a disulfide bond at the protein surface and decarboxylation of several aspartic and glutamic acid side chains.[34] The active site was characterized by *Cys530* (*D. gigas* numbering, see Figure 2A) displaying two conformations, no evidence for a significantly populated diatomic bridging species, and a small electron density peak close to the Ni−Fe bridging thiolate of *Cys68*. At that time we did not model this latter density that we attributed to noise, but recent reanalysis of the orthorhombic crystal structure using quantum refinement suggests that *Cys68* and *Cys530* are 5 and 20% modified to sulfenic acid, respectively.[180]

In contrast with the orthorhombic crystal structure, the 1.8 Å resolution structure determination of as-prepared hydrogenase using a monoclinic crystal form showed significantly fewer indications of radiation damage.[34] At this point in time, it is difficult to understand why the two structures display such different responses to radiation damage, as only standard buffers and common chemicals were used in both cases.

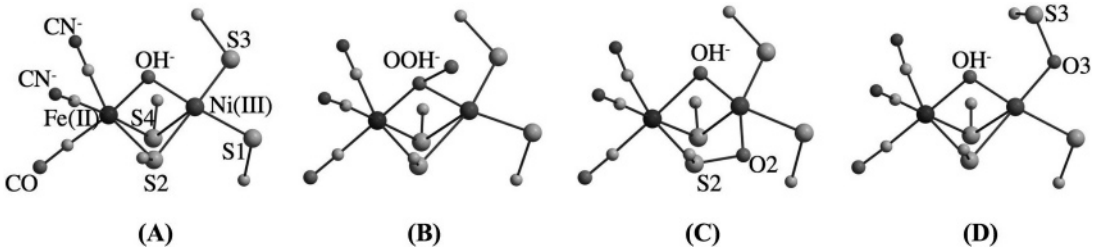

Figure 8. Oxidized forms of the Ni−Fe active site: **(**A**)** ready enzyme (Ni-B);[40] **(**B−D**)** three possible structures for unready Ni-A enzyme [**(B)** and **(C)** correspond to a mixture of states assigned to a single crystal, leading to some uncertainty in the exact atomic positions];[36,40] **(**D**)** partial structure obtained from quantum refinement of another disordered crystal.[180] Terminal and bridging cysteine ligands are labeled S1, S3 and S2, S4, respectively. Sulfenic acids are labeled O2 and O3.

Recently, we have revised the structure of the monoclinic form[40] and showed that its active site shares both an alternative conformation of *Cys530* and the partial modification of *Cys68* to sulfenic acid (about 30%) with the revised orthorhombic structure described above.[180] In addition, it also contains about 70% of a peroxide bridging species. The thiolates of the residues corresponding to *Cys68* and *Cys530* are also partially modified to sulfenates (53 and 39%, respectively) in the recent crystal structure of an unready state of *D. vulgaris* (Miyazaki) [NiFe]-hydrogenase.[36] In addition, and as in the monoclinic *D. fructosovorans* structure, there is a partially occupied peroxo ligand (59%) that bridges the Ni and Fe ions.

Thus, in all of the recent crystal structures containing oxidized unready enzyme, the active site displays a mixture of species. It seems to be fairly well-established that the ready Ni-B form corresponds to Ni(III) with a bridging hydroxo ligand (Figure 8A).[29,181,182] In the crystal structure of as-prepared enzyme, the peroxo oxygen atom closer (proximal) to the Fe ion refines to higher occupancy than the distal one, indicating that the proximal site is occupied by a (hydr)oxo ligand in a significant fraction of the hydrogenase molecules. Therefore, compared to the Ni-B form, the structures of the unready Ni-A and Ni-SU states (see Figure 3) are less well defined with both the peroxo ligand and cysteine sulfenates being, in principle, possible components (Figure 8B−D).

At room temperature, reaction of partially reduced hydrogenase with molecular oxygen most likely produces a (hydro)peroxo bridging species according to

$$O_2 + \text{Ni(II)} + e^- + H^+ \rightarrow \text{Ni(III)}-\text{OOH}^- \qquad (1)$$

The electron in reaction 1 is thought to come from the oxidation of the $[Fe_3S_4]^0$ cluster. The resulting (hydro)peroxo ligand can react with a cysteine ligand to give a bridging (hydr)oxo plus a sulfenate species according to

$$\text{Ni(III)}-\text{OOH}^- + \text{Cys-S}^- \rightarrow \text{Ni(III)}-\text{OH}^- + \text{Cys}-\text{SO}^- \qquad (2)$$

In a previous crystallographic publication[40] it was argued that the (hydro)peroxo bridging species, with an occupancy of about 0.70, was responsible for the Ni-A EPR signal. It was also suggested that Ni-SU could correspond to Ni(II)−OH^-/Cys−SO^- because ENDOR results from Carepo et al. indicated that after the oxidation of the Ni-C state by air, the labeled oxygen atom of $H_2{}^{17}O$ from the solvent medium is bound to Ni in the Ni-A form.[183] It was thought then that Ni(II)−OH^-/Cys−SO^- was more likely to exchange with solvent $H_2{}^{17}O$ than Ni(II)−OOH^-/Cys−S^- but, as we will argue below, this may not be the case. Because $^{17}O_2$ also modifies the EPR spectra of the oxidized states of hydrogenases,[184] it was implicitly necessary to invoke the oxidation of Ni(II)−OH^-/Cys−SO^- (Ni-SU) to yield Ni(III)−OOH^-/Cys−S^-(Ni-A),[40] that is, the reverse of reaction (2). However, although the reactivity of sulfenates seems to be significantly dependent on the microenvironment,[185] the equilibrium of reaction 2 should lie far to the right because S−O bonds are stronger than O−O bonds. Thus, according to a recent DFT analysis of [NiFe]-hydrogenase, the ΔG^0 of reaction 2 is about −180 kJ/mol.[180] Not surprisingly, in many biochemical reactions involving CysS−OH intermediates, these decay by forming the stronger CysS−SCys bond.[185] On the basis of these observations, we now conclude that in the hydrogenase active site the (hydro)peroxo ligand represents a species that is stable in air and observable by X-ray crystallography because the activation energy is too high to completely displace the reaction to the right side of eq 2.

Another possibility would be that Ni-A is Ni(III)−OH^-/Cys−SO as suggested by its higher stability, according to DFT calculations.[180] However, there are problems with this interpretation. For instance, it is difficult to explain why, if the Ni-A form corresponds to Ni(III)−OH^-/Cys−SO^-, its OH^- ligand does not exchange with solvent $H_2{}^{17}O$.[183] Also, the peroxo ligand is the major component in two independently determined structures,[36,40] which are known to contain a large fraction of unready enzyme.

In summary, the Ni-A signal most probably arises from a Ni(III)−OOH^-/Cys−S^- species, which corresponds to the major component in as-prepared, relatively X-ray undamaged, hydrogenase crystals. However, and because of the problems with the reversibility of eq 2, it is difficult to conclude that Ni-SU could correspond to Ni(II)−OH^-/Cys−SO. An alternative model for Ni-SU is Ni(II)−OOH^-/Cys−S^- and it is more likely that the sulfenate species represent dead enzyme as hinted by the fact that anaerobically purified hydrogenases display significantly higher activity than reactivated, aerobically purified ones.[40] Also, sulfenic acid formation according to reaction 2 might explain the gradual irreversible enzyme inactivation that is observed in electrochemical studies.[186,187] Indeed, there is a fraction of enzyme activity that is unrecovered after O_2 treatment and which is not accounted for by film loss, as determined by comparison with anaerobic control experiments.[187] An −SO ligand will stabilize the lower accessible redox state of Ni, in this case Ni(II), because sulfenate is a less good σ donor than thiolate.[188]

It remains to be explained how, if the Ni-A and Ni-SU states are Ni(III)−OOH^-/Cys−S^- and Ni(II)−OOH^-/Cys−S^-, respectively, an oxygen atom from either $H_2{}^{17}O$ or $^{17}O_2$ can be found in the peroxo ligand.[183,184] A possibility is provided by the following reaction, analogous to the reported

exchange reaction of peroxide with water in the model heme catalyst, microperoxidase-8:[189]

$$\mathrm{Ni(II)-OOH^- - Fe(II) + e^- + H^+ \rightarrow Ni(III)-O^{2-} - Fe(II) + H_2O \rightarrow Ni(II)-OOH^- - Fe(II) + e^- + H^+} \quad (3)$$

The (hydro)peroxo-containing species is obtained from eq 1, and the bridging ligand will be labeled if this reaction is carried out in the presence of $^{17}O_2$. Conversely, if activation is carried out in the presence of $H_2{}^{17}O$, the labeled oxygen atom could exchange according to eq 3. Again, the electron should come from the oxidation of $[Fe_3S_4]^0$. This reaction nicely explains the absence of $H_2{}^{17}O$ exchange in the Ni-A state because it has no electrons available to form a Ni(III)−Fe(II) oxide. According to the active site structures of unready hydrogenase, both oxygen atoms of the peroxo ligand are close to Ni, explaining the previous $^{17}O_2$ EPR and $H_2{}^{17}O$ ENDOR spectroscopic results.

The possibility of O exchange between H_2O and a peroxo ligand has already been evoked by Lamle et al.[190] Their recent electrochemical results suggest that in the activation process the unready Ni-A state is first reduced to Ni-SU and subsequently undergoes a slow, reversible step to a novel transient P state. This state does not oxidize to Ni-B, so it cannot correspond to a ready Ni-SI form. Lamle et al. have suggested that the reversible step could consist of proton transfer to, or a rearrangement of, the oxygen-derived active site ligand. Addition of either H_2 or CO to the P-state activates the enzyme fully and very rapidly.[190] Because the activation is not a redox process and CO is known to form a tightly bound terminal ligand to the Ni,[35] the authors proposed that CO could displace a Ni-bound H_2O_2 molecule when the enzyme is in the P-state.

Oxidative damage may also occur at FeS clusters, as reported for the [NiFe]-hydrogenase from *D. desulfuricans* ATCC 27774. In this case the $[Fe_4S_4]$ cluster next to the Ni−Fe active site was modified into a $[Fe_4S_3O_3]$ cluster, presumably due to a reaction with dioxygen and water.[13]

6.2. Oxidative Damage of FeS Clusters in [FeFe]-Hydrogenases

As isolated, aerobically purified, *D. vulgaris* hydrogenase exhibits a nearly isotropic EPR signal at $g = 2.02$ and a derivative-type signal at $g = 2.00$, very similar to the one found for a $[Fe_3S_4]$ cluster in *D. gigas* ferredoxin II. For various hydrogenase preparations, quantitations of 0.02−0.2 spin/molecule have been reported for the $g = 2.0$ signal, which is an artifact due to the oxidation of a $[Fe_4S_4]$ cluster.[191] We have observed that the $[Fe_3S_4]$ signal is absent when the enzyme is purified anaerobically in a glovebox.

The choloroplastic *Chlamydomonas* enzyme is extremely sensitive to oxygen, which irreversibly inhibits H_2 evolution within minutes. In the absence of dithionite, the enzyme was inactivated with a half-time of several hours, even under strictly anaerobic conditions.[54] *C. pasteurianum* contains two very different hydrogenases: CpI and CpII. CpII is very active in H_2 oxidation with methylene blue but catalyzes H_2 evolution from reduced methylviologen (MV) at very low rates. On the other hand, CpI catalyzes the two reactions at extremely high rates. Also, this hydrogenase can be reversibly oxidized and reduced with ferricyanide and H_2 or dithionite. On the other hand, when CpII was treated with a 200-fold excess ferricyanide under anaerobic conditions, no hydrogenase activity could be detected after a 5 min of incubation. When dithionite was subsequently added, the solution turned red, indicating that iron had been released from the enzyme by the ferricyanide treatment. The EPR spectra of the damaged enzyme revealed the presence of only two $[Fe_4S_4]$ clusters. Thus, the ferricyanide treatment may have involved the intermediate formation of $[Fe_3S_4]$ centers.

D. desulfuricans [FeFe]-hydrogenase is reversibly inhibited by oxygen when it is purified under aerobic conditions, but it can be reactivated under H_2 and MV. In this resting state the enzyme is O_2-insensitive and not very active. However, when the enzyme is reductively activated, it becomes O_2-sensitive. The O_2-stable state can be regenerated by anaerobic oxidation using 2,6-dichlorophenol-indophenol (DCIP).

As isolated CpI, CpII, and *Megasphera elsdenii* [FeFe]-hydrogenases are extremely O_2-sensitive and have to be purified under anaerobic conditions. Low O_2 concentrations induce the same changes as CO in the EPR properties of the oxidized CpI and CpII hydrogenases, that is, conversion of the rhombic $g = 2.10$ signal into the photosensitive axial $g = 2.07$ type signal.[49] However, added CO does not irreversibly inactivate the enzyme. It is now clear that the O_2-induced axial $g = 2.07$ signal does not reflect enzyme inactivation. In fact, O_2-induced inactivation is indicated by a decrease in the intensity of both rhombic and axial EPR signals to much less than stoichiometric values, presumably as a result of cluster degradation. In contrast to CO, prolonged exposure to O_2 leads to destruction of the H-cluster.[49] This may be due to the generation of oxygen-derived and partially reduced reactive species that react with the thiolate ligands or other potentially reactive species at the active site.

It remains to be determined why the various [FeFe]-hydrogenases, having almost identical active sites, display so widely different sensitivities toward oxygen. One possible explanation resides in their different FeS cluster compositions and their exposure to oxygen attack. The algal enzyme is a minimal species that contains only the H-cluster, whereas CpI has extra FeS clusters in a plant ferredoxin-like domain. However, CpII has the same FeS cluster structure as the *D. desulfuricans* enzyme but a much higher oxygen sensitivity.

6.3. Hydrophobic Tunnels in [NiFe]-Hydrogenases

[NiFe]-hydrogenases contain specific hydrophobic tunnels that regulate H_2 access to the Ni−Fe site. The same tunnels are most probably also used by the bulkier O_2. The first study concerning gas diffusion inside calculated internal tunnels in [NiFe]-hydrogenases was published by Montet et al. in 1997, based on the enzymes from *D. gigas* and *D. fructosovorans*.[11] Very similar tunnels involving residues from both the large and the small subunit are also present in the less-related enzyme from *Dm. baculatum*.[165] To determine the possible role of the tunnels in catalysis, we collected 6 Å resolution X-ray diffraction data from a *D. fructosovorans* hydrogenase crystal exposed to 9 bar of Xe pressure. Xe was chosen because it is a gas rich in electrons and, consequently, readily visible in electron density maps when specifically bound to the protein. From our map it was possible to identify 10 Xe sites, all located inside the calculated hydrophobic tunnels (Figure 9). However, none of these sites was found at the active site or very near it. The Xe concentration in the tunnels greatly exceeds its water solubility, indicating that the gas partition coefficient favors its binding inside the protein. To further explore the role of the tunnels in gas diffusion, a molecular dynamics (MD)

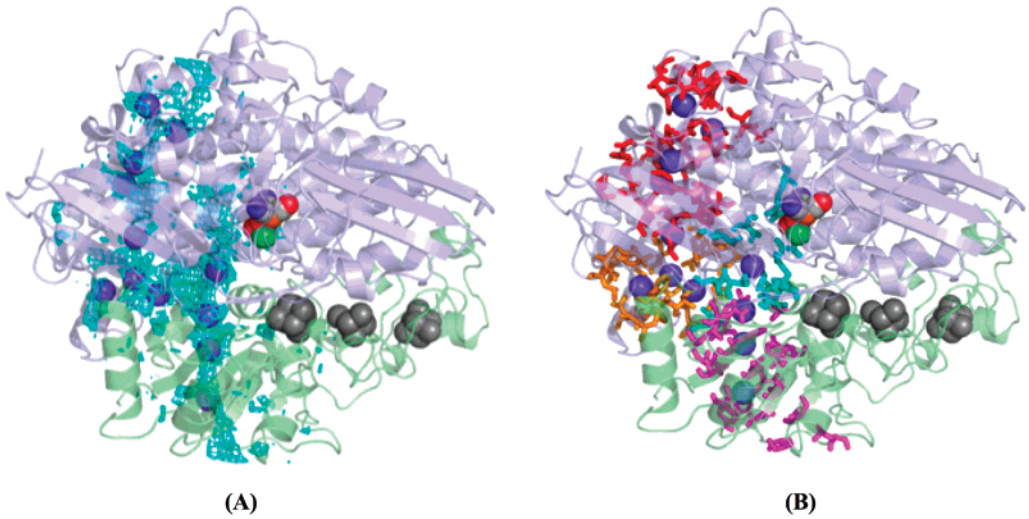

Figure 9. Structure of *Desulfovibrio fructosovorans* hydrogenase depicting internal hydrophobic tunnels. The large subunit is shown in light blue, the small one in green. Iron−sulfur clusters are shown as gray spheres, the active site as color-coded spheres, and observed xenon-binding sites as dark blue spheres. **(A)** A blue grid depicts internal regions accessible to a probe of 1 Å radius. **(B)** Residues lining the different hydrophobic cavities are shown in blue, magenta, orange, and red, as in Figure 9. This figure and Figures 10 and 14 were made with the program PyMol.[256]

study using the time-dependent Hartree approximation[192] was carried out with the experimentally determined Xe sites as starting points. During the simulation Xe atoms were left to diffuse for 50−200 ps in the fluctuating protein matrix. Again, no Xe atom approached the Ni−Fe center, suggesting that even when subjected to MD, the enzyme did not allow the passage of the bulky Xe atom to the active site. The experimental Xe sites were also used as starting points for a simulation including hydrogen molecules. In several trajectories H_2 approached the active site with minimal gas-Fe and gas-Ni distances of 1.8 and 1.4 Å, respectively. Hydrogen left the enzyme through four different tunnels (Figure 9). The average of 80 trajectories indicated that statistically the gas did not occupy potential holes in the protein matrix other than the ones obtained in the cavity calculations.

Very recently, Teixeira and co-workers have carried out a similar theoretical study with the program GROMACS, using the three-dimensional model of the *D. gigas* [NiFe]-hydrogenase.[193] These authors used a dodecahedral box filled with hydrogen and water molecules with a minimal distance of 8 Å between the protein and the simulation box. The hydrogen concentration in the box was much higher than the value determined from its solubility in water, but this had no effect on the protein structure and was required to get reliable statistics. The study was extended to an in silico Val67Ala mutant, a position in the tunnel near the active site, to determine whether increasing the tunnel girth could affect hydrogen diffusion toward the Fe−Ni center. Hydrogen readily entered the protein molecule, and there were 47 H_2 molecules inside the hydrogenase after 5 ns into the simulation. Once inside, the H_2 molecules did not tend to leave the protein, supporting our earlier proposal that the tunnels may function as hydrogen reservoirs.[11] Whenever hydrogen penetrated hydrogenase through paths other than the tunnels, it did not reach the active site.[193] Teixeira et al. also found that few hydrogen molecules actually reached the active site during their study, a situation that may be due to the short time period of 9 ns used. However, in the work reported by Montet et al., in which an even shorter period of 200 ps was applied, the number of hydrogen molecules approaching the active site was significant (see Figure 1D in ref 11). The difference may be due to the starting positions of the gas molecules in the two simulations: outside in[193] and inside in.[11] Teixeira et al. have also calculated H_2 probability density maps that reflect the degree of gas population in different regions of the tunnels.[193] Their conclusions are very similar to the ones reached in the previous study by Montet et al.,[11] namely, that hydrogen preferentially occupies tunnels that connect the active site to the molecular surface. Similarly, they conclude that hydrogen approaches the active side at the Ni side as already pointed out by Montet et al.

The simulations carried out with the in silico Val67Ala mutant indicate that more hydrogen molecules can get inside the enzyme (55 vs 47) and that they get closer to the active site than in the wild type hydrogenase. The consequences of mutations at this position have already been discussed by some of us[34] and are being the subject of intense scrutiny (Cournac et al., unpublished results). In summary, the two studies concerning gas diffusion reach similar conclusions and underscore the importance of the hydrophobic tunnels for both (correct) substrate access to the active site and hydrogen storage inside [NiFe]-hydrogenases.

Four tunnels can be distinguished in [NiFe]-hydrogenases. Figures 9 and 10 depict the position of tunnel residues in the tertiary and primary structures, respectively. Residues coded in blue correspond to the most conserved tunnel. Those in magenta the next most conserved cavities, whereas residues shown in orange and red are less conserved in their respective tunnels. The amino acid sequences of the three *Desulfovibrio* hydrogenases of known structure are very similar, including the residues lining the tunnel. On the other hand, the tunnel residues in *Dm. baculatum* [NiFeSe]-hydrogenase are less conserved. The role of the selenocysteine at the active site of this enzyme is not immediately obvious, but it may be related to its high resistance to oxygen inactivation. On the one hand, Se may be harder to oxidize than S in the corresponding *Cys530*. On the other hand, Se is larger than S and partially blocks access to the Ni−Fe unit. This effect may be enough to allow H_2 diffusion while obstructing the entrance of the bulkier O_2 to the active site cavity. In addition, as noted before,[34] a leucine substitutes the nearby tunnel residue *Val110*, also resulting in a narrower

Small subunit:

```
Df    SVVWLHNAECTGCTEAAIRTIKPYIDALILDT-ISLDYQETIMAAAGETSEAALHQ 62
Dg    SVVYLHNAECTGCSESLLRTVDPYVDELILDV-ISMDYHETLMAGAGHAVEEALHE 62
DvM   SVVYLHNAECTGCSESVLRAFEPYIDTLILDT-LSLDYHETIMAAAGDAAEAALEQ
Dmb   PVIWVQGQGCTGCSVSLLNAVHPRIKEILLDV-ISLEFHPTVMASEGEMALAHMYE
SH    KVATIGLCGCWGCTLSFLDMDER----L-----LPLLEKVTLLRSSLTDIKRIPER
RH    -VLWIQSGGCGGCSMSLLCADTTDFTGMLKSAGIHMLWHPSLSLESGVEQLQILED
MBH   PVLWLHGLECTCCSESFIRSAHPLAKDVVLSM-ISLDYDDTLMAAAGHQAEAILEE

Df    AL-EGKDGYYLVVEGGLPTIDGG--QWGMVAGH----------PMIETTKKAAAKA 105
Dg    AI-KGD--FVCVIEGGIPMGDGG--YWGKVGRR----------NMYDICAEVAPKA 103
DvM   AV-NSPHGFIAVVEGGIPTAANG--IYGKVANH----------TMLDICSRILPKA
Dmb   IAEKFNGNFFLLVEGAIPTAKEG--RYCIVGETLDAKGHHHEVTMMELIRDLAPKS
SH    CAIGF-------VEGGVSSEEN----------------------IETLEHFRENC
RH    CLQGRVALHALCVEGAMLRGPHGTGRFHLLAGT--------GVPMIEWVSRLAAVA
MBH   IMTKYKGNYILAVEGNPPLNQDG--MSCIIGGR----------PFIEQLKYVAKDA

Df    KGIICIRHLP-HGGVQKAKPNPSQAKGVS----------E--AL---GVKTINIPG 146
Dg    KAVIAIGTCATYGGVQAAKPNPTGTVGVN----------E--ALGKLGVKAINIAG 147
DvM   QAVIAYGTCATFGGVQAAKPNPTGAKGVN----------D--ALKHLGVKAINIAG
Dmb   LATVAVGTCSAYGGIPAAEGNVTGSKSVR----------DFFADEKIEKLLVNVPG
SH    DILISVGACAVWGGVPAMRNVFELKDCLA----------EAYVNSATAVPGAKAV-
RH    DYTLAVGTCAAYGGITAGGGNPTDACGLQYEGDQPGGLLGLNYRSRAGLPVINVAG
MBH   KAISWGSCASWGCVQAAKPNPTQATPVH----------K--VI--TDKPIIKVPG

Df    CPPNPINFVGAVV----HVL---TKGIPDLDE 171
Dg    CPPNPMNFVGTVV----HLL---TKGMPELDK 172
DvM   CPPNPYNLVGTIV----YYL--KNKAAPELDS
Dmb   CPPHPDWMVGTLVAAWSHVLNPTEHPLPELDD
SH    VPFHPDIPRITTKVYPCHEVVKMDYFIPGCPP
RH    CPTHPGWVTDALA-----LLSARLLTASDLDT
MBH   CPPIAEVMTGVIT----YML--TFDRIPELDR
```

Large subunit :

```
Df    GVCTYVHALASSRCVDDAVKV------SIPANARMMRNLVMASQYLHDHLVHFYHL 122
Dg    GVCTYVHALASVRAVDNCVGV------KIPENATLMRNLTMGAQYMHDHLVHFYHL 115
DvM   GVCTYTHALASTRCVDNAVGV------HIPKNATYIRNLVLGAQYLHDHIVHFYHL
Dmb   GVCPTAHCTASVMAQDDAFGV------KVTTNGRITRNLIFGANYLQSHILHFYHL
SH    GICFVSHHLCGAKALDDMVGVGLKSGIHVTPTAEKMRRLGHYAQMLQSHTTAYFYL
RH    GICSVSQSVAASRALADLAGV------TVPANGMLAMNLMLATENLADHLTHFYLF
MBH   GVCTGCHALASVRAVENALDI------RIPKNAHLIREIMAKTLQVHDHAVHFYHL

Df    HALDWVDVTAALKADPNKAAKLAASIDTARTGNSEKALKAVQDKLKAFVESGQLGI 178
Dg    HALDWVNVANALNADPAKAARLANDLSPRKT--TTESLKAVQAKVKALVESGQLGI 169
DvM   HALDFVDVTAALKADPAKAAKVASSISPRKT--TAADLKAVQDKLKTFVETGQLGP
Dmb   AALDYVKGPDVSPFVPRYANA----------DLLTDRIKDGAKAD
SH    IVPEMLFGMDAPPAQRNVLGL----------IEANPDLVKRVVMLRKWG-
RH    FMPDFTREIYAGRPWHTDATA---RFSPTHGKHHRLAIAARQRWFTLMGTLGGKWP
MBH   HALDWVDVMSALKADPKRTSELQQLVSPAHPLSSAGYFRDIQNRLKRFVESGQLGP

Df    FTNAYFLGGHKAYYLPPEVNLIATAHYLEALHMQVKAASAMAILGGKNPHTQFTVV 234
Dg    FTNAYFLGGHPAYVLPAEVDLIATAHYLEALRVQVKAARAMAIFGAKNPHTQFTVV 225
DvM   FTNAYFLGGHPAYYLDPETNLIATAHYLEALRLQVKAARAMAVFGAKNPHTQFTVV
Dmb   ATNTY----------GLNQYLKALEIRRICHEMVAMFGGRMPHVQGMVV
SH    ----------QEVIKAV-FGKKMHGINSVPGGVNNNLSIA--
RH    HTESVQPGG----------SSRAIDAAE-RVRLLGRVREFRCFLEQTLYAA-
MBH   FMNGYW--GSKAYVLPPEANLMAVTHYLEALDLQKEWVKIHTIFGGKNPHPNYLVG
```

Figure 10. Structure-based alignment of partial amino acid sequences of different [NiFe]-hydrogenases (Df, *Desulfovibrio desulfuricans*; Dg, *Desulfovibrio gigas*; DvM, *Desulfovibrio vulgaris* Miyazaki; Dmb, *Desulfomicrobium baculatum*; SH, *Ralstonia eutropha* H16 soluble cytoplasmic hydrogenase; RH, *Ralstonia eutropha* H16 regulatory hydrogenase; MBH, *Ralstonia eutropha* H16 membrane-bound hydrogenase. Because no structures are known for the *Ralstonia* enzymes, their sequence alignment is only tentative. Residues lining the different hydrophobic cavities are shown in cyan, magenta, orange, and red (see Figure 9). Only segments containing residues lining to tunnels are depicted.

tunnel. A putative effect of the tunnel diameter on the O_2 tolerance of *R. eutropha* enzymes is discussed below.

6.4. Hydrophobic Tunnels in [FeFe]-Hydrogenase

The hydrophobic tunnel structure of [FeFe]-hydrogenase was first explored by Nicolet et al. in the *D. desulfuricans* structure.[15] Cavity calculations showed the presence of a short tunnel connecting the molecular surface to a vacant coordination site of the active site Fe_D (Figure 5A). Xenon-binding experiments, similar to the ones performed with [NiFe]-hydrogenase crystals,[11] revealed only one well-occupied site in the largest section of the tunnel (Y. Nicolet and J. C. Fontecilla-Camps, unpublished results). More recently,[194] passive H_2 and O_2 transport in CpI has been investigated using the maximum volumetric solvent accessibility method (VSAM). It was concluded that differences between gas permeation dynamics were caused only by dissimilar probe sizes. This, in turn, suggested that hydrophobic gases diffuse through pathways that are mainly determined by density fluctuations within the protein. To focus only on their size difference, and to remove the variation in behavior between the two gases due to their mass difference, the hydrogen atom mass was set to that of O_2 (hH_2, heavy H_2). These theoretical simulations of gas diffusion, using the temperature-controlled locally enhanced sampling (TLES) dynamics have thus suggested different transport mechanisms for O_2 and H_2.

Besides the channel found in the crystal structure, called A, the study had identified a second, dynamically determined, channel B (Figure 11). Both pathways meet at the large central cavity next to the active site where we observed the only experimental Xe site in the enzyme (Y. Nicolet and J. C. Fontecilla-Camps, unpublished results). Molecular oxygen left the central cavity through pathway B in only one of five simulations. In the other cases, O_2 remained in the cavity. It was concluded that the initial failure of O_2 to exit through pathway A was due to insufficient sampling of the protein degrees of freedom. When the sampling was expanded, O_2 diffused along channel A in three simulations but in no case could it leave the protein completely. This was probably due to O_2 hydrophobicity.

The hH_2 probe could diffuse in a broader region and on shorter timescales than O_2, which was limited to the described A and B pathways. Different copies of hH_2 spread out into a diffuse cloud covering the entire protein−water system. On the other hand, O_2 probes typically clustered together as a single cloud, although occasionally they split into several ones. This clustering behavior was not observed with hH_2. Also, O_2 fills up some little cavities that are themselves dynamic and fluctuate in both size and in their connections to neighboring cavities. Thus, O_2 transport seems to be determined more by the protein random peristaltic motions than by simple diffusion. The theoretical approach suggests that transient cavities are present even in the absence of gas and the maximum VSAM can predict the accessibility of both O_2 and H_2. The gas-transport pathways are not fully described by a simple analysis of the [FeFe]-hydrogenase crystal structures. As mentioned above, pathway A was described in *D. desulfuricans* hydrogenase, but it was discontinuous unless a small probe of 0.75 Å radius was used.[14] No indication of the more fluctuating pathway B was found in the crystal. In fact, in the study by Cohen et al. only very few cavities are large enough to accommodate O_2,

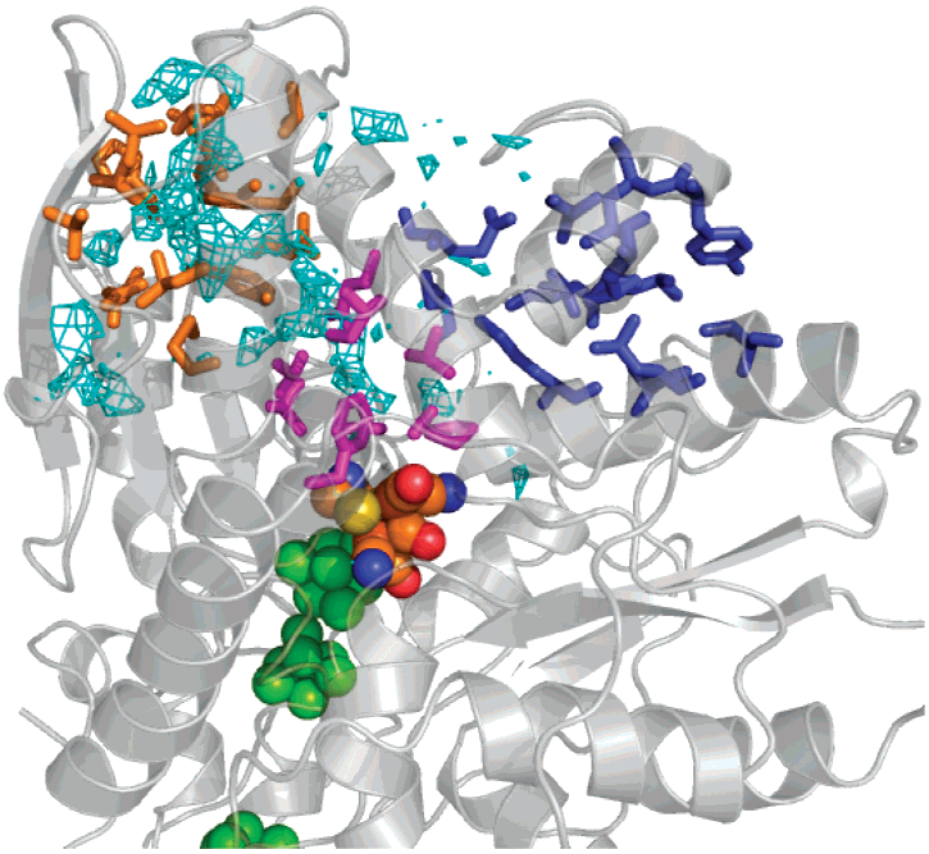

Figure 11. Hydrophobic tunnels in [FeFe]-hydrogenase (cyan) with conserved residues depicted in magenta (common central cavity), orange (pathway A), and blue (pathway B). Iron−sulfur clusters are shown as green spheres and the active site as color-coded spheres. Only a part of the structure is depicted as gray ribbons and arrows.

and this gas moves from cavity to cavity as these are created within the protein.[194] The transient H_2-filled cavities connect in more places as well as more often, allowing for easier diffusion than in the case of O_2. Most pathway regions are open 5−8% of the time for O_2 and 30−35% of the time for H_2. The central cavity is accessible to O_2 and to H_2 2 and 20% of the time, respectively. Other studies on gas transport in protein cavities suggest that the presence of a gas strongly influences the internal conformations of the protein near it, as in catalase and myoglobin.[195,196] In the case of [FeFe]-hydrogenase, although gases can strongly bias the size and shape of cavities, they do not create new ones. Thus, the presence of gas is not needed to open and activate the pathways.

When amino acid sequences are compared, it becomes clear that [FeFe]-hydrogenases can vary to a significant extent: the algal *Chlamydomonas renhardii* enzyme contains no ferredoxin-like domain, whereas the hydrogenase from *T. maritima* is bifunctional with a NADP-reducing subunit. However, the common central cavity found close to the active site is strictly conserved (Figure 12). Residues lining the crystallographically characterized pathway A are globally conserved, but this is not the case for the more dynamic theoretical pathway B.

6.5. Hydrogen Sensors Related to [NiFe]-Hydrogenases

In the Knallgas bacterium *Ralstonia eutropha*, a signal transduction apparatus consisting of the response regulator HoxA and its cognate histidine protein kinase HoxJ directs H_2-dependent transcription. H_2 sensing is mediated by an additional third component, the regulatory hydrogenase (RH) or hydrogen sensor, which belongs to a subclass of [NiFe]-hydrogenases[197] also found in *Rhodobacter capsulatus*. As in *Ralstonia*, in addition to the sensor protein (Hup UV), *Rhodobacter* has a histidine kinase and a response regulator (HupT and HupR), forming a two-component regulatory system that functions by phosphate transfer.[198] The sensors are able to catalyze the three typical reactions of [NiFe]-hydrogenases: H_2 uptake, H_2 evolution, and H−D exchange. As isolated, RH is found only in the Ni-SI and Ni-C states depending on the redox environment, the oxygen-modified Ni-A and Ni-B forms being inaccessible in this protein, which is both O_2- and CO-insensitive. In addition, the coupling between the active site Ni and the proximal cluster typical of standard [NiFe]-hydrogenases is not observed in RH.[199]

The *D. gigas* [NiFe]-hydrogenase active site is embedded in a cavity formed by five fairly conserved motifs of the large subunit (L1-L5), but only L1 (RGxE) and L5 (DPCxx-CxxH/R) are strictly invariant in all known [NiFe]-hydrogenase sequences.[200] H_2 sensors display significant changes in the remaining motifs: for instance, the conserved Pro of motif L4 (Gx4PRGx3H) is replaced by Ala, and only two His residues of motif L3 (HxHxxHxxHLHxL) are present. However, this motif is not strictly conserved in the standard enzymes (Figure 10). The most striking change takes place at position 67 in the L2 motif because the conserved equivalent *His72* in *D. gigas* hydrogenase interacts directly with the active site *Cys533* that coordinates both the nickel and iron ions (Figure 2A). In all H_2-sensing hydrogenases this histidine residue is substituted by glutamine (Gln 67 of

```
CpI  INFGADMTIMEEATELVQRI--E------NNGPFPMFTSCCPGWVRQAENYYPELLN316
Dd   TEFTADVTIWEEGSEFVERLTKK------SDMPLPQFTSCCPGWQKYAETYYPELLP195L
Cr1  TLFGADLTIMEEGSELLHRLTEHLEAHPHSDEPLPMFTSCCPGWIAMLEKSYPDLIP186
Tm   VSFGADLVAYEEAHEFYERL--K------KGERLPQFTSCCPAWVKHAEHTYPQYLQ311

CpI  NLSSAKSPQQIFGTASKTYYPSISGLDPKNVFTVTVMPCTSKKFEADRPQM---EKD370
Dd   HFSTCKSPIGMNGALAKTYGAERMKYDPKQVYTVSIMPCIAKKYEGLRPEL---KSS249L
Cr1  YVSSCKSPQMMLAAMVKSYLAEKKGIAPKDMVMVSIMPCTRKQSEADRDWFCVDADP243
Tm   NLSSVKSPQQALGTVIKKIYARKLGVPEEKIFLVSFMPCTAKKFEAERE-----EHE363

CpI  GLRDIDAVITTRELAKMIKDAKIPFAKLEDSEADPAMGEYSGAGAIFGATGGVMEAA427
Dd   GMRDIDATLTTRELAYMIKKAGIDFAKLPDGKRDSLMGESTGGATIFGVTGGVMEAA306L
Cr1  TLRQLDHVITTVELGNIFKERGINLAELPEGEWDNPMGVGSGAGVLFGTTGGVMEAA300
Tm   GI--VDIVLTTRELAQLIKMSRIDINRVEPQPFDRPYGVSSQAGLGFGKAGGVFSCV418

CpI  LRSAKDFAENAELEDIEYKQVRGLNGIKEAEVEI----------------------461
Dd   LRFAYEAVTGKKPDSWDFKAVRGLDGIKEATVNV----------------------340L
Cr1  LRTAYELFTGTPLPRLSLSEVRGMDGIKETNITMVPAPGSKFEELLKHRAAARAEAA357
Tm   LSVLN---EEIGIEKVDVKSPE--DGIRVAEVTL----------------------447

CpI  ----------------------NNNKYNVAVINGASNLFKFMKSGMINEKQYHFIEVM496
Dd   ----------------------GGTDVKVAVVHGAKRFKQVCDDVKAGKSPYHFIEYM374L
Cr1  AHGT-PGPLAWDGGAGFTSEDGRGGITLRVAVANGLGNAKKLITKMQAGEAKYDFVEIM415
Tm   ----------------------KDGTSFKGAVIYGLGKVKKFLEE----RKDVEIIEVM480

CpI  ACHGGCVNGGGQPHVNPKDLEKV-----DIKKVRASVLYNQDEHLSKRKSHENTALVKM551
Dd   ACPGGCVCGGGQP-VMPGVLEAAVKQIKDYMLDRINGVYGADAKFPVRASQDNTQVKAL71S
Cr1  ACPAGCVGGGGQPRSTDKAITQK----------RQAALYNLDEKSTLRRSHENPSIREL464
Tm   ACNYGCVGGGGQPYPNDSR----------IREHRAKVLRDTMGIKSLLTPVENLFLMKL529

CpI  YQNYFGKPGEGRAHEILHFK571
Dd   YKSYLEKPLGHKSHDLLHTH91S
Cr1  YDTYLGEPLGHKAHELLHTH484
Tm   YEEDL--KDEHTRHEILHTT547
```

Figure 12. Partial amino acid sequences of various Fe hydrogenases (CpI, *Clostridium pasteurianum* I; Dd, *Desulfovibrio desulfuricans*; Cr, *Chlamydomonas reinhardtii* HydA1; Tm, *Thermotoga maritima*). Residues lining the common central cavity are depicted in magenta, residues lining pathway A are shown in orange, and residues lining pathway B are shown in blue. Only segments containing residues lining the hydrophobic tunnels are depicted. The sequence alignment of the Cr and Tm enzymes is tentative, as no structures are known for them yet.

RH large subunit HoxC). However, EPR studies have shown that the Ni−Fe center has similar structures in native RH and the RH Gln67His mutant.[201] Model building shows that the glutamine side chain could substitute for the histidine by forming a hydrogen bond to *Cys533*, but a ^{14}N quadrupole coupling was observed only in the Gln67His mutant. Mutagenesis of RH Gln67 to Glu results in an unstable protein, showing that a negatively charged residue is deleterious at this position. The Gln67His and the Gln67Asn mutants display between 51 and 60% decrease in activity. A similar result is observed when using the D_2/H^+ exchange assay.[201]

The basis for the resistance to oxygen-induced damage in the sensors has been investigated. One obvious possibility is restricted access of O_2, which is bulkier than hydrogen, to the active site. In standard [NiFe]-hydrogenases, the gas tunnel that connects the molecular surface to the active site peters out near the nickel ion (Figure 9),[11] where two highly conserved and relatively small hydrophobic amino acids, valine and leucine, are found. In the H_2-sensing hydrogenases RH and HupUV, these amino acids are replaced by the bulkier Ile and Phe, respectively (see also Figure 10).[34] It is reasonable to conclude that they will make this region of the gas channel narrower, thereby limiting the transit of molecules larger than H_2. To test this concept, the channel Ile62 and Phe110 of the RH large subunit HoxC were mutated to Val and Leu, respectively.[202] When purified under air, the Ile62Val, Phe110Leu, and Ile62Val/Phe110Leu mutants displayed drastically decreased H_2 uptake activities. The double Ile62Val/Phe110Leu mutant was totaly inactive, whereas the Ile62Val and Phe110Leu mutants had 6 and 18% residual activity, respectively. These mutants could be reactivated by dithionite + H_2, showing that, as in standard [NiFe]-hydrogenases, their oxidative inactivation is reversible. In *R. capsulatus*, the equivalent double-mutant Ile65Val/Phe113Leu lost 80% of its activity after being exposed for 1.5 days to air.[203] The same enzyme preparation lost about 50% activity during a similar period when stored under N_2, probably due to inactivation by traces of O_2. For the wild type HupUV, the activity and the rate of HD and H_2 formation were similar under aerobic and anaerobic conditions, whereas the activity was twice as high for the mutant in the absence of O_2. Concerning the effect of methylviologen on activity, the wild type HupUV is not reductively reactivated, whereas the mutant displays a 4-fold increase in activity after reactivation.[203] From these studies it can be concluded that the diameter of the hydrophobic channel serves as a filter, modulating gas access on the basis of molecular size.

Table 2. Nomenclature of Related Subunits of Complex I and Hydrogenase

NAD^+:Q oxidoreductase[a]	H_2-$NAD(P)^+$ oxidoreductase[b]	H_2-$NADP^+$ oxidoreductase[c]	Ech hydrogenase[d]	cofactors/reactants, special features
51K-Nqo1-NuoF	HoxF	HydB		NADH, FMN, $[Fe_4S_4]$
24K-Nqo2-NuoE	HoxE	HydC		$[Fe_2S_2]$
75K-Nqo3-NuoG	**HoxU**	**HydA**		$[Fe_2S_2]$**, 2**$[Fe_4S_4]$[e]
49K-Nqo4-NuoD	**HoxH**		E	**quinone or Ni−Fe**
30K-Nqo5-NuoC			D	
PSST-Nqo6-NuoB	**HoxY**		**C**	****$[Fe_4S_4]$**
TYKY-Nqo9-NuoI			F	2$[Fe_4S_4]$
ND1-Nqo8-NuoH			B	membrane-bound
ND2-Nqo14-NuoN				membrane-bound
ND3-Nqo7-NuoA				membrane-bound
ND4-Nqo13-NuoM				membrane-bound
ND4L-Nqo11-NuoK				membrane-bound
ND5-Nqo12-NuoL			A	membrane-bound
ND6-Nqo10-NuoJ				membrane-bound

[a] Complex I subunits in bovine mitochondrion (this has at least 32 other subunits), *T. thermophilus*, and *E. coli*.[212] [b] *Synechocystis* [NiFe]-hydrogenase.[220] [c] *T. maritima* [FeFe]-hydrogenase.[51] [d] *M. barkeri* [NiFe]-hydrogenase.[136] [e] These clusters are located in the N-terminal domain. The C-terminal domain is different: in HydA of *T. maritima* this contains the H-cluster.

6.6. Oxygen-Insensitive [NiFe]-Hydrogenases from *Ralstonia eutropha*

The Knallgas bacterium *R. eutropha* has two energy-conserving [NiFe]-hydrogenases: a membrane-bound enzyme coupled to the respiratory chain via a *b*-type cytochrome and a cytoplasmic soluble hydrogenase (SH), which can directly reduce NAD^+ at the expense of H_2.[204] Both enzymes are remarkably resistant to oxygen and CO.[204] Unfortunately, their structures have not been determined yet. MBH has been used by Armstrong et al. (see the Armstrong's paper)[175] to build a bio-fuel cell that can operate with low hydrogen concentrations in air. Overall, this enzyme is similar to oxygen-sensitive hydrogenases from *Desulfovibrio* sp. (Figure 10), so the basis for its resistance is not well understood. SH is a NAD^+-reducing enzyme with a reported $HoxFUYHI_2$ subunit stoechiometry.[205] It contains two heterodimeric complexes (HoxFU and HoxHY) that display the diaphorase and hydrogenase activities, respectively. Both heterodimers bind FMN.[206] Friedrich et al.[207−209] have carried out an extensive mutagenesis program concerning this enzyme. A surprising proposition concerns the structure of the active site. FTIR studies have shown the presence of extra high-frequency bands that have been assigned as corresponding to two extra CN^- ligands as compared to the active sites depicted in Figure 2.[210] One of these extra ligands would be terminally bound to Ni, whereas the second would bridge the two metal ions. In addition, an XAS study has suggested that some cysteine ligands could be modified to sulfenates.[211] Clearly, an X-ray crystallographic study of this enzyme is in order.

7. Evolutionary Relationships of Hydrogenases to Other Proteins

7.1. Comparison of [NiFe]-Hydrogenase with Complex I

In the 1990s, surprising relationships were noted between hydrogenase and NADH:quinone oxidoreductase. This multisubunit membrane-bound enzyme, also known as complex I, couples the oxidation of NADH by ubiquinone with the translocation of four protons through a membrane.[212,213] The resulting proton gradient is a fundamental biological solution for the storage of energy.[214] The first sequence similarities with complex I were noted for three open reading frames of the *E. coli* formate hydrogenlyase operon,[95,215] one of which corresponds to the [NiFe]-hydrogenase large subunit. Two diaphorase subunits of the soluble NAD^+-reducing hydrogenase of *R. eutropha* (at the time known as *Alcaligenes eutrophus*) were found to be related to the 75- and 51-kDa subunits of bovine mitochondrial complex I.[216] Significant additional similarities were subsequently found with the N-terminal flavodoxin-like domain of the [NiFe]-hydrogenase small subunit,[217] two diaphorase subunits of the NADP-reducing heterotetrameric *D. fructosovorans* [FeFe]-hydrogenase, and the N-terminal region of the H-cluster-containing subunit.[218,219]

Significant similarities to complex I have since been noted in many other hydrogenases: the heterotrimeric [FeFe]-hydrogenase from *Thermotoga maritima*,[51] the heteropentameric $NAD(P)^+$-reducing hydrogenase from *Synechocystis* sp. strain PCC 6803,[220] and the membrane-bound multisubunit [NiFe]-hydrogenases. These enzymes, which have six conserved core subunits related to complex I,[136,221] include hydrogenases 3 and 4 of *E. coli* formate hydrogen lyase system, a CO-induced hydrogenase of *Rhodospirillum rubrum* that is complexed with a homodimeric carbon monoxide dehydrogenase, and energy-converting hydrogenases from archaea. Like complex I, the latter also function as an ion pump. Eleven of the 13 subunits of the $F_{420}H_2$ dehydrogenase complex, which archaea also use for proton translocation, are homologous to complex I subunits.[137] The archaean system uses $F_{420}H_2$ instead of NAD(P)H as hydride donor and methanophenazine instead of quinone as electron acceptor. Related complex I and hydrogenase subunits are grouped in Table 2. Electron microscopic analyses have indicated that complex I may function in respiratory chain supercomplexes with the electrochemical-proton-gradient-generating enzymes ubiquinol:cytochrome *c* oxidoreductase (complex III) and cytochrome *c* oxidase (complex IV).[222] The similarities with hydrogenases have been very recently confirmed by the 3.3 Å resolution crystal structure of the hydrophilic domain of *Thermus thermophilus* complex I.[170] Many structural similarities with other proteins were observed as well (Table 3). As indicated schematically in Figure 13A, an electron-transfer pathway is formed by seven FeS clusters located between the FMN of the diaphorase active site in Nqo1 and the quinone-reducing site in Nqo4. The distal $[Fe_2S_2]$ cluster in Nqo2, being within electron acceptor

Table 3. Superposition Statistics for Complex I Nqo Subunits (PDB Code 2FUG)

protein 1 (residues)	description	protein 2	residues	Δrms (Å)	identities (%)
Nqo1 (80−220)	Rossman-like fold	thymidyltransferase[a]	105	3.0	nd
Nqo1 (241−335)	ubiquitin-like	NEDD8 protein[b]	64	2.7	nd
Nqo2 (76−180)	thioredoxin-like	[2Fe-2S]-ferredoxin[c]	75	1.5	19
Nqo3 (1−240)	[FeFe]-H_2ase-like	[FeFe]-H_2ase domain 1[d]	173	1.7	23
Nqo3 (241−767)	"molybdopterin" fold	NO_3-reductase[e]	428	2.7	18
Nqo4 (35−409)	[NiFe]-H_2ase-like	[NiFe]-H_2ase (L)[f]	274	1.9	16
Nqo6 (15−175)	flavodoxin-like	[NiFe]-H_2ase (S)[f]	87	2.0	26
Nqo9 (26−179)	ferredoxin-like	2[Fe_4S_4]-ferredoxin[g]	58	1.9	34
Nqo15 (3−129)	frataxin-like	human frataxin[h]	96	3.3	11

[a] PDB code 1H5R. [b] PDB code 1R4M [c] PDB code 1M2D. [d] PDB code 1FEH. [e] PDB code 2NAP. [f] PDB code 1YQW. [g] PDB code 1H98. [h] PDB code 1EKG.

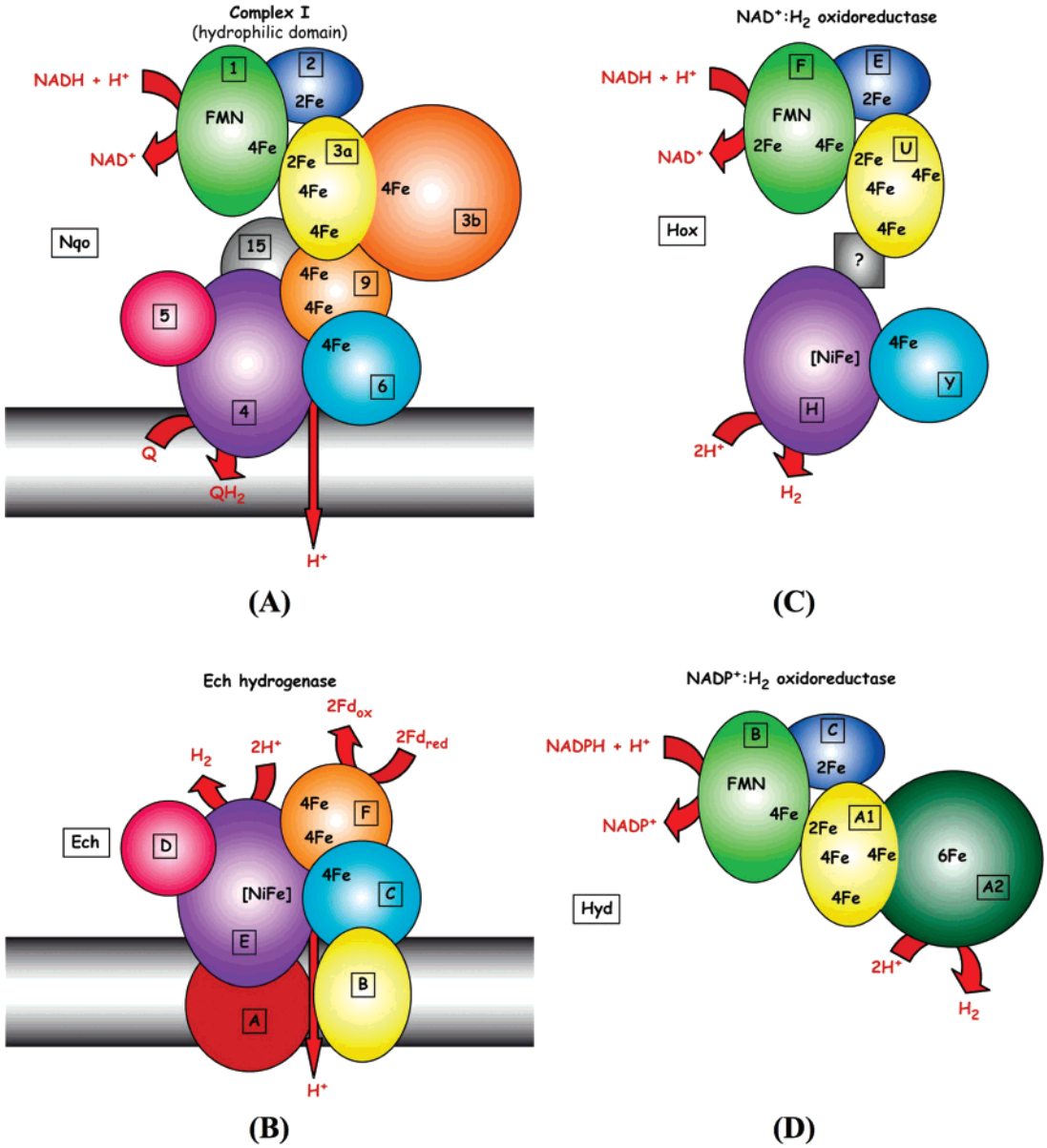

Figure 13. Schematic picture of complex I−hydrogenase relationships: **(**A**)** hydrophilic domain of *T. thermophilus* complex I;[170] **(**B**)** energy converting (Ech) hydrogenase from *M. barkeri*;[136] **(**C**)** NAD(P)$^+$-reducing [NiFe]-hydrogenase from *Synechocystis* sp. strain PCC 6803,[220] with unknown connection between the diaphorase and the hydrogenase part; **(**D**)** NADP$^+$-reducing [FeFe]-hydrogenase of *T. maritima*.[51] Each homologous subunit/domain is represented by a specifically colored ellipsoid. The gray rectangle represents the membrane.

distance from the FMN, may function as an antioxidant.[223] An extra FeS cluster in the Nqo3 C-terminal domain is too remote to be involved in fast electron transfer. However, in some other species this cluster may be rendered accessible by an additional, intervening [Fe_4S_4] cluster, as predicted by sequence similarities with the mesial [Fe_4S_4] cluster ligands in [FeFe]-hydrogenase.[47] In that case, the FeS cluster in the Nqo3 domain could provide an interaction site with an external redox partner.

Two of the seven hydrophobic membrane-bound subunits of complex I, namely, Nqo12 and Nqo8, are respectively homologous to *M. barkeri* energy-converting hydrogenase

(Ech) subunits A and B (Figure 13B). Moreover, Nqo12 and Nqo8 are homologous to bacterial K^+ or Na^+/H^+ antiporters, in agreement with a proton pumping function.[136] A Hox-EFUYH-type enzyme from *A. vinosum* has been recently used to study the similarities between complex I and NAD^+-reducing [NiFe]-hydrogenases.[224] The latter is predicted to contain two additional FeS clusters (shown in *italics* in Figure 13C), but because it does not have a subunit or domain homologous to Nqo9, it is not clear how diaphorase and hydrogenase communicate. This problem does not arise in $NADP^+$-reducing [FeFe]-hydrogenases (Figure 13D), because their H-cluster-containing domain is known to be tightly connected to the Nqo3a-related N-terminal region.[15] For the *D. fructosovorans* [FeFe]-enzyme, the thioredoxin-like fold of the C-terminal domain of its Nqo2-related HndA subunit has recently been confirmed by an NMR solution structure.[225]

The structural homology between the quinone-binding Nqo4 subunit and the [NiFe]-hydrogenase large subunit is extensive, including most of the secondary structure elements of the former. This is quite remarkable because their active sites catalyze different reactions. A hydrophobic gas tunnel between the small and the large subunit that leads to the active site in hydrogenase overlaps with a much wider tunnel in complex I that originates at the presumed membrane surface (Figure 13A). It seems likely that part of the long hydrophobic tail of the ubiquinone substrate binds here.[170] The two enzymes might share proton-transfer mechanisms, and it has been postulated that there may exist common pathways for these.[226] In the complex I structure water molecules are not resolved due to the limited 3.3 Å resolution, but there is a hydrophilic cavity between the conserved *Asp528*, which has been proposed to be involved in proton transfer in [NiFe]-hydrogenase,[13] and *Asp129* (Figure 14; see also section 5). The latter residue is exposed at the membrane surface, where it may interact with proton-translocating subunits. In hydrogenase there is no such cavity, the corresponding space being occupied by the three partially conserved *His111*, *His116*, and *His525*. Domain movements could help proton transfer in this region.

In complex I (and in energy converting hydrogenases) protons should arrive through a pathway that is connected to the cytoplasm and depart through a different pathway, connected to the membrane. To prevent proton leakage these pathways should not be active at the same time. Their functionality could be regulated by a change of redox state, which possibly triggers a dynamic change of the protein structure.[227] In the known [NiFe]-hydrogenase structures there are three kinked α-helices in the large subunit four-helix bundle (Figure 14). A shift of these kinked helices to a straight conformation could separate domains I_L and III_L, thus leading to the formation of a hydrophilic cavity between *Asp528* and *Asp129*, as observed in complex I. This might facilitate proton transfer in the membrane direction.

Other pathways may also benefit from domain movements. For example, the proximal cluster is connected via the invariant large subunit *His219* and *Arg63* to bulk solvent through a water network at the interface of the small subunit flavodoxin-like and C-terminal domains. The latter is replaced by a ferredoxin-like subunit in complex I, but *His219* and *Arg63* are conserved. Recently, it has been shown that the complex I histidine homologous to *His219* is responsible for the pH dependence of the $[Fe_4S_4]$ cluster midpoint potential.[228] Its substitution by methionine abolished this pH dependence without affecting the proton pumping efficiency. Therefore, the redox state of the cluster does not seem to affect proton pumping. Proton flow is probably controlled by the various redox and protonation states of the quinone substrate in complex I and probably this also applies to the Ni−Fe active site in hydrogenase.

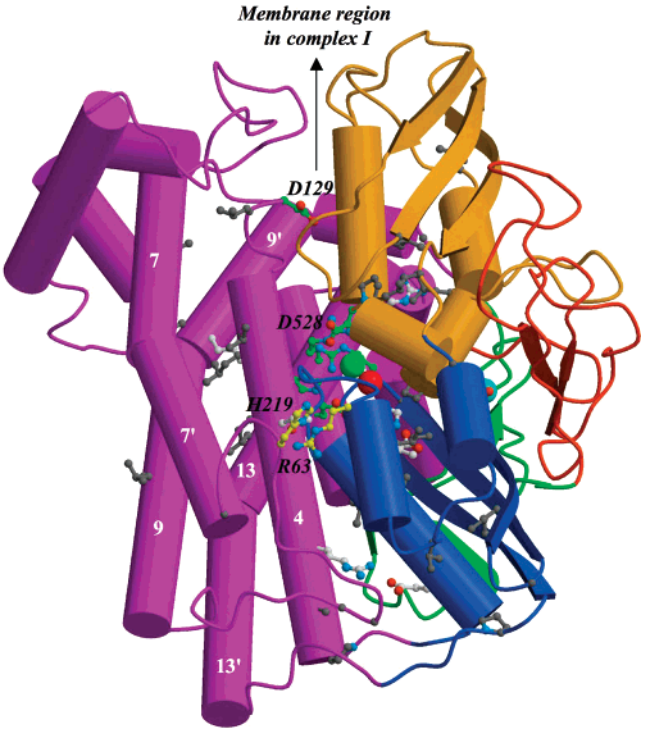

Figure 14. Structure of the large subunit of [NiFe]-hydrogenase (PDB code 1YQW), highlighting invariant residues in the Nqo4 subunit of complex I (PDB code 2FUG). Domains and metals are colored as in Figure 1. Carbons and bonds are depicted in gray for hydrophobic residues, white for hydrophilic ones, yellow for residues interacting with the proximal $[Fe_4S_4]$ cluster, and green for those that are involved in a putative dynamic proton-transfer pathway. The four-helix bundle with its three kinked α-helices 7, 9, and 13 is labeled.

7.2. Comparison of [FeFe]-Hydrogenase to Narf-like Proteins

The current efforts in genome sequencing of eukaryotic organisms have unexpectedly revealed the existence of genes coding for proteins that bear a remarkable similarity with [FeFe]-hydrogenases (Figure 15).[229,230] These proteins have been so far identified in yeast, plants, and humans. Their presence in these organisms is surprising, and it is generally assumed that they have acquired new functions. The first reported hydrogenase-like protein was the human Nar protein that was found to be associated to the cell nucleus-associated prelamin A.[229] Further work concerning the related yeast Nar1p has linked it to the maturation of cytosolic and nuclear FeS proteins.[231] In addition, this protein has been associated with ribosome biogenesis.[232] There are two novel observations more relevant to the subject of this chapter. In a very recent report Huang et al. have demonstrated that the [FeFe]-hydrogenase-like human protein IOP1 is involved in a network regulating genes as a function of oxygen pressure in mammal cells.[233] Mondy et al. have identified a dwarf mutant of the model plant *Medicago trunculata* affecting the Narf-like protein GOLLUM, the phenotype of which is observable at atmospheric partial oxygen pressure but is

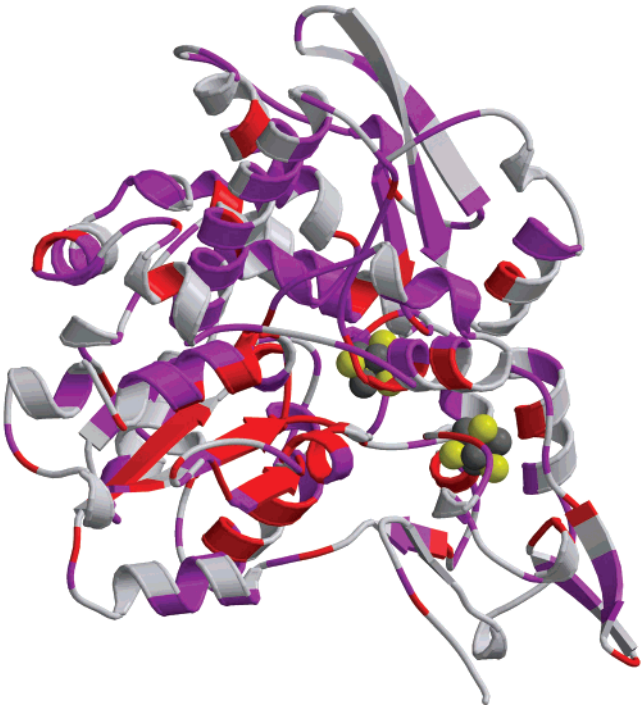

Figure 15. Ribbon drawing of *C. pasteurianum* Fe-hydrogenase (accession no. GI:4139441) from residue 133 to residue 574. The invariant residues in *Nar1p* are depicted in red, conserved substitutions are depicted in purple, and not conserved residues are depicted in gray. The iron and sulfur atoms of the clusters are respectively shown as gray and yellow balls.

absent at the lower oxygen pressure of 5 kPa (submitted for publication). These observations, along with the results from Fournier et al. involving the [FeFe]-hydrogenase from *D. vulgaris* that is proposed to be implicated in protective mechanisms against oxidative stress,[234] suggest that these enzymes may be ancestral to proteins possessing an oxygen-response function in eukaryotes. Using an approach combining EPR and cysteine mutagenesis we have found that GOLLUM coordinates two $[Fe_4S_4]$ clusters, one of which corresponds to the cubane of the H-cluster in [FeFe]-hydrogenases (unpublished results). However, it is not clear what substitutes the Fe−Fe subcluster in Narf-like proteins, which do not display hydrogenase activity (unpublished results).

8. Substrate Binding And Catalysis

8.1. [NiFe]-Hydrogenases

Hydrogenases have three different substrates/products: molecular hydrogen, protons, and electrons. Because hydrogen cleavage is heterolytic, the active site must also bind hydride. Hydrons are not detectable by X-ray crystallography at the resolutions that have been obtained so far. Therefore, the hydrogenase crystal structures provide only indirect information on substrate binding. Many different stable Ni−Fe site intermediates have been observed by EPR and FTIR spectroscopy (Figure 3). Crystallographic evidence has been discussed in section 6.1 concerning the nature of bound oxygen species in the active site of unready (Ni-A and Ni-SU) and ready enzyme states (Ni-B). In crystal structures of reduced, active enzyme there is no evidence for the presence of an exogenous ligand.[12,41] However, a hydride may be bound at the E2 site (Figure 2) because in the reduced active site there is no significant change in the conformation of the Ni thiolate ligands. A bound hydride would make the otherwise peculiar Ni coordination square pyramidal. Moreover, the Ni−Fe distance is 2.6 Å, compatible with the binding of a bridging hydride between these two metal ions.[235]

Because of redox reactions with the FeS clusters and proton-transfer reactions, different Ni−Fe states are normally at thermodynamic equilibrium. It is therefore rather difficult to obtain hydrogenase crystals in a single homogeneous state. A microstate formalism has been proposed to describe the enzyme as ensembles of redox states, the compositions of which depend on the pH and the potential of the environment. Redox titrations of *D. gigas* [NiFe]-hydrogenase that were fitted to theoretical curves favored a model where the Ni-C state is two electrons more reduced than the Ni-B state.[236] Because these two EPR active states are best described as corresponding to Ni(III) species,[237] the two-electron difference would arise from the presence of a hydride in Ni-C. Only the Ni-C/Ni-R and one of the $[Fe_4S_4]^{2+}/[Fe_4S_4]^{+}$ redox couples have been found to be in redox equilibrium with molecular hydrogen.[236,238] If the enzyme in the Ni-C state can react with hydrogen, as this result implies, then both E1 and E2 should be able to bind hydrons. One possibility mentioned above is that the putative hydride in Ni-C is bound at the bridging E2 site, leaving E1 available for substrate binding. In agreement with this hypothesis, added CO was observed to bind terminally to the Ni at the E1 site in the crystal structure of *D. vulgaris* Miyazaki F hydrogenase.[35] This result confirmed previous IR data that indicated that the vibrational frequency of bound CO was not compatible with a bridging binding mode in either *A. vinosum* or *D. fructosovorans* [NiFe]-hydrogenase.[29,239]

Recent direct evidence for bound hydride in the Ni-C state of the regulatory [NiFe]-hydrogenase from *R. eutropha* has been obtained using HYSCORE and ENDOR spectroscopies.[240] Furthermore, the single-crystal EPR study of the same state of *D. vulgaris* Miyazaki F hydrogenase indicated that, on the basis of the g-tensor orientation, the hydride was bound to the Ni-Fe bridging E2 position,[241] a result confirmed by a more recent ENDOR/HYSCORE study of the same enzyme.[242] As observed previously,[243] the ^1H hyperfine coupling assigned to the bound hydride was lost upon exposure of the hydrogenase sample to light.[240] This indicated photolytic cleavage of metal−hydride bonds resulting in the EPR-active Ni-L state. According to DFT calculations this state corresponds to a formal Ni^+ species, suggesting that the two electrons from the hydride are taken by the Ni ion and the hydron dissociates as a proton.[244] As XAS studies do not show a significant shift of the Ni absorption edge between the Ni-C and Ni-L states,[243,245] the electron density is probably highly delocalized over the active site. The proton photodissociated from Ni may have several potential binding sites, as suggested by the finding of three different Ni-L states (see, e.g., Dole et al.[246]). Different protonation states have also been observed for the Ni-SI and Ni-R forms.[32,247] One of the protonation sites is probably a Ni thiolate ligand (Figure 7A), a likely candidate being *Cys530* (see Figure 2A and section 5), which is close (perpendicular) to both the E1 and E2 sites. Table 4 shows the catalytic activity of selected [NiFe]-hydrogenases.

8.2. [FeFe]-Hydrogenases

Prior to the X-ray structural analyses, spectroscopic studies have been complicated by problems in determining the

Table 4. Specific Activities of [NiFe]-Hydrogenases[a]

	H_2 uptake (U)		H_2 evolution (U)	
	as isolated	activated	as isolated	activated
Desulfovibrio gigas	30[b]	1500[bc]	nd	440[b,c]
Desulfovibrio fructosovorans				
aerobic purification[b]	40	700	nd	400
anaerobic purification[d]	1250	nd	nd	nd
Dm. baculatum ([NiFeSe]-hydrogenase)	190[b]	1700[b]	2000[e]	nd
DvH ([NiFeSe]-hydrogenase)[f]	900	nd	6908	nd
Ralstonia eutropha SH	202	nd	8	nd
Ralstonia eutropha MBH[h]	40.5	nd	nd	nd
Ralstonia eutropha RH[i]				
aerobic purification	1.67	nd	nd	nd
anaerobic purification	1.78	nd	nd	nd

[a] Temperature, 30 °C; substrates, methylviologen for *Desulfovibrio* and *Desulfomicrobium* (*Dm.*) enzymes, idem for *Desulfovibrio vulgaris* (Hildenborough) (DvH) [NiFeSe]-hydrogenase H_2 evolution, benzylviologen for DvH [NiFeSe]-hydrogenase H_2 uptake, benzylviologen, NAD^+ or NADH for *Ralstonia* enzymes; U, μmol of $H_2 \cdot min^{-1} \cdot$mg of protein^{-1}; nd, not determined. [b] C. Cavazza, unpublished results. [c] Fauque et al. *FEMS Microbiol. Rev.* **1988**, *54*, 299. [d] Reference 40. [e] Reference 22. [f] Reference 178. [g] Van der Linden et al. *J. Biol. Inorg. Chem.* **2006**, *11*, 247−260. [h] Schneider et al. *Biochem. J.* **1983**, *213*, 391−398. [i] Reference 202.

composition of the H-cluster and the presence of unprecedented magnetic signals. One of the major obstacles had been establishing the number of Fe ions involved in the active site. Although metal content analysis may be accurate, determining the number of metal ions per protein molecule heavily relies on the way the protein concentration is determined. In this respect, colorimetric methods are not reliable enough; only amino acid composition determination seems to be accurate. In addition, spin concentrations, as measured by EPR spectroscopy, often indicate substoichiometric amounts of paramagnetic species in the active site. Initial estimates of iron content in the H-cluster ranged from one to six atoms. The last model published prior to the X-ray studies proposed a $[Fe_4S_4]$ cubane linked to a mononuclear low-spin iron coordinated by one CN^- and one CO.[57] The diatomic ligands were included because FTIR studies of DvH had shown the presence of high-frequency bands similar to those observed in [NiFe]-hydrogenases.[64]

EPR-monitored redox titrations[191,248] have indicated that, besides signals arising from two ferredoxin-like $[Fe_4S_4]$ clusters, [FeFe]-hydrogenases from *Desulfovibrio* sp. display two rhombic signals generated by the H-cluster: although aerobically prepared oxidized DvH enzyme is EPR silent (the H_{ox}^{inact} state), one-electron reduction results in an oxidized paramagnetic species with g_x equal to 2.06 called $H_{ox2.06}$ or H_{trans}.[249,250] These species have not been detected in CpII, an enzyme that is irreversibly damaged if purified aerobically. Further treatment with H_2 reductively activates the Dd enzyme, giving rise to a state with a rhombic $g_x = 2.10$ signal called $H_{ox2.10}$. $H_{ox2.06}$ and $H_{ox2.10}$ were thought to be isoelectronic,[191,251] but recent redox titrations monitored by FTIR spectroscopy[250] indicate that the latter is two electrons more reduced than the former. However, the two electrons do not reduce the Fe−Fe unit.[251] Of the two paramagnetic species only $H_{ox2.10}$ is found in both CpII and Dd hydrogenases, where it is catalytically relevant and at redox equilibrium with molecular hydrogen.[57] Thus, in this respect $H_{ox2.10}$ is analogous to the Ni-C species in [NiFe]-hydrogenases (Figure 3). $H_{ox2.06}$ is thought to contain some oxygen-derived species, also present in the H_{ox}^{inact} state, which must dissociate to generate $H_{ox2.10}$. Although H_{ox}^{inact} is stable under air, subsequent reduction and reoxidation in the presence of oxygen damages the active site. Thus, the putative oxygen-derived species bound to the H-cluster in H_{ox}^{inact} seems to afford protection against air exposure.[252] Further reduction of the H-cluster generates H_{red} that is diamagnetic.

After the crystal structures of CpI and Dd hydrogenases indicated that the H-cluster is composed of a standard cubane and a binuclear Fe center, re-interpretation of the spectroscopic data was in order. Thus, Popescu and Münck reanalyzed the Mössbauer and ENDOR data collected earlier from CpII,[253] an enzyme similar to the Dd hydrogenase. Pereira et al. have carried out a similar Mössbauer analysis with the DvH enzyme.[251] Both groups have addressed the assignment of valence to the different H-cluster states. Popescu and Münck concluded that the cubane in the H-cluster is in the 2+ state in all of the spectroscopically observable forms of the active site of CpII.[253] This implies that all of the detected electronic changes in this hydrogenase must take place either at the Fe−Fe cluster or at a ligand bound to it. In the fully oxidized EPR-silent H_{ox}^{inact} state of DvH hydrogenase the cluster is proposed to be electronically coupled $Fe_D(III)-Fe_P(III)$ (where D and P denote, respectively, distal and proximal positions relative to the cubane, see Figure 5). As mentioned above, it is possible that some oxygen-derived species binds to Fe_D in this state. Indeed, Peters et al. modeled a water molecule bound to Fe_D in the CpI hydrogenase structure.[15] One-electron reduction of H_{ox}^{inact} results in the inactive $H_{ox2.06.}$ Pereira et al. concluded that H_{ox}^{inact} could be either $Fe_D(II)-Fe_P(II)$ or antiferromagnetically coupled $Fe_D(III)-Fe_P(III)$ and that the one-electron reduction to the $H_{ox2.06}$ concerns the cubane that is now in the 1+ state.[251] It seems more reasonable to postulate an $Fe_D(II)-Fe_P(II)$ unit than an $Fe_D(III)-Fe_P(III)$ unit sitting next to a cubane in the 1+ state and, consequently, only the former proposition will be discussed. The two electrons required to generate the active $H_{ox2.10}$ from $H_{ox2.06}$ could in principle reduce the Fe−Fe unit, but Mössbauer results suggests this is not the case.[251] Reduction should then affect the putative oxygen-derived species and force its dissociation. One possibility is the reduction of a peroxo ligand to a hydroxo ligand plus water as postulated for the Ni-SU to Ni-Si transition in [NiFe]-hydrogenases.[40] Thus, $Hox_{2.10}$ could be assigned to an $Fe_D(II)-Fe_P(I)$ species with the cubane in the 2+ redox state. Further reduction generates the H_{red} form with H^--$Fe_D(II)-Fe_P(II)$ as a plausible structure (Figure 16).[251,253] CO binds to the H-cluster and forms a paramagnetic complex that is isoelectronic with $H_{ox2.10}$. Again, this observation favors an $Fe_D(II)-Fe_P(I)$ unit for $Hox_{2.10}$ because CO binds well to electron-rich metal centers. Table 5 shows

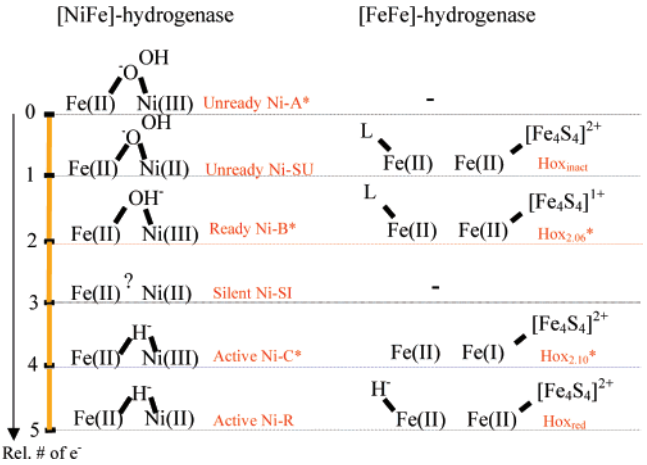

Figure 16. Comparison of proposed redox states in [NiFe]- and [FeFe]-hydrogenases. The oxidized [NiFe]-hydrogenase states are assigned as discussed in section 6.1. The asterisk indicates an EPR-active species. "L" might be a partially reduced oxygen species such as peroxide.

the catalytic activities of selected [FeFe]-hydrogenases.

8.3. Comparison of Active Redox States in [NiFe]- and [FeFe]-Hydrogenases

During catalysis by [FeFe]-hydrogenases, and by analogy with CO, hydrogen should bind at Fe_D of the $Hox_{2.10}$ species. Polarization of the H−H bond would be induced by the bridgehead N atom of the small active site organic molecule and Fe_D. Assuming, as above, that $Hox_{2.10}$ is an $Fe_D(II)-Fe_P(I)$ species, the uptake reaction could take place as follows:

$$H_2 + Fe_D(II)-Fe_P(I) \rightarrow H^- - Fe_D(II)-Fe_P(II) + H^+ + e^- \rightarrow Fe_D(I)-Fe_P(I) + H^+ \rightarrow Fe_D(II)-Fe_P(I) + e^-$$

This hypothesis puts forward a H_{red} species $H^- - Fe_D(II)-Fe_P(II)$ similar to the proposed Ni-R state in [NiFe]-hydrogenases (Figure 3). In these enzymes, the active site Ni−Fe center is thought to go initially from Ni(II)−Fe(II) (the Ni-SI state) to Ni(III)−H^-−Fe(II) (Ni-C) + H^+ + e^- upon reaction with molecular hydrogen. However, during turnover only Ni-C and Ni-R [Ni(II)−H^-−Fe(II)] are thought to be in redox equilibrium with H_2.[236,238] The same seems to apply to [FeFe]-hydrogenases, where $H_{2.10}$ and H_{red} are the only observable active species. Consequently, in both enzymes there should be an unobserved, transient state that is two electrons more reduced than Ni-C or $Hox_{2.10}$, that is, $H^- - Ni(III) - H^- - Fe(II)$ [formally equivalent to $H^+ - Ni(I) - H^- - Fe(II)$] and $H^- - Fe_D(II) - Fe_P(I)$, respectively. This state decays rapidly to yield Ni-R or H_{red} by transferring one electron to one of the $[Fe_4S_4]$ clusters. The first electron is then not transferred to the other redox centers from the hydride but from a metal ion. This may be a requirement of the reaction as electrons are transferred one at a time and the hydride is a two-electron species. In the reduced (H_{red}) [FeFe] enzyme, the intrinsic bridging CO becomes terminally bound to Fe_D, suggesting that its role is to mitigate the effect of the additional electron density contributed by the hydride bound trans to it (see Figure 5).[47] Figure 16 summarizes these ideas.

9. Concluding Remarks

In this paper we have tried to give a coherent view of how the crystal structures of [NiFe]- and [FeFe]-hydrogenases have contributed to our understanding of hydrogen biocatalysis in general. The three-dimensional structures cannot provide a complete picture of this process. However, without the spatial models, especially of the active sites, the interpretation of spectroscopic data, EPR, XAS, FTIR, etc., is severely handicapped. This is also true for the molecular biology of active site cluster assembly and the electrochemical studies of hydrogenases. Besides allowing plausible models for catalysis to be put forward from the active site structures, these serve as a source of inspiration for the synthesis of biomimetic models.

A particular aspect of hydrogenase research has become especially popular: the oxygen sensitivy of these enzymes. In a world that is increasingly concerned by the greenhouse effects derived from fossil fuel utilization, the production of biohydrogen by oxygen-evolving photosynthetic organisms has become a plausible solution to global energy requirements. Thus, either designing or discovering oxygen-resistant hydrogenases seems to be urgent. Initial steps in the right direction are being taken by the site-directed mutagenesis of amino acid residues lining the hydrophobic tunnels within hydrogenases. Acting as sieves, the tunnels can be made to discriminate between oxygen and hydrogen molecules on the basis of their size. Here, the availability of crystal structures has been essential.

In spite of the wealth of information obtained from the crystallographic studies, there is still much to be done. We badly need the structure of Knallgas bacterial hydrogenases, naturally significantly resistant to oxygen, to better under-

Table 5. Specific Activities of [FeFe]-Hydrogenases[a]

	H_2 uptake (U)		H_2 evolution (U)	
	as isolated	activated	as isolated	activated
Desulfovibrio desulfuricans[b]				
aerobic purification	19300	62200	8200	8200
anaerobic purification	60000		nd	nd
Chlamydomonas reinhardtii[c]				
anaerobic purification	nd	nd	935	nd
Clostridium pasteurianum I[d]				
anaerobic purification	24000	nd	5500	nd
Clostridium pasteurianum II[d]				
anaerobic purification	34000	nd	10	nd
Megasphaera elsdenii[d]				
anaerobic purification	9000	nd	7000	nd

[a] Substrates, methylviologen for H_2 evolution, methylviologen, benzylviologen, or methylene blue for H_2 uptake; U, μmol of $H_2 \cdot min^{-1} \cdot mg$ of $protein^{-1}$; nd, not determined. [b] Hatchikian et al. *Eur. J. Biochem.* **1992**, *209*, 357−365. [c] Reference 54. [d] Reference 49.

stand the basis of this resistance. We also need more structures where the active sites are poised at well-defined redox states to establish meaningful structure/function relationships. Last but not least, we need to better understand the evolutionary relationships between hydrogenases, complex I, and Narf-like proteins.

The next few years should provide answers to these important questions.

10. Acknowledgments

We thank the CEA and the CNRS for institutional support and the reviewers for their careful reading and correction of the original manuscript.

11. Note Added after ASAP Publication

This paper was published ASAP on September 13, 2007. A reference and its citation in the text were amended, and the paper was reposted on September 14, 2007.

12. References

(1) Collman, J. P. *Nat. Struct. Biol.* **1996**, *3*, 213.
(2) Zirngibl, C.; Hedderich, R.; Thauer, R. K. *FEBS Lett.* **1990**, *261*, 112.
(3) Lyon, E. J.; Shima, S.; Buurman, G.; Chowdhuri, S.; Batschauer, A.; Steinbach, K.; Thauer, R. K. *Eur. J. Biochem.* **2004**, *271*, 195.
(4) Shima, S.; Lyon, E. J.; Sordel-Klippert, M.; Kauss, M.; Kahnt, J.; Thauer, R. K.; Steinbach, K.; Xie, X.; Verdier, L.; Griesinger, C. *Angew. Chem.* **2004**, *43*, 2547.
(5) Shima, S.; Lyon, E. J.; Thauer, R. K.; Mienert, B.; Bill, E. *J. Am. Chem. Soc.* **2005**, *127*, 10430.
(6) Lyon, E. J.; Shima, S.; Boecher, R.; Thauer, R. K.; Grevels, F. W.; Bill, E.; Roseboom, W.; Albracht, S. P. J. *J. Am. Chem. Soc.* **2004**, *126*, 14239.
(7) Korbas, M.; Vogt, S.; Meyer-Klaucke, W.; Bill, E.; Lyon, E. J.; Thauer, R. K.; Shima, S. *J. Biol. Chem.* **2006**, *281*, 30804.
(8) Pilak, O.; Mamat, B.; Vogt, S.; Hagemeier, C. H.; Thauer, R. K.; Shima, S.; Vonrhein, C.; Warkentin, E.; Ermler U. *J. Mol. Biol.* **2006**, *358*, 796.
(9) Volbeda, A.; Charon, M. H.; Piras, C.; Hatchikian, E. C.; Frey, M.; Fontecilla-Camps, J. C. *Nature* **1995**, *373*, 580.
(10) Higuchi, Y.; Yagi, T.; Yasuoka, N. *Structure* **1997**, *5*, 1671.
(11) Montet, Y.; Amara, P.; Volbeda, A.; Vernéde, X.; Hatchikian, E. C.; Field, M. J.; Frey, M.; Fontecilla-Camps, J. C. *Nat. Struct. Biol.* **1997**, *4*, 523.
(12) Garcin, E.; Vernede, X.; Hatchikian, E. C.; Volbeda, A.; Frey, M.; Fontecilla-Camps, J. C. *Structure* **1999**, *7*, 557.
(13) Matias, P. M.; Soares, C. M.; Saraiva, L. M.; Coelho, R.; Morais, J.; Le Gall, J.; Carrondo, M. A. *J. Biol. Inorg. Chem.* **2001**, *6*, 63.
(14) Nicolet, Y.; Piras, C.; Legrand, P.; Hatchikian, C. E.; Fontecilla-Camps, J. C. *Structure* **1999**, *7*, 13.
(15) Peters, J. W.; Lanzilotta, W. N.; Lemon, B. J.; Seefeldt, L. C. *Science* **1998**, *282*, 1853.
(16) Higuchi, Y.; Yasuoka, N.; Kakudo, Y.; Katsube, Y.; Yagi, T.; Inokuchi, H. *J. Biol. Chem.* **1987**, *262*, 2823.
(17) Niviére, V.; Hatchikian, E. C.; Cambillaud C.; Frey, M. *J. Mol. Biol.* **1987**, *195*, 969.
(18) Cammack, R.; Fernandez, V. M.; Hatchikian, E. C. *Methods Enzymol.* **1994**, *243*, 43.
(19) Smith, W. W.; Burnett, R. M.; Darling, G. D.; Ludwig, M. L. *J. Mol. Biol.* **1977**, *117*, 195.
(20) Volbeda, A.; Piras, C.; Charon, M.-H.; Hatchikian, E. C.; Frey, M.; Fontecilla-Camps, J. C. *ESF/CCP4 Newsl.* **1993**, *28*, 30.
(21) Higuchi, Y.; Okamoto, T.; Fujimoto, K.; Misaki, S. *Acta Crystallogr., D* **1994**, *50*, 781.
(22) He, S. H.; Teixeira, M.; Le Gall, J.; Patil, D. S.; Moura, I.; Moura, J. J.; DerVartanian, D. V.; Huynh, B. H.; Peck, Jr., H. D. *J. Biol. Chem.* **1989**, *264*, 2678.
(23) Eidsness, M. K.; Scott, R. A.; Prickril, B. C.; DerVartanian, D. V.; LeGall, J.; Moura, I.; Moura, J. J.; Peck, Jr., H. D. *Proc. Natl. Acad. Sci. U.S.A.* **1989**, *86*, 147.
(24) Sorgenfrei, O.; Klein, A.; Albracht, S. P. J. *FEBS Lett.* **1993**, *332*, 291.
(25) Hatchikian, E. C.; Bruschi, M.; LeGall, J. *Biochem. Biophys. Res. Commun.* **1978**, *82*, 451.
(26) Volbeda, A.; Garcin, E.; Piras, C.; De Lacey, A. L.; Fernandez, V. M.; Hatchikian, E. C.; Frey, M.; Fontecilla-Camps, J. C. *J. Am. Chem. Soc.* **1996**, *118*, 12989.
(27) Menon, N. K.; Robbins, J.; DerVartanian, M.; Patil, D.; Peck, Jr., H. D.; Menon, A. L.; Robson, R. L.; Przybyla, A. E. *FEBS Lett.* **1993**, *331*, 91.
(28) Sorgenfrei, O.; Linder, D.; Karas, M.; Klein, A. *Eur. J. Biochem.* **1993**, *213*, 1355.
(29) Bagley, K. A.; Van Garderen, C. J.; Chen, M.; Duin, E. C.; Albracht, S. P.; Woodruff, W. H. *Biochemistry* **1994**, *33*, 9229.
(30) Bagley, K. A.; Duin, E. C.; Roseboom, W.; Albracht, S. P. J.; Woodruff, W. H. *Biochemistry* **1995**, *34*, 5527.
(31) Happe, R. P.; Roseboom, W.; Pierik, A. J.; Albracht, S. P. J.; Bagley, K. A. *Nature* **1997**, *385*, 126.
(32) De Lacey, A. L.; Hatchikian, E. C.; Volbeda, A.; Frey, M.; Fontecilla-Camps, J. C.; Fernandez, V. M. *J. Am. Chem. Soc.* **1997**, *119*, 7181.
(33) Pierik, A. J.; Roseboom, W.; Happe, R. P.; Bagley, K. A.; Albracht, S. P. J. *J. Biol. Chem.* **1999**, *274*, 3331.
(34) Volbeda, A.; Montet, Y.; Vernède, X.; Hatchikian, E. C.; Fontecilla-Camps, J. C. *Int. J. Hydr. Energy* **2002**, *27*, 1449.
(35) Ogata, H.; Mizoguchi, Y.; Mizuno, N.; Miki, K.; Adachi, S.; Yasuoka, N.; Yagi, T.; Yamauchi, O.; Hirota, S.; Higuchi, Y. *J. Am. Chem. Soc.* **2002**, *124*, 11628.
(36) Ogata, H.; Hirota, S.; Nakahara, A.; Komori, H.; Shibata, N.; Kato, T.; Kano, K.; Higuchi, Y. *Structure* **2005**, *13*, 1635.
(37) Fichtner, C.; Laurich, C.; Bothe, E.; Lubitz, W. *Biochemistry* **2006**, *45*, 9706.
(38) Volbeda, A.; Fontecilla Camps, J. C. *Coord. Chem. Rev.* **2005**, 1609.
(39) Fernandez, V. M.; Hatchikian, E. C.; Cammack, R. *Biochim. Biophys. Acta* **1985**, 832, 69.
(40) Volbeda, A.; Martin, L.; Cavazza, C.; Matho, M.; Faber, B. W.; Roseboom, W.; Albracht, S. P.; Garcin, E.; Rousset, M.; Fontecilla-Camps, J. C. *J. Biol. Inorg. Chem.* **2005**, *10*, 239.
(41) Higuchi, Y.; Ogata, H.; Miki, K.; Yasuoka, N.; Yagi, T. *Structure* **1999**, *7*, 549.
(42) Voordouw, G.; Brenner, S. *Eur. J. Biochem.* **1985**, *148*, 515.
(43) Meyer, J.; Gagnon, J. *Biochemistry* **1991**, *30*, 9697.
(44) Gorwa, M. F.; Croux, C.; Soucaille, P. *J. Bacteriol.* **1996**, *178*, 2668.
(45) Atta, M.; Meyer, J. *Biochim. Biophys. Acta* **2000**, *1476*, 368.
(46) Hatchikian, E. C.; Magro, V.; Forget, N.; Nicolet, Y.; Fontecilla-Camps, J. C. *J. Bacteriol.* **1999**, *181*, 2947.
(47) Nicolet, Y.; Lemon, B. J.; Fontecilla-Camps, J. C.; Peters, J. W. *Trends Biochem. Sci.* **2000**, *25*, 138.
(48) Chen, J. S.; Mortenson, L. E. *Biochim. Biophys. Acta* **1974**, *371*, 283.
(49) Adams, M. W. W. *Biochim. Biophys. Acta* **1990**, *1020*, 115.
(50) Kaji, M.; Taniguchi, Y.; Matsushita, O.; Katayama, S.; Miyata, S.; Morita, S.; Okabe, A. *FEMS Microbiol. Lett.* **1999**, *181*, 329.
(51) Verhagen, M. F.; O'Rourke, T.; Adams, M. W. *Biochim. Biophys. Acta* **1999**, *1412*, 212.
(52) Soboh, B.; Linder, D.; Hedderich, R. *Microbiology* **2004**, *150*, 2451.
(53) Erbes, D. L.; King, D.; Gibbs, M. *Plant Physiol.* **1979**, *63*, 1138.
(54) Happe, T.; Naber, J. D. *Eur. J. Biochem.* **1993**, *214*, 475.
(55) Florin, L.; Tsokoglou, A.; Happe, T. *J. Biol. Chem.* **2001**, *276*, 6125.
(56) Winkler, M.; Heil, B.; Heil, B.; Happe, T. *Biochim. Biophys. Acta* **2002**, *1576*, 330.
(57) Pierik, A. J.; Hulstein, M.; Hagen, W. R.; Albracht, S. P. J. *Eur. J. Biochem.* **1998**, *258*, 572.
(58) Nicolet, Y.; De Lacey, A. L.; Vernède, X.; Fernandez, V. M.; Hatchikian, E. C.; Fontecilla-Camps, J. C. *J. Am. Chem. Soc.* **2001**, *123*, 1596.
(59) Lemon, B. J.; Peters, J. W. *Biochemistry* **1999**, *38*, 12969.
(60) Curtis, C. J.; Medaner, A.; Clancanelli, R.; Ellis, W. W.; Noll, B. C.; Rakowski Dubois, M.; Dubois, D. L. *Inorg. Chem.* **2003**, *42*, 216.
(61) Thomann, H.; Bernardo, M.; Adams, M. W. W. *J. Am. Chem. Soc.* **1991**, *113*, 7044.
(62) Williams, R.; Cammack, R.; Hatchikian, E. C. *J. Chem. Soc., Faraday Trans.* **1993**, *89*, 2869.
(63) Van Dam, P. J.; Reijerse, E. J.; Hagen, W. R. *Eur. J. Biochem.* **1997**, *248*, 355.
(64) Van der Spek, T. M.; Arendsen, A. F.; Happe, R. P.; Yun, S.; Bagley, K. A.; Stufkens, D. J.; Hagen, W. R.; Albracht, S. P. J. *Eur. J. Biochem.* **1996**, *237*, 629.
(65) Posewitz, M. C.; King, P. W.; Smolinski, S. L.; Zhang, L.; Seibert, M.; Ghirardi, M. L. *J. Biol. Chem.* **2004**, *279*, 25711.
(66) Brazzolotto, X.; Rubach, J. K.; Gaillard, J.; Ganbarelli, S.; Atta, M.; Fontecave, M. *J. Biol. Chem.* **2006**, *281*, 769.
(67) Johnson, D. C.; Dean, D. R.; Smith, A. D.; Johnson, M. K. *Annu. Rev. Biochem.* **2005**, *74*, 247.
(68) Kiley, P. J.; Beinert, H. *FEMS Microbiol. Rev.* **1999**, *22*, 341.
(69) Vignais, P. M.; Colbeau, A. *Curr. Issues Mol. Biol.* **2004**, *6*, 159.

(70) Valko, M.; Morris, H.; Cronin, M. T. D. *Curr. Med. Chem.* **2005**, *12*, 1161.
(71) Schreiter, E. R.; Wang, S. C.; Zamble, D. B.; Drennan, C. L. *Proc. Natl. Acad. Sci. U.S.A.* **2006**, *103*, 13676.
(72) Cherrier, M. V.; Martin, L.; Cavazza, C.; Jacquamet, L.; Lemaire, D.; Gaillard, J.; Fontecilla-Camps, J. C. *J. Am. Chem. Soc.* **2005**, *127*, 10075.
(73) Jacobi, A.; Rossmann, R.; Böck, A. *Arch. Microbiol.* **1992**, *158*, 444.
(74) Barrett, E. L.; Kwan, H. S.; Macy, J. *J. Bacteriol.* **1984**, *158*, 972.
(75) Paschos, A.; Glass, R. S.; Böck, A. *FEBS Lett.* **2001**, *488*, 9.
(76) Wolf, I.; Buhrke, T.; Dernedde, J.; Pohlmann, A.; Friedrich, B. *Arch. Microbiol.* **1998**, *170*, 451.
(77) Rosano, C.; Zuccotti, S.; Bucciantini, M.; Stefani, M.; Ramponi, G.; Bolognesi, M. *J. Mol. Biol.* **2002**, *321*, 785.
(78) Rain, J. C.; Selig, L.; De Reuse, H.; Battaglia, V.; Reverdy, C.; Simon, S.; Lenzen, G.; Petel, F.; Wojcik, J.; Schachter, V.; Chemama, Y.; Labigne, A.; Legrain, P. *Nature* **2001**, *409*, 211.
(79) Blokesch, M.; Paschos, A.; Bauer, A.; Reissmann, S.; Drapal, N.; Böck, A. *Eur. J. Biochem.* **2004**, *271*, 3428.
(80) Jones, A. K.; Lenz, O.; Strack, A.; Buhrke, T.; Friedrich, B. *Biochemistry* **2004**, *43*, 13467.
(81) Li, C.; Kappock, T. J.; Stubbe, J.; Weaver, T. M.; Ealick, S. E. *Structure* **1999**, *7*, 1155.
(82) Reissmann, S.; Hochleitner, E.; Wang, H.; Paschos, A.; Lottspeich, F.; Glass, R. S.; Böck, A. *Science* **2003**, *299*, 1067.
(83) Roseboom, W.; Blokesch, M.; Böck, A.; Albracht, S. P. J. *FEBS Lett.* **2005**, *579*, 469.
(84) Magalon, A.; Böck, A. *J. Biol. Chem.* **2000**, *275*, 21114.
(85) Blokesch, M.; Albracht, S. P. J.; Matzanke, B. F.; Drapal, N. M.; Jacobi, A.; Böck, A. *J. Mol. Biol.* **2004**, *344*, 155.
(86) Waugh, R.; Boxer, D. H. *Biochimie* **1986**, *68*, 157.
(87) Magalon, A.; Blokesch, M.; Zehelein, E.; Böck, A. *FEBS Lett.* **2001**, *499*, 73.
(88) Maier, T.; Jacobi, A.; Sauter, M.; Böck, A. *J. Bacteriol.* **1993**, *175*, 630.
(89) Gasper, R.; Scrima, A.; Wittinghofer, A. *J. Biol. Chem.* **2006**, *281*, 27492.
(90) Lee, M. H.; Mulrooney, S. B.; Renner, M. J.; Markowicz, Y.; Hausinger, R. P. *J. Bacteriol.* **1992**, *174*, 4324.
(91) Kerby, R. L.; Ludden, P. W.; Roberts, G. P. *J. Bacteriol.* **1997**, *179*, 2259.
(92) Olson, J. W.; Maier, R. J. *J. Bacteriol.* **2000**, *182*, 1702.
(93) Leach, M. R.; Sandal, S.; Sun, H.; Zamble, D. B. *Biochemistry* **2005**, *44*, 12229.
(94) Menon, N. K.; Chatelus, C. Y.; Der Vartanian, M.; Wendt, J. C. Shanmugam, K. T.; Peck, H. D., Jr.; Przybyla, A. E. *J. Bacteriol.* **1994**, *176*, 4416.
(95) Böhm, R.; Sauter, M.; Böck, A. *Mol. Microbiol.* **1990**, *4*, 231.
(96) Zhang, J. W.; Butland, G.; Greenblatt, J. F.; Emili, A.; Zamble, D. B. *J. Biol. Chem.* **2005**, *280*, 4360.
(97) Theodoratou, E.; Huber, R.; Böck, A. *Biochem. Soc. Trans.* **2005**, *33*, 108.
(98) Fritsche, E.; Paschos, A.; Beisel, H. G.; Böck, A.; Huber, R. *J. Mol. Biol.* **1999**, *288*, 989.
(99) Rossmann, R.; Maier, T.; Lottspeich, F.; Böck, A. *Eur. J. Biochem.* **1995**, *227*, 545.
(100) Menon, A. L.; Robson, R. L. *J. Bacteriol.* **1994**, *176*, 291.
(101) Theodoratou, E.; Paschos, A.; Magalon, A.; Fritsche, E.; Huber, R.; Böck, A. *Eur. J. Biochem.* **2000**, *267*, 1995.
(102) Theodoratou, E.; Paschos, A.; Mintz-Weber, S.; Böck, A. *Arch. Microbiol.* **2000**, *173*, 110.
(103) King, P. W.; Posewitz, M. C.; Ghirardi, M. L.; Seibert, M. *J. Bacteriol.* **2006**, *188*, 2163.
(104) Pan, G.; Menon, A. L.; Adams, M. W. W. *J. Biol. Inorg. Chem.* **2003**, *8*, 469.
(105) Chirpich, T. P.; Zappia, V.; Costilow, R. N.; Barker, H. A. *J. Biol. Chem.* **1970**, *245*, 1778.
(106) Frey, P. A.; Reed, G. H. *Arch. Biochem. Biophys.* **2000**, *382*, 6.
(107) Sofia, H. J.; Chen, G.; Hetzler, B. G.; Reyes-Spindola, J. F.; Miller, N. E. *Nucleic Acids Res.* **2001**, *29*, 1097.
(108) Cosper, M. M.; Jameson, G. N.; Davydov, R.; Eidsness, M. K.; Hoffman, B. M.; Huynh, B. H.; Johnson, M. K. *J. Am. Chem. Soc.* **2002**, *124*, 14006.
(109) Walsby, C. J.; Hong, W.; Broderick, W. E.; Cheek, J.; Ortillo, D.; Broderick, J. B.; Hoffman, B. M. *J. Am. Chem. Soc.* **2002**, *124*, 3143.
(110) Chen, D.; Walsby, C.; Hoffman, B. M.; Frey, P. A. *J. Am. Chem. Soc.* **2003**, *125*, 11788.
(111) Walsby, C. J.; Ortillo, D.; Yang, J.; Nnyepi, M. R.; Broderick, W. E.; Hoffman, B. M.; Broderick, J. B. *Inorg. Chem.* **2005**, *44*, 727.
(112) Frey, P. A. *Annu. Rev. Biochem.* **2001**, *70*, 121.
(113) Frey, P. A.; Magnusson, O. T. *Chem. Rev.* **2003**, *103*, 2129.
(114) Fontecave, M.; Atta, M.; Mulliez, E. *Trends Biochem. Sci.* **2004**, *29*, 243.
(115) Marsh, E. N.; Patwardhan, A.; Huhta, M. S. *Bioorg. Chem.* **2004**, *32*, 326.
(116) Layer, G.; Kervio, E.; Morlock, G.; Heinz, D. W.; Jahn, D.; Retey, J.; Schubert, W. D. *J. Biol. Chem.* **2005**, *386*, 971.
(117) Allen, R. M.; Chatterjee, R.; Ludden, P. W.; Shah, V. K. *J. Biol. Chem.* **1995**, *270*, 26890.
(118) Dos Santos, P. C.; Dean, D. R.; Hu, Y.; Ribbe, M. W. *Chem. Rev.* **2004**, *104*, 1159.
(119) Cosper, N. J.; Booker, S. J.; Ruzicka, F.; Frey, P. A.; Scott, R. A. *Biochemistry* **2000**, *39*, 15668.
(120) Henshaw, T.; Cheek, J.; Broderick, J. *J. Am. Chem. Soc.* **2000**, *122*, 8331.
(121) Wu, W.; Booker, S.; Lieder, K. W.; Bandarian, V.; Reed, G. H.; Frey, P. A. *Biochemistry* **2000**, *39*, 9561.
(122) Berkovitch, F.; Nicolet, Y.; Wan, J. T.; Jarrett, J. T.; Drennan, C. L. *Science* **2004**, *303*, 76.
(123) Layer, G.; Moser, J.; Heinz, D. W.; Jahn, D.; Schubert, W. D. *EMBO J.* **2003**, *22*, 6214.
(124) Hanzelmann, P.; Schindelin, H. *Proc. Natl. Acad. Sci. U.S.A.* **2004**, *101*, 12870.
(125) Lepore, B. W.; Ruzicka, F. J.; Frey, P. A.; Ringe, D. *Proc. Natl. Acad. Sci. U.S.A.* **2005**, *102*, 13819.
(126) Nicolet, Y.; Drennan, C. L. *Nucleic Acids Res.* **2004**, *32*, 4015.
(127) Jarrett, J. T. *Chem. Biol.* **2005**, *12*, 409.
(128) Rubach, J. K.; Brazzolotto, X.; Gaillard, J.; Fontecave, M. *FEBS Lett.* **2005**, *579*, 5055.
(129) Peters, J. W.; Szilagyi, R. K.; Naumov, A.; Douglas, T. *FEBS Lett.* **2006**, *580*, 363.
(130) Posewitz, M. C.; King, P. W.; Smolinski, S. L.; Smith, R. D.; Ginley, A. R.; Ghirardi, M. L.; Seibert, M. *Biochem. Soc. Trans.* **2005**, *33*, 102.
(131) Leonardi, R.; Fairhurst, S. A.; Kriek, M.; Lowe, D. J.; Roach, P. L. *FEBS Lett.* **2003**, *539*, 95.
(132) McGlynn, S. E.; Ruebush, S. S.; Naumov, A.; Nagy, L. E.; Dubini, A.; King, P. W.; Broderick, J. B.; Posewitz, M. C.; Peters, J. W. *J. Biol. Inorg. Chem.* **2007**, *12*, 443.
(133) Vignais, P. M.; Billoud, B.; Meyer, J. *FEMS Microbiol. Rev.* **2001**, *25*, 455.
(134) Czjzek, M.; ElAntak, L.; Zambonie, V.; Morelli, X.; Dolla, A.; Guerlesquin, F.; Bruschi, M. *Structure* **2002**, *10*, 1677.
(135) Matias, P. M.; Coelho, A. V.; Valente, F. M. A.; Placido, D.; JeGall, J.; Xavier, A. V.; Pereira, I. A. C.; Carrondo, M. A. *J. Biol. Chem.* **2002**, *277*, 47907.
(136) Hedderich, R. *J. Bioenerg. Biomembr.* **2004**, *36*, 65.
(137) Deppenmeier, U. *J. Bioenerg. Biomembr.* **2004**, *36*, 55.
(138) Vignais, P. M.; Billoud, B. *Chem. Rev.* **2007**, *107*, 4206−4272.
(139) Page, C. C.; Moser, C. C.; Dutton, P. L. *Curr. Opin. Chem. Biol.* **2003**, *7*, 551.
(140) Leys, D.; Scrutton, N. S. *Curr. Opin. Struct. Biol.* **2004**, *14*, 642.
(141) Teixeira, M.; Moura, I.; Xavier, A. V.; Moura, J. J. G.; LeGall, J.; DerVartanian, D. V.; Peck Jr., H. D. *J. Biol. Chem.* **1989**, *264*, 16435.
(142) Démentin, S.; Belle, V.; Bertrand, P.; Guigliarelli, B.; Adryanczyk-Perrier, G.; De Lacey, A. L.; Fernandez, V. M.; Rousset, M.; Léger, C. *J. Am. Chem. Soc.* **2006**, *128*, 5209.
(143) Rousset, M.; Montet, Y.; Guigliarelli, B.; Forget, N.; Asso, M.; Bertrand, P.; Fontecilla-Camps, J. C.; Hatchikian, E. C. *Proc. Natl. Acad. Sci. U.S.A.* **1998**, *95*, 11625.
(144) Bingemann, R.; Klein, A. *Eur. J. Biochem.* **2000**, *267*, 6612.
(145) Bertrand, P.; Dole, F.; Asso, M.; Guigliarelli, B. *J. Biol. Inorg. Chem.* **2000**, *5*, 682.
(146) Czjzek, M.; Guerlesquin, F.; Bruschi, M.; Haser, R. *Structure* **1996**, *4*, 395.
(147) Niviére, V.; Hatchikian, E. C.; Bianco, P.; Haladjian, J. *Biochim. Biophys. Acta* **1988**, *935*, 34.
(148) Nørager, S.; Legrand, P.; Pieulle, L.; Hatchikian, E. C.; Roth, M. *J. Mol. Biol.* **1999**, *290*, 881.
(149) Valente, F. M. A.; Saraiva, L. M.; LeGall, J.; Xavier, A. V.; Teixeira, M.; Pereira, I. A. C. *ChemBioChem* **2001**, *2*, 895.
(150) Matias, P. M.; Coelho, R.; Pereira, I. A. C.; Coelho, A.; Thompson, A. W.; Sieker, L. C.; LeGall, J.; Carrondo, M. A. *Structure* **1999**, *7*, 119.
(151) Umhau, S.; Fritz, G.; Diederichs, K.; Breed, J.; Welte, W.; Kroneck, P. M. *Biochemistry* **2001**, *40*, 1308.
(152) Simões, P.; Matias, P. M.; Morais, J.; Wilson, K.; Dauter, Z.; Carrondo, M. A. *Inorg. Chim. Acta* **1998**, *273*, 213.
(153) Yahata, N.; Saitoh, T.; Takayama, Y.; Ozawa, K.; Ogata, H.; Higuchi, Y.; Akutsu, H. *Biochemistry* **2006**, *45*, 1653.
(154) Harada, E.; Fukuoka, Y.; Ohmura, T.; Fukunishi, A.; Kawai, G.; Fujiwara, T.; Akutsu, H. *J. Mol. Biol.* **2002**, *319*, 767.
(155) Park, J.-S.; Ohmura, T.; Kano, K.; Sagara, T.; Niki, K.; Kyogoku, Y.; Akutsu, H. *Biochim. Biophys. Acta* **1996**, *1293*, 45.

(156) Pieulle, L.; Morelli, X.; Gallice, P.; Lojou, E.; Barbier, P.; Czjzek, M.; Bianco, P.; Guerlesquin, F.; Hatchikian, E. C. *J. Mol. Biol.* **2005**, *18*, 73.
(157) Morelli, X.; Czjzek, M.; Hatchikian, E. C.; Bornet, O.; Fontecilla-Camps, J. C.; Palma, N. P.; Moura, J. J. G.; Guerlesquin, F. *J. Biol. Chem.* **2000**, *275*, 23204.
(158) Sebban-Kreuzer, C.; Blanchard, L.; Bersch, B.; Blackledge, M. J.; Marion, D.; Dolla, A.; Guerlesquin, F. *Eur. J. Biochem.* **1998**, *251*, 787.
(159) Morelli, X.; Guerlesquin, F. *FEBS Lett.* **1999**, *460*, 77.
(160) ElAntak, L.; Morelli, X.; Bornet, O.; Hatchikian, C.; Czjzek, M.; Dolla, A.; Guerlesquin, F. *FEBS Lett.* **2003**, *548*, 1.
(161) Liang, Z.-X.; Klinman, J. P. *Curr. Opin. Struct. Biol.* **2004**, *14*, 648.
(162) Clegg, W.; Henderson, R. A. *Inorg. Chem.* **2002**, *41*, 1128.
(163) Démentin, S.; Burlat, B.; De Lacey, A. L.; Pardo, A.; Adryanczyk-Perrier, G.; Guigliarelli, B.; Fernandez, V. M.; Rousset, M. *J. Biol. Chem.* **2004**, *279*, 10508.
(164) Cammack, R. In *Hydrogen as a Fuel; Learning from Nature*; Cammack, R., Robson, R., Frey, M., Eds.; Taylor and Francis: London, U.K., 2001; p 164.
(165) Frey, M.; Fontecilla-Camps, J. C.; Volbeda, A. In *Handbook of Metalloproteins*; Messerschmidt, A., Huber, R., Poulos, T., Wieghardt, K., Eds.; Wiley: Chichester, U.K., 2001; p 880.
(166) Louro, R. O.; Catarino, T.; LeGall, J.; Xavier, A. V. *J. Biol. Inorg. Chem.* **1997**, *2*, 488.
(167) Cukierman, S. *Biochim. Biophys. Acta* **2006**, *1757*, 876.
(168) Brzezinski, P.; Ädelroth, P. *Curr. Opin. Struct. Biol.* **2006**, *16*, 465.
(169) Kato, M.; Pisliakov, A. V.; Warshel, A. *Proteins* **2006**, *64*, 829.
(170) Sazanov, L. A.; Hinchliffe, P. *Science* **2006**, *311*, 1430.
(171) Ullmann, G. M. *J. Phys. Chem. B* **2000**, *104*, 6293.
(172) Klingen, A. R.; Bombarda, E.; Ullmann, G. M. *Photochem. Photobiol. Sci.* **2006**, *5*, 588.
(173) Namslauer, A.; Aagaard, A.; Katsonouri, A.; Brzezinski, P. *Biochemistry* **2003**, *42*, 1488.
(174) Garczarek, F.; Gerwert, K. *Nature* **2006**, *439*, 109.
(175) Armstrong, F. A. *Chem. Rev.* **2007**, *107*, 4366−4413.
(176) Rieder, R.; Cammack, R.; Hall, D. O. *Eur. J. Biochem.* **1984**, *145*, 637.
(177) Teixeira, M.; Fauque, G.; Moura, I.; Lespinat, P. A.; Berlier, Y.; Prickril, B.; Peck, H. D.; Xavier, A. V.; Legall, J.; Moura, J. J. G. *Eur. J. Biochem.* **1987**, *167*, 47.
(178) Valente, F. M.; Oliveira, A. S.; Gnadt, N.; Pacheco, I.; Coelho, A. V.; Xavier, A. V.; Teixeira, M.; Soares, C. M.; Pereira, I. A. *J. Biol. Inorg. Chem.* **2005**, *10*, 667.
(179) Montet, Y. Thesis, Université Joseph Fourier, Grenoble, France, 1998.
(180) Söderhjelm, P.; Ryde, U. *J. Mol. Struct. THEOCHEM* **2006**, 770, 199.
(181) Stein, M.; Van Lenthe, E.; Baerends, E. J.; Lubitz, W. *J. Am. Chem. Soc.* **2001**, *123*, 5839.
(182) Stadler, C.; De Lacey, A. L.; Montet, Y.; Volbeda, A.; Fontecilla-Camps, J. C.; Conesa, J. C.; Fernandez, V. M. *Inorg. Chem.* **2002**, *41*, 4424.
(183) Carepo, M.; Tierney, D. L.; Brondino, C. D.; Yang, T. C.; Pamplona, A.; Telser, J.; Moura. I.; Moura, J. J.; Hoffman, B. M. *J. Am. Chem. Soc.* **2002**, *124*, 281.
(184) Van der Zwaan, J. W.; Coremans, J. M.; Bouwens, E. C.; Albracht, S. P. J. *Biochim. Biophys. Acta* **1990**, 1041, 101.
(185) Claiborne, A.; Yeh, J. I.; Mallet, T. C.; Luba, J.; Crane, E. J.; Charrier, C.; Parsonage, D. *Biochemistry* **1999**, *38*, 15407.
(186) Lamle, S. E.; Albracht, S. P. J.; Armstrong, F. A. *J. Am. Chem. Soc.* **2004**, *126*, 14899.
(187) Vincent, K. A.; Parkin, A.; Lenz, O.; Albracht, S. P.; Fontecilla-Camps, J. C.; Cammack, R.; Friedrich, B.; Armstrong, F. A. *J. Am. Chem. Soc.* **2005**, *127*, 18179.
(188) Farmer, P. J.; Reibenspies, J. H.; Lindahl, P. A.; Darensbourg, M. Y. *J. Am. Chem. Soc.* **1993**, *115*, 4665.
(189) Primus, J. L.; Teunis, K.; Mandon, D.; Veeger, C.; Rietjens, I. M. C. M. *Biochem. Biophys. Res. Commun.* **2000**, *272*, 551.
(190) Lamle, S. E.; Albracht, S. P. J.; Armstrong, F. A. *J. Am. Chem. Soc.* **2005**, *127*, 6595.
(191) Patil, D. S.; Moura, J. J.; He, S. H.; Teixeira, M.; Prickril, B. C.; DerVartanian, D. V.; Peck, H. D., Jr.; LeGall, J.; Huynh, B. H. *J. Biol. Chem.* **1988**, *263*, 18732.
(192) Elber, R.; Karplus M. *J. Am. Chem. Soc.* **1990**, *112*, 9161.
(193) Teixeira, V. H.; Baptista, A. M.; Soares, C. *Biophys. J.* **2006**, *91*, 2035.
(194) Cohen, J.; Kim, K.; King, P.; Seibert, M.; Schulten, K. *Structure* **2005**, *13*, 1321.
(195) Amara, P.; Andreoletti, P.; Jouve, H. M.; Field, M. J. *Protein Sci.* **2001**, *10*, 1927.
(196) Bossa, C.; Anselmi, M.; Roccatano, D.; Amadei, A.; Vallone, B.; Brunori, M.; Nola, A. D. *Biophys. J.* **2004**, *86*, 3855.
(197) Kleihues, L.; Lenz, O.; Bernhard, M.; Buhrke, T.; Friedrich, B. *J. Bacteriol.* **2000**, *182*, 2716.
(198) Elsen, S.; Duché, O.; Colbeau, A. *J. Bacteriol.* **2003**, *185*, 7111.
(199) Bernhard, M.; Buhrke, T.; Bleijlevens, B.; De Lacey, A. L.; Fernandez, V. M.; Albracht, S. P. J.; Friedrich, B. *J. Biol. Chem.* **2001**, *276*, 15592.
(200) Albracht, S. P. J. *Biochim. Biophys. Acta* **1994**, *1188*, 167.
(201) Buhrke, T.; Brecht, M.; Lubitz, W.; Friedrich, B. *J. Biol. Inorg. Chem.* **2002**, *7*, 897.
(202) Buhrke, T.; Lenz, O.; Krauss, N.; Friedrich, B. *J. Biol. Chem.* **2005**, *280*, 23791.
(203) Duché, O.; Elsen, S.; Cournac, L.; Colbeau, A. *FEBS J.* **2005**, *272*, 3899.
(204) Burgdorf, T.; Lenz, O.; Buhrke, T.; Van der Linden, E.; Jones, A. K.; Albracht, S. P.; Friedrich, B. *J. Mol. Microbiol. Biotechnol.* **2005**, *10*, 181.
(205) Burgdorf, T.; Van der Linden, E.; Bernhard, M.; Yin, Q. J.; Back, J. W.; Hartog, A. F.; Muijsers, A. O.; De Koster, C. G.; Albracht, S. P. J.; Friedrich, B. *J. Bacteriol.* **2005**, *187*, 3122.
(206) Van der Linden, E.; Faber, B. W.; Bleijlevens, B.; Burgdorf, T.; Bernhard, M.; Friedrich, B.; Albracht, S. P. *Eur. J. Biochem.* **2004**, *271*, 801.
(207) Massanz, C.; Friedrich, B. *Biochemistry* **1999**, *38*, 14330.
(208) Burgdorf, T.; De Lacey, A. L.; Friedrich, B. *J. Bacteriol.* **2002**, *184*, 6280.
(209) Friedrich, B. Personal communication.
(210) Van der Linden, E.; Burgdorf, T.; Bernhard, M.; Bleijlevens, B.; Friedrich, B.; Albracht, S. P. *J. Biol. Inorg. Chem.* **2004**, *9*, 616.
(211) Burgdorf, T.; Löscher, S.; Liebisch, P.; Van der Linden, E.; Galander, M.; Lendzian, F.; Meyer-Klaucke, W.; Albracht, S. P. J.; Friedrich, B.; Dau, H.; Haumann, M. *J. Am. Chem. Soc.* **2005**, *127*, 576.
(212) Yagi, T.; Matsuno-Yagi, A. *Biochemistry* **2003**, *42*, 2266.
(213) Brandt, U. *Annu. Rev. Biochem.* **2006**, *75*, 69.
(214) Mitchell, P. *Science* **1979**, *206*, 1148.
(215) Fearnley, I. M.; Walker, J. E. *Biochim. Biophys. Acta* **1992**, *1140*, 105.
(216) Pilkington, S. J.; Skehel, J. M.; Gennis, R. B.; Walker, J. E. *Biochemistry* **1991**, *30*, 2166.
(217) Albracht, S. P. J. *Biochim. Biophys. Acta* **1993**, *1144*, 221.
(218) Malki, S.; Saimmaime, I.; De Luca, G.; Rousset, M.; Dermoun, Z.; Belaich, J.-P. *J. Bacteriol.* **1995**, *177*, 2628.
(219) Albracht, S. P. J.; De Jong, A. M. P. *Biochim. Biophys. Acta* **1997**, *1318*, 92.
(220) Cournac, L.; Guedeney, G.; Peltier, G.; Vignais, P. M. *J. Bacteriol.* **2004**, *186*, 1737.
(221) Friedrich, T.; Scheide, D. *FEBS Lett.* **2000**, *479*, 1.
(222) Schäfer, E.; Seeler, H.; Reifscheider, N. H.; Krause, F.; Dencher, N. A.; Vonck, J. *J. Biol. Chem.* **2006**, *281*, 15370.
(223) Hinchliffe, P.; Sazanov, L. A. *Science* **2005**, *309*, 771.
(224) Long, M.; Liu, J.; Chen, Z.; Bleijlevens, B.; Roseboom, W.; Albracht, S. P. *J. Biol. Inorg. Chem.* **2007**, *12*, 62.
(225) Nouailler, M.; Morelli, X.; Bornet, O.; Chetrit, B.; Dermoun, Z.; Guerlesquin, F. *Protein Sci.* **2006**, *15*, 1369.
(226) Albracht, S. P.; Hedderich, R. *FEBS Lett.* **2000**, *485*, 1.
(227) Hosler, J. P.; Ferguson-Miller, S.; Mills, D. A. *Annu. Rev. Biochem.* **2006**, *75*, 165.
(228) Zwicker, K.; Galkin, A.; Dröse, S.; Grgic, L.; Kerscher, S.; Brandt, U. *J. Biol. Chem.* **2006**, *281*, 23013.
(229) Barton, R. M.; Worman, H. J. *J. Biol. Chem.* **1999**, *274*, 30008.
(230) Hackstein, J. H. *Biochem. Soc. Trans.* **2005**, *33*, 47.
(231) Balk, J.; Pierik, A. J.; Netz, D. J.; Muhlenhoff, U.; Lill, R. *EMBO J.* **2004**, *23*, 2105.
(232) Yarunin, A.; Panse, V. G.; Petfalski, E.; Dez, C.; Tollervey, D.; Hurt, E. C. *EMBO J.*, **2005**, *24*, 580.
(233) Huang, J.; Song, D.; Flores, A.; Zhao, Q.; Mooney, S. M.; Shaw, L. M.; Lee, F. S. *Biochem. J.* **2007**, *401*, 341.
(234) Fournier, M.; Dermoun, Z.; Durand, M. C.; Dolla, A. *J. Biol. Chem.* **2004**, *279*, 1787.
(235) Ceriotti, A.; Chini, P.; Fumagalli, A.; Koetzle, T. F.; Longoni, G.; Tagusagawa, F. *Inorg. Chem.* **1984**, *23*, 1363.
(236) Roberts, L. M.; Lindahl, P. A. *J. Am. Chem. Soc.* **1995**, *117*, 2565.
(237) Salerno, J. C. In *The Bioinorganic Chemistry of Nickel*; Lancaster, J. R., Ed.; VCH: Weinheim, Germany, 1988; p 53.
(238) Coremans, J. M. C. C.; Van Garderen, C. J.; Albracht, S. P. J. *Biochim. Biophys. Acta* **1992**, *1119*, 148.
(239) De Lacey, A. L.; Stadler, C.; Fernandez, V. M.; Hatchikian, E. C.; Fan, H.-J.; Li, S.; Hall, M. B. *J. Biol. Inorg. Chem.* **2002**, *7*, 318.
(240) Brecht, M.; Van Gastel, M.; Buhrke, T.; Friedrich, B.; Lubitz, W. *J. Am. Chem. Soc.* **2003**, *125*, 13075.
(241) Foerster, S.; Stein, M.; Brecht, M.; Ogata, H.; Higuchi, Y.; Lubitz, W. *J. Am. Chem. Soc.* **2003**, *125*, 83.
(242) Foerster, S.; Van Gastel, M.; Brecht, M.; Lubitz, W. *J. Biol. Inorg. Chem.* **2005**, *10*, 51.

(243) Whitehead, J. P.; Gurbiel, R. J.; Bagyinka, C.; Hoffman, B. M.; Maroney, M. J. *J. Am. Chem. Soc.* **1993**, *115*, 5629.
(244) Stein, M.; Lubitz, W. *J. Inorg. Biochem.* **2004**, *98*, 862.
(245) Davidson, G.; Choudhury, S. B.; Gu, Z.; Bose, K.; Roseboom, W.; Albracht, S. P. J.; Maroney, M. J. *Biochemistry* **2000**, *39*, 7468.
(246) Dole, F.; Medina, M.; More, C.; Cammack, R.; Bertrand, P.; Guigliarelli, B. *Biochemistry* **1996**, *35*, 16399.
(247) Bleijlevens, B.; Van Broekhuizen, F. A.; De Lacey, A. L.; Roseboom, W.; Fernandez, V. M.; Albracht, S. P. J. *J. Biol. Inorg. Chem.* **2004**, *9*, 743.
(248) Grande, H. J.; Dunham, W. R.; Averill, B.; Van Dijk, C.; Sands, R. H. *Eur. J. Biochem.* **1983**, *136*, 201.
(249) Albracht, S. P. J.; Roseboom, W.; Hatchikian, E. C. *J. Biol. Chem.* **2006**, *11*, 88.
(250) Roseboom, W.; De Lacey, A. L.; Fernandez, V. M.; Hatchikian, E. C; Albracht, S. P. J. *J. Biol. Chem.* **2006**, *11*, 102.
(251) Pereira, A. S.; Tavares, P.; Moura, I.; Moura, J. J. G.; Huynh, B. H. *J. Am. Chem. Soc.* **2001**, *123*, 2771.
(252) Parkin, A.; Cavazza, C.; Fontecilla-Camps, J. C.; Armstrong, F. A. *J. Am. Chem. Soc.* **2006**, *128*, 16808.
(253) Popescu, C. V.; Münck, E. *J. Am. Chem. Soc.* **1999**, *121*, 7877.
(254) Kraulis, P. J. *J. Appl. Crystallogr.* **1991**, *24*, 946.
(255) Merrit, E. A.; Bacon, D. J. *Methods Enzymol.* **1997**, *277*, 520.
(256) http://www.pymol.org.

CR050195Z